NUCLEAR WASTE MANAGEMENT ORGANIZATION
SOCIÉTÉ DE GESTION DES DÉCHETS NUCLÉAIRES

Phase 2 Geoscientific Preliminary Assessment, Lineament Interpretation

TOWNSHIP OF SCHREIBER, ONTARIO



APM-REP-06145-0007

FEBRUARY 2015

This report has been prepared under contract to the NWMO. The report has been reviewed by the NWMO, but the views and conclusions are those of the authors and do not necessarily represent those of the NWMO.

All copyright and intellectual property rights belong to the NWMO.

For more information, please contact:
Nuclear Waste Management Organization
22 St. Clair Avenue East, Sixth Floor
Toronto, Ontario M4T 2S3 Canada
Tel 416.934.9814
Toll Free 1.866.249.6966
Email contactus@nwmo.ca
www.nwmo.ca

Phase 2 Geoscientific Preliminary Assessment,

Lineament Interpretation, Township of Schreiber, Ontario

Report Prepared for

Nuclear Waste Management Organization

nwmo
NUCLEAR WASTE MANAGEMENT ORGANIZATION
SOCIÉTÉ DE GESTION DES DÉCHETS NUCLÉAIRES

Report Prepared by

srk consulting 1974 40 2014

SRK Consulting (Canada) Inc.
SRK Project Number: 3CN020.003
NWMO Report Number: APM-REP-06145-0007
February, 2015

Phase 2 Geoscientific Preliminary Assessment,

Lineament Interpretation, Township of Schreiber, Ontario

SRK Consulting (Canada) Inc.
Suite 1300, 151 Yonge Street
Toronto, Ontario
M5C 2W7
E-mail: toronto@srk.com
Website: www.srk.com
Tel: +1 416 601 1445
Fax: +1 416 601 9046

SRK Project Number: 3CN020.003
NWMO Report Number: APM-REP-06145-0007

February 2015

Authored by:



Simon Craggs, MSc
Senior Consultant (Structural Geology)

Reviewed by:



James Siddorn, PhD, PGeo
Principal Consultant (Structural Geology)

Executive Summary

This technical report documents the results of an updated surficial and geophysical lineament interpretation study conducted as part of the Phase 2 Geoscientific Preliminary Assessment, to further assess the suitability of the Schreiber area to safely host a deep geological repository (Geofirma, 2015). This study followed the successful completion of a Phase 1 Geoscientific Desktop Preliminary Assessment (NWMO, 2013; AECOM, 2013). The desktop study identified two potentially suitable areas warranting further studies such as high-resolution surveys and geological mapping.

The purpose of the Phase 2 lineament interpretation was to provide an updated interpretation of the geological and structural characteristics of the bedrock units within the potentially suitable areas identified in Phase 1 desktop assessment. The assessment area considered for the lineament study includes the areas covered by the newly acquired Phase 2 airborne surveys (Geofirma, 2015). The interpretation of lineaments was conducted using the new high-resolution airborne magnetic and topographic data, as well as high-resolution satellite data.

The lineament interpretation followed a systematic workflow involving three steps. The first step included an independent lineament interpretation by two separate interpreters for each data set and assignment of certainty level (low certainty, medium certainty, or high certainty). The second step involved the integration of interpreted lineaments for each individual data set and first determination of reproducibility. The third and final step involved the integration of lineament interpretations for the surficial data sets (topography and satellite) followed by integration of the combined surficial data set with the magnetic data set, with determination of coincidence in each integration step. Over the course of these three steps, a comprehensive list of attributes for each lineament was compiled. The four key lineament attributes and characteristics used in the assessment include certainty, length, density and orientation.

Geophysical lineaments were interpreted using the newly acquired high-resolution magnetic data (SGL 2015), which provides an improvement to the overall resolution and quality of magnetic data compared with the available data interpreted during the Phase 1 preliminary assessment. Lineaments interpreted using the magnetic data are typically less affected by the presence of overburden than surficial datasets, and more likely reflect potential structures at depth that may or may not have surficial expressions. In general, the geophysical lineament densities observed in the two survey areas show a similar uniform lineament density, with some areas showing decreased density.

Surficial lineaments were interpreted using the high-resolution topographic data (DEM) from the airborne surveys, and high-resolution satellite data with a cell resolution of 0.46 m. Surficial lineaments were interpreted as linear traces along topographic valleys, escarpments, and drainage patterns such as river streams and linear lakes. These linear traces may represent the expression of fractures on the ground surface. However, it is uncertain what proportion of surficial lineaments represent actual geological structures and if so, whether the structures extend to significant depth. The observed distribution and density of surficial lineaments is highly influenced by the presence of overburden cover and water bodies, which can mask the surface expressions of potential fractures. The observed surficial lineament density is generally uniform and relatively high throughout the Schreiber area, due in part to the use of high-resolution satellite imagery and extensive bedrock exposure, which makes surficial lineaments readily interpretable.

Table of Contents

Executive Summary ii

Table of Contents iii

List of Tables iv

List of Figures iv

1 Introduction 1
- 1.1 Scope of Work and Work Program 1
- 1.2 Assessment Area 2
- 1.3 Qualifications of SRK and SRK Team 2

2 Summary of Geology 4
- 2.1 Geological Setting 4
- 2.2 Bedrock Geology 4
  - 2.2.1 Granitoid Intrusive Rocks 4
  - 2.2.2 Schreiber-Hemlo Greenstone Belt 5
  - 2.2.3 Mafic dykes 5
- 2.3 Metamorphism 5
- 2.4 Structural History 6
- 2.5 Quaternary Geology 9

3 Methodology 11
- 3.1 Source Data Description 11
  - 3.1.1 High-Resolution Magnetic Data 11
  - 3.1.2 Digital Elevation Model 12
  - 3.1.3 High-Resolution Satellite Imagery 12
- 3.2 Lineament Interpretation Workflow 13
  - 3.2.1 Step 1: Lineament Interpretation and Certainty Level 14
  - 3.2.2 Step 2: Lineament Reproducibility Assessment 1 (RA_1) 16
  - 3.2.3 Step 3: Coincidence Assessment (RA_2) 17
  - 3.2.4 Lineament Length 19
  - 3.2.5 Lineament Trends 19
  - 3.2.6 Lineament Density 19

4 Lineament Interpretation Results 21
- 4.1 Geophysical Lineaments 21
- 4.2 Surficial Lineaments 22
  - 4.2.1 DEM lineaments 22
  - 4.2.2 Satellite Imagery Lineaments 23
- 4.3 Integrated Surficial Lineaments (RA_2) 24
- 4.4 Integrated Final Lineaments (RA_2) 24

5 Discussion 26
- 5.1 Lineament Reproducibility (RA_1) and Coincidence (RA_2) 26
- 5.2 Lineament Trends 27
  - 5.2.1 Relationship between Lineament Trends and Regional Stress Field 28
- 5.3 Lineament Length 28
- 5.4 Density 29
  - 5.4.1 Lineament Density 30
  - 5.4.2 Intersection Density 31
- 5.5 Lineament Truncation and Relative Age Relationships 31

5.5.1 Mapped Fault and Lineament Relationships 33
6 Summary of Results 34
7 References 36
8 APPENDIX 41

List of Tables

Table 1: Bounding Coordinates of the Schreiber Phase 2 Assessment Areas shown in Figure 1 (UTM NAD83 Zone 16N) 2
Table 2: Summary of the Geological and Structural History of the Schreiber area (adapted from AECOM, 2013a) 8
Table 3: Spectral Ranges and Spatial Resolution for the Primary World View-2 Visible Bands....12
Table 4: Attribute Table Fields Populated for the Lineament interpretation 14

List of Figures

Figure 1: Location and Overview of the Schreiber Area
Figure 2: Bedrock Geology of the Schreiber Area
Figure 3: Terrain Features of the Schreiber Area
Figure 4: Pole Reduced Magnetic Data (First Vertical Derivative) of the Schreiber Area
Figure 5: Digital Elevation Data of the Schreiber Area
Figure 6: Satellite Imagery Data of the Schreiber Area
Figure 7: Ductile Features of the Schreiber Area
Figure 7a: Ductile Features of the Schreiber Area - Block A
Figure 7b: Ductile Features of the Schreiber Area - Block B
Figure 8: Interpreted Lineaments (RA-1) from Pole Reduced Magnetic Data (1VD) of the Schreiber Area
Figure 8a: Interpreted Lineaments (RA-1) from Pole Reduced Magnetic Data (1VD) of the Schreiber Area - Block A
Figure 8b: Interpreted Lineaments (RA-1) from Pole Reduced Magnetic Data (1VD) of the Schreiber Area - Block B
Figure 9: Interpreted Lineaments from Digital Elevation Data of the Schreiber Area
Figure 9a: Interpreted Lineaments from Digital Elevation Data of the Schreiber Area - Block A
Figure 9b: Interpreted Lineaments from Digital Elevation Data of the Schreiber Area - Block B
Figure 10: Interpreted Lineaments from Satellite Imagery Data of the Schreiber Area
Figure 10a: Interpreted Lineaments from Satellite Imagery Data of the Schreiber Area - Block A
Figure 10b: Interpreted Lineaments from Satellite Imagery Data of the Schreiber Area - Block B
Figure 11: Interpreted Lineaments from Surficial Data of the Schreiber Area
Figure 11a: Interpreted Lineaments from Surficial Data of the Schreiber Area - Block A

Figure 11b: Interpreted Lineaments from Surficial Data of the Schreiber Area - Block B
Figure 12: Interpreted Lineaments from Pole Reduced Magnetic Data of the Schreiber Area
Figure 12a: Interpreted Lineaments from Pole Reduced Magnetic Data of the Schreiber Area - Block A
Figure 12b: Interpreted Lineaments from Pole Reduced Magnetic Data of the Schreiber Area - Block B
Figure 13: Final Integrated Interpreted Lineaments (RA-2) of the Schreiber Area
Figure 13a: Final Integrated Interpreted Lineaments (RA-2) of the Schreiber Area - Block A
Figure 13b: Final Integrated Interpreted Lineaments (RA-2) of the Schreiber Area - Block B
Figure 14: Geophysical Lineaments by Length of the Schreiber Area - Block A
Figure 15: Geophysical Lineaments by Length of the Schreiber Area - Block B
Figure 16: Surficial Lineaments by Length of the Schreiber Area - Block A
Figure 17: Surficial Lineaments by Length of the Schreiber Area - Block B
Figure 18: Final Integrated Lineaments by Length of the Schreiber Area - Block A
Figure 19: Final Integrated Lineaments by Length of the Schreiber Area - Block B
Figure 20: Geophysical Lineament Density of the Schreiber Area - Block A
Figure 21: Geophysical Lineament Density of the Schreiber Area - Block B
Figure 22: Surficial Lineament Density of the Schreiber Area - Block A
Figure 23: Surficial Lineament Density of the Schreiber Area - Block B
Figure 24: Final Integrated Lineament Density of the Schreiber Area - Block A
Figure 25: Final Integrated Lineament Density of the Schreiber Area - Block B
Figure 26: Geophysical Lineament Intersection Density of the Schreiber Area - Block A
Figure 27: Geophysical Lineament Intersection Density of the Schreiber Area - Block B
Figure 28: Surficial Lineament Intersection Density of the Schreiber Area - Block A
Figure 29: Surficial Lineament Intersection Density of the Schreiber Area - Block B
Figure 30: Final Integrated Lineament Intersection Density of the Schreiber Area - Block A
Figure 31: Final Integrated Lineament Intersection Density of the Schreiber Area - Block B
Figure 32: Relative Age Relationships Interpreted Lineaments (RA-2) of the Schreiber Area

Copyright

Both parties retain all rights to methodology, knowledge, and data brought to the work and used therein. No rights to proprietary interests existing prior to the start of the work are passed hereunder other than rights to use same as provided for below. All title and beneficial ownership interests to all intellectual property, including copyright, of any form, including, without limitation, discoveries (patented or otherwise), software, data (hard copies and machine readable) or processes, conceived, designed, written, produced, developed or reduced to practice in the course of the work, shall vest in and remain with NWMO. For greater certainty, all rights, title and interest in the work or deliverables will be owned by NWMO and all intellectual property created, developed or reduced to practice in the course of creating a deliverable or performing the work will be exclusively owned by NWMO.

1 Introduction

This technical report documents the results of an updated surficial and geophysical lineament interpretation study conducted as part of the Phase 2 Geoscientific Preliminary Assessment, to further assess the suitability of the Schreiber area to safely host a deep geological repository (Geofirma, 2015). This study followed the successful completion of a Phase 1 Geoscientific Desktop Preliminary Assessment (NWMO, 2013; AECOM, 2013). The desktop study identified two potentially suitable areas warranting further studies such as high-resolution surveys and geological mapping.

The purpose of the Phase 2 lineament interpretation was to provide an updated interpretation of the geological and structural characteristics of the bedrock units within the potentially suitable areas identified in Phase 1 desktop assessment. The assessment area considered for the lineament study includes the areas covered by the newly acquired Phase 2 airborne surveys (Geofirma, 2015).

The interpretation of geophysical and surficial lineaments was conducted using newly acquired high-resolution airborne magnetic surveys (SGL, 2015). The interpretation of surficial lineaments was conducted using newly acquired topographic data (SGL, 2015) and high-resolution satellite imagery of the area (World View-2).

1.1 Scope of Work and Work Program

The scope of work includes the completion of a structural lineament interpretation of remote sensing and geophysical data for the Schreiber area in northwestern Ontario (Figure 1). The lineament study involved the interpretation of remotely-sensed data sets, including surficial (satellite imagery, digital elevation) and geophysical (magnetic) data sets (SGL, 2015) for the Schreiber area. The investigation interpreted the implication of lineament location and orientation as potential bedrock structural features (e.g., individual fractures or fracture zones) and evaluated their relative timing relationships within the context of the local and regional geological setting. For the purpose of this report, a lineament was defined as, ‘an extensive linear or arcuate geophysical or topographic feature’. The approach undertaken in this lineament investigation is based on the following:

- Lineaments were interpreted using newly acquired high-resolution magnetic and digital elevation data (SGL, 2015), and purchased high-resolution satellite imagery (World View-2);
- Lineament interpretations for each data set were made by two specialist interpreters using a standardized workflow;
- Lineaments were interpreted as being brittle, dyke or ductile features by each interpreter;
- Lineaments were analyzed based on an evaluation of the quality and limitations of the available data sets;
- Lineaments were evaluated using: age relationships; reproducibility tests, particularly the coincidence of lineaments extracted by different interpreters; coincidence of lineaments extracted from different data sets; and comparison to literature; and
- Classification was applied to indicate the significance of lineaments based on certainty, length and reproducibility.

These elements address the issues of subjectivity and reproducibility normally associated with lineament investigations and their incorporation into the methodology increases the confidence in the resulting lineament interpretation.

1.2 Assessment Area

The Phase 2 lineament assessment and interpretation in the Schreiber area was done for two subareas totalling approximately 174 square kilometres (km^2) in area (Figure 1; Blocks (A) and (B)) and was provided by NWMO as a shape file. The approximate coordinates defining the boundaries of the two assessment areas are listed in Table 1 (UTM NAD83, Zone 16N).

The rectangular Block (A) covers 91.24 km^2 and is located west of the approximately square-shaped Block (B), which covers 82.48 km^2 (Figure 1).

Table 1: Bounding Coordinates of the Schreiber Phase 2 Assessment Areas shown in Figure 1 (UTM NAD83 Zone 16N)

X UTM	Y UTM	Block
464,222	5,430,741	A
471,657	5,430,741	A
471,657	5,418,469	A
464,222	5,418,469	A
491,043	5,425,584	B
491,043	5,416,950	B
481,490	5,416,950	B
481,490	5,425,584	B

1.3 Qualifications of SRK and SRK Team

The SRK Group comprises more than 1,400 professionals, offering expertise in a wide range of resource engineering disciplines. The independence of the SRK Group is ensured by the fact that it holds no equity in any project it investigates and that its ownership rests solely with its staff. These facts permit SRK to provide its clients with conflict-free and objective recommendations on crucial issues. SRK has a proven track record in undertaking independent assessments of mineral resources and mineral reserves, project evaluations and audits, technical reports and independent feasibility evaluations to bankable standards on behalf of exploration and mining companies, and financial institutions worldwide. Through its work with a large number of major international mining companies, the SRK Group has established a reputation for providing valuable consultancy services to the global mining industry.

The lineament interpretation and the compilation of this report were completed by Mr. Simon Craggs and Mr. Carl Nagy. Dr. James P. Siddorn, PGeo served as a technical advisor and reviewed lineament interpretations and drafts of this report prior to their delivery to the NWMO as per SRK internal quality management procedures.

Following is a brief description of the qualifications of the project team members.

Mr. Simon Craggs, MSc is a Senior Consultant (Structural Geology) who specializes in regional mapping, detailed analysis of fracture/fluid flow mechanics, and the structural controls on epithermal ore deposit formation. Mr. Craggs has conducted several structural interpretations for vein-type precious metal deposits in poly-deformed terranes across Canada. He recently completed structural

lineament interpretations for the Phase 1 Schreiber, Manitouwadge, and White River areas for the NWMO. In this study, Mr. Craggs was the lead interpreter and the report author.

Mr. Carl Nagy, MSc is a Consultant (Structural Geology) with SRK who specializes in regional bedrock mapping, structural analysis and 2D GIS compilations and interpretations. He has recently completed several regional to detailed scale lineament interpretations of remotely sensed data for projects across the Abitibi. He has also completed Phase 1 lineament interpretations for the Manitouwadge and White River areas for the NWMO. In this study, Mr. Nagy was the second interpreter.

Dr. James Siddorn, PGeo is a Practice Leader (Structural Geology) and specialist in applied structural interpretation of geophysical data sets combined with the structural analysis of ore deposits. Dr. Siddorn has conducted numerous detailed interpretations of magnetic and electromagnetic data sets for gold and diamond exploration, and rock mechanics/hydrogeological engineering studies. He completed a Phase 1 structural lineament interpretation of the Ignace area for the NWMO. He oversaw the structural lineament interpretations for Phase 1 Schreiber and Ear Falls in 2012 and for White River and Manitouwadge in 2013 for NWMO. In this study, Dr. Siddorn was the senior reviewer.

Mr. Jason Adam is an Associate Consultant (GIS) who has a broad experience in GIS. Mr. Adam provided GIS support for the study, mainly for the preparation of figures, under the direction of Mr. Craggs.

2 Summary of Geology

Details of the geology of the Schreiber area were described in the Phase 1 Geoscientific Desktop Preliminary Assessment (AECOM, 2013a). The following sections provide a brief description of the geologic setting, bedrock geology, structural history and mapped structures, metamorphism and Quaternary geology, with a focus on the areas identified during Phase 1 as being potentially suitable (Crossman Lake batholith), its surrounding bedrock units and important structural features.

2.1 Geological Setting

The Schreiber area is primarily located in the Archean Wawa Subprovince, Superior Province. The Wawa Subprovince comprises a volcano-sedimentary-plutonic terrane bounded to the east by the Kapuskasing structural zone (beyond the Schreiber area) and to the north by the metasedimentary-dominated Quetico Subprovince. The western end of the Wawa Subprovince is bordered by the Proterozoic Trans-Hudson orogen. To the south, it is flanked by the Early Proterozoic Southern Province.

The Wawa Subprovince is composed of two semi-linear zones of greenstone belts, the northern of which includes the Shebandowan, Schreiber-Hemlo, Manitouwadge-Hornepayne, White River, Dayohessarah, and Kabinakagami greenstone belts. The Schreiber area occurs in the western portion of the Schreiber-Hemlo greenstone belt (Figure 2). The Schreiber-Hemlo greenstone belt consists of a number of narrow, arcuate segments of supracrustal rocks that are bounded and intruded by granitoid bodies, including the Crossman Lake and Whitesand Lake batholiths.

2.2 Bedrock Geology

The bedrock geology of the Schreiber Phase 2 assessment areas (Blocks (A) and (B), Figure 2) is dominated by granitoid rocks of the Crossman Lake batholith, and also includes supracrustal rocks of the Schreiber-Hemlo greenstone belt, and several suites of mafic diabase dykes. The bedrock in the Schreiber assessment areas is overprinted by several sets of brittle faults and has been subjected to varying amounts of metamorphism. Each of these rock units is discussed in more detail below.

2.2.1 Granitoid Intrusive Rocks

The Crossman Lake batholith within the Schreiber area underlies the majority of the Phase 2 assessment areas (Figure 2). It is predominantly massive and consists of a mixture of medium-grained, quartz-monzonite and monzodiorite, (alkali-feldspar) granite, tonalite and granodiorite. Tonalite and granodiorite phases have weak foliation, while the granite phase has been affected by brittle deformation. Minor dykes and irregular masses of microgranite, quartz (-feldspar) porphyry and aplite occur along the margins of the batholith. Gneissosity and porphyritic facies are seen only in the southwestern and southern part of the batholith to the west of the Township of Schreiber, where the rocks are associated with partially melted metasedimentary rocks (Carter, 1988). Minor phases comprise microgranitic rocks, porphyries, aplites, pegmatites and irregular bodies of quartz are noted within the contact zone (Carter, 1988).

Metamorphism is constrained to an aureola at the contact of the intrusion with the greenstone belt. The thickness of the Crossman lake batholith is not known. Carter (1988) considered the Whitesand Lake and Crossman Lake batholiths to be of the same age. Although the absolute age of

emplacement of the Crossman Lake batholiths is not known, its emplacement would have occurred sometime between 2.75 and 2.677 Ga (Turek et al., 1992; Polat and Kerrich, 1999; Zaleski et al., 1999; Davis and Lin, 2003).

2.2.2 Schreiber-Hemlo Greenstone Belt

The structurally and lithologically complex Schreiber-Hemlo greenstone belt is divided into three lithotectonic assemblages: the Schreiber, Hemlo-Black River, and Heron Bay assemblages (Williams et al. 1991). Supracrustal rocks in the Schreiber area occur in the western part of the Schreiber-Hemlo greenstone belt are considered to be part of the Schreiber assemblage (Williams et al., 1991; Figure 2).

Carter (1988) identified three major types of supracrustal rocks in the Schreiber assemblage: 1) tholeiitic, mafic metavolcanic rocks comprising mainly massive to pillow basalt, tuff and related breccias; 2) calc-alkalic, mafic to felsic metavolcanic rocks dominated by pyroclastic units; and 3) clastic metasedimentary rocks of turbiditic origin interbedded with minor banded iron formation.

2.2.3 Mafic dykes

Several suites of mafic dykes crosscut the Schreiber area and are known regionally (Figure 2), including:

- Northwest-trending Matachewan Suite dykes (ca. 2.473 Ga; Buchan and Ernst, 2004). This dyke swarm is one of the largest in the Canadian Shield. Individual dykes are generally up to 10 m wide, and have vertical to subvertical dips. The Matachewan dykes comprise mainly quartz diabase dominated by plagioclase, augite and quartz (Osmani, 1991).
- North-trending Marathon Suite dykes (ca. 2.121 Ga; Buchan et al. 1996). These form a fan-shaped distribution pattern around the northern, eastern, and western flanks of Lake Superior. The dykes vary in orientation from northwest to northeast, and occur as steep to subvertical sheets, typically a few metres to tens of metres thick, but occasionally up to 75 m thick (Hamilton et al., 2002). The Marathon dykes are quartz tholeiite dominated by equigranular to subophitic clinopyroxene and plagioclase.
- East-west trending, reversely polarized Keweenawan Suite dykes related to ca. 1.100 Ga mid-continental rifting centred on proto-Lake Superior (Thurston, 1991).

A western extension of the ca. 2.167 Ga Biscotasing dyke swarm may also occur in the Schreiber area (Hamilton et al., 2002). These generally trend northeast; however, how these may be distinguished from northeast-trending Marathon dykes in the Schreiber area is undefined.

2.3 Metamorphism

Studies on metamorphism in Precambrian rocks across the Canadian Shield have been summarized in a few publications since the 1970s (e.g., Fraser and Heywood 1978; Kraus and Menard, 1997; Menard and Gordon, 1997; Berman et al., 2000; Easton, 2000a and Easton, 2000b; and Berman et al., 2005) and the thermochronologic record for large parts of the Canadian Shield is documented in a number of studies (Berman et al., 2005; Bleeker and Hall, 2007; Corrigan et al., 2007; and Pease et al., 2008).

The Superior Province of the Canadian Shield largely preserves low pressure – high temperature Neoarchean (ca. 2.710-2.640 Ga) metamorphic rocks. The relative timing and grade of regional

metamorphism in the Superior Province corresponds to the lithological composition of the subprovinces (Easton, 2000a; Percival et al., 2006). Subprovinces comprising volcano-sedimentary assemblages and synvolcanic to syntectonic plutons (i.e., granite-greenstone terranes) are affected by relatively early lower greenschist to amphibolite facies metamorphism. Subprovinces comprising both metasedimentary- and migmatite-dominated lithologies, such as the English River and Quetico, and dominantly plutonic and orthogneissic domains, such as the Winnipeg River, are affected by relatively late middle amphibolite to granulite facies metamorphism (Breaks and Bond, 1993; Corfu et al., 1995). Subgreenschist facies metamorphism in the Superior Province is restricted to limited areas, notably within the central Abitibi greenstone belt (e.g., Jolly, 1978; Powell et al., 1993).

Overall, most of the Canadian Shield preserves a complex episodic history of Neoarchean tectonometamorphism overprinted by Paleoproterozoic tectonothermal events culminating at the end of the Grenville orogeny ca. 0.950 Ga. The distribution of contrasting metamorphic domains in the Canadian Shield is a consequence of relative uplift, block rotation and erosion resulting from Neoarchean orogenesis, subsequent local Proterozoic orogenic events and broader epeirogeny during later Proterozoic and Phanerozoic eons.

In the Schreiber area, the metamorphic grade of exposed Archean rocks is upper greenschist facies (Williams et al., 1991). Locally, higher metamorphic grades up to upper amphibolite facies are recorded in rocks along the margins of plutons. No records exist that suggest that rocks in the Schreiber area may have been affected by thermotectonic overprints related to post-Archean events.

2.4 Structural History

Direct information on the structural geological history of the Schreiber area is limited. The structural geological history summarized below and in Table 2 integrates the results from studies undertaken proximal to the area shown in Figure 2, including structural investigations on the Hemlo gold deposit and surrounding region (i.e., the eastern portion of the Schreiber-Hemlo greenstone belt). It is understood that there are potential problems in applying a regional D_x numbering system into a local geological history. Nonetheless, the summary below represents an initial preliminary interpretation for the Schreiber area, which may be modified after site-specific information has been collected.

Regional studies revealed that the region has undergone complicated polyphase deformation, but do not clarify the relationship between various structures and their significance for the regional tectonic evolution (Polat et al., 1998). Since the various structural studies were carried out on various scales and from different perspectives, disparate structural models and associated terminologies have developed for the Schreiber-Hemlo greenstone belt. In addition, because more than one generation of structures may develop in a single episode of progressive deformation, correlating the different structural studies is a challenge.

The most comprehensive structural study of the Schreiber-Hemlo greenstone belt was conducted by Muir (2003). Since no previous detailed structural studies have been undertaken in the Schreiber area, Muir's (2003) findings on the structural history are included in the summary below, and may be used as a best-fit for the structural history of the Schreiber area. The summary below integrates findings from Muir (2003) with information based on Carter (1988), Polat et al. (1998), Jackson (1998), Polat and Kerrich (1999), Lin (2001), and Davis and Lin (2003).

Muir (2003) defined at least six generations of structures, including two that account for most of the ductile strain, and although others can be distinguished on the basis of crosscutting relationships, they are likely the products of progressive strain events. The main characteristics of these deformation phases are described below.

D_1 deformation is associated with the development of S_1 slaty cleavage and asymmetric boudins in metasedimentary rocks, and asymmetric boudins, mesoscopic closed to isoclinal (overturned) F_1 folds and associated D_1 thrust faults in the metavolcanic rocks. Muir (2003) included the development of S_1 compositional layering as part of this deformation event. The orientation of F_1 folds was modified during subsequent deformation; however, the regionally consistent asymmetry of the F_1 overturned folds, combined with S-C fabrics along ductile D_1 thrust faults, suggests a south-southeast tectonic vergence. Muir (2003) suggested that D_1 likely occurred from ca. 2.719 to ca. 2.691 Ga.

D_2 deformation structures (D_1 in Jackson, 1998) are ubiquitous in the Schreiber-Hemlo greenstone belt and include dominantly east-northeast trending overturned tight to isoclinal F_2 folds, D_2 thrust faults, and northeast- to east-trending D_2 strike-slip faults (collectively forming D_2 fold and thrust duplexes) that overprint or fold D_1 structural elements. During D_2 deformation, the dominantly steeply northward dipping S_2 foliation was developed. The S_2 foliation is characterized by a preferred alignment of phyllosilicate and mafic minerals and flattening and (or) elongation of clasts (Davis and Lin, 2003; Muir, 2003). Several kilometre-scale F_2 folds, with dominant S-shaped asymmetry developed during D_2 deformation (Muir, 2003). Whereas Polat et al. (1998) interpreted that D_2 developed during dextral transpression, Lin (2001) interpreted D_2 deformation as an episode of sinistral transpression based on local observations from the Hemlo shear zone. Muir (2003) suggested that D_2 likely initiated at ca. 2.691 Ga and continued until ca. 2.683 Ga.

Lin (2001) further distinguished open to tight folds with a well-developed axial planar cleavage associated with north over south compression with a dextral strike-slip component. It is not clear whether these structures represent a separate deformation event. If D_2 deformation represents a stage of dextral transpression, as interpreted by Polat et al. (1998), these structures can be interpreted to result from the prolongation of D_2 deformation. However, if D_2 represents a stage of sinistral transpression, it follows that these structures must be related to a separate D_3 deformation phase.

Based on observations in the vicinity of the Hemlo gold deposit, Muir (2003) distinguished a variably developed S_3 mineral and (or) crenulation foliation associated with F_3 folds, which overprint D_2 structural elements. Muir (2003) noted that these features are particularly well-developed within schistose units. Local D_3 S-C shear fabrics and extensional shear bands record a dextral sense of shear, which conforms to their development during dextral transpression as interpreted by Lin (2001). Muir (2003) interpreted that a period of near peak metamorphic temperatures overlapped with the D_2-D_3 transition from ca. 2.688 to ca. 2.675 Ga.

Again, founded on observations in the vicinity of the Hemlo gold deposit, Lin (2001) and Muir (2003) recognized D_4 structural elements, including F_4 kink folds and various sets of D_4 fractures and small-scale faults. Muir (2003) interpreted that the orientation of conjugate sets of D_4 contractional kink bands is consistent with their development during northwest- to west-northwest directed shortening. Northwest-directed D_3-D_4 shortening is estimated to have occurred from ca. 2.682 to ca. 2.679 Ga (Muir, 2003).

Based on this summary, it may be surmised that a protracted period of brittle-ductile deformation spanning D_1 to D_4 comprising elements of compression and sinistral and dextral transpression occurred between ca. 2.719 and ca. 2.679 Ga. It should be noted that this age range partly overlaps with the inferred ages for granitoid intrusions (ca. 2.690 to ca. 2.680 Ga) which suggests that these intrusions may have been affected by D_2-D_4 deformation.

Table 2: Summary of the Geological and Structural History of the Schreiber area (adapted from AECOM, 2013a)

Time period (years before present)	Geological Event
ca. 3.0 to 2.770 Ga	Progressive growth of the Wawa-Abitibi terrane by accretion of oceanic plateau sequences; volcanic island arc sequences; and arc-derived, synkinematic siliciclastic trench turbidites collages along a south-southeast-facing convergent plate margin through compressional and transpressional collisions (Polat et al., 1998).
ca. 2.770 to 2.678 Ga	An extended period of volcanism and sedimentation associated with the formation of the Schreiber-Hemlo greenstone belt. - ca. 2.770 Ga: Formation of the Hemlo-Black River Assemblage (Williams et al., 1991) - ca. 2.700 Ga: Formation of the Heron Bay Assemblage (Williams et al., 1991) - ca. 2.697 to ca. 2.688: Mafic, calc-alkalic and felsic volcanism (Corfu and Muir, 1989; Muir, 2003) - ca. 2.693 to ca. 2.685: Deposition of clastic and chemical sedimentary rocks (Muir, 2003) - ca. 2690-2680: Inferred emplacement of granitoid intrusions in the Schreiber area (Smyk and Schnieders, 1995; Corfu and Muir, 1989. During the formation of the greenstone belt, four periods of ductile-brittle deformation (D_1-D_4) are recognized as occurring between ca. 2.719 and 2.679 Ga (Muir, 2003).
ca. 2.690 to 2.684 Ga	Coalescence of the Wawa and Quetico subprovinces (D_2) (Corfu and Stott, 1996).
ca. 2.688 to 2.675 Ga	Regional metamorphism (Muir, 2003) ($D_2 – D_4$).
ca. 2.688 to 2.675 Ga	Emplacement of granitoid intrusions including the Terrace Bay, Crossman Lake and Whitesand Lake batholiths, and the Mount Gwynne pluton (Santaguida, 2002).
ca. 2.473 Ga	Emplacement of northwest-trending Matachewan Suite of dykes (Buchan and Ernst, 2004).
ca. 2.400 to 2.200 Ga	Development of the Southern Province; possible deposition and subsequent erosion of sedimentary rocks in the Schreiber area (Young et al., 2001).
ca. 2.167 Ga	Possible emplacement of the northeast trending Biscotasing dyke swarm (Hamilton et al., 2002). These dykes cannot be separated with confidence from the Marathon dykes.
ca. 2.121 Ga	Emplacement of north-trending Marathon Suite of dykes (Hamilton et al., 2002; Buchan et al., 1996).
ca. 2.100 to 1.860 Ga	Penokean Orogen (post-D_4); deposition of the Animikie Group sediment rocks to the west. Possible deposition and subsequent erosion in the Schreiber area (Sutcliffe, 1991; Fralick et al., 2002).
ca. 1.540 Ga	Possible deposition and subsequent erosion of Mesoproterozoic Sibley Group clastic sedimentary rocks (Sutcliffe, 1991).
ca. 1.150 to 1.090 Ga	Formation of the Midcontinent Rift that resulted in the deposition of volcanic rocks and minor sedimentary units. Emplacement of west–trending Keweenawan Suite of dykes related to mid-continental rifting that was centred on proto-Lake Superior (Sutcliffe, 1991; Thurston, 1991).
ca.1.100 to 1.086 Ga	Deposition of the Osler Group (Sutcliffe, 1991).
ca. 540 to 355 Ma	Possible coverage of the area by marine seas and deposition of carbonate and clastic rocks subsequently removed by erosion (Johnson et al., 1992).
ca. 145 to 65 Ma	Possible deposition of marine and terrestrial sediments of Cretaceous age subsequently removed by erosion.
ca. 2.6 to 0.01 Ma	Periods of glaciation and deposition of glacial sediments (Barnett, 1992).

Lin (2001) highlighted the presence of post-D_4 brittle faults at various scales and with various orientations in the Schreiber-Hemlo greenstone belt. One set of post-D_4 brittle faults is parallel to the S_2 foliation, contains cataclasite, fault breccia and local pseudotachylite, and commonly offsets Proterozoic diabase dykes. Another post-D_4 brittle fault set strikes southeast and displays a consistent dextral sense of shear. Other than that these faults post-date the intrusion of Proterozoic diabase dykes, no estimates for the timing of this post-D_4 brittle deformation are present in literature. Peterman and Day (1989) recorded reactivation of the Late Archean Quetico and Rainy Lake-Seine River faults at ca. 1.943 Ga in the Rainy Lake region of Minnesota and Ontario. It is possible that at least one stage of post-D_4 faulting occurred during this regional tectonic event, which coincides with the ca. 2.100 to 1.860 Ga Penokean Orogen.

Mapped Structures and Named Faults

Several northwest and northeast-trending faults have been mapped in the Schreiber area (OGS, 2011). These include the Sox Creek, and Ross Lake northwest-trending faults and the northeast trending Syenite Lake fault (Figure 2). South of the Schreiber area shown in Figure 2, other mapped faults include: the northwest-trending Cook Lake fault; and the northeast-trending Worthington Bay, Schreiber Point and Ellis Lake faults (AECOM, 2013a).

Carter (1988) conducted a field mapping program and developed a geological map for the Schreiber area, primarily on the basis of 1:15,840 scale aerial photographs and north-south trending traverse mapping at roughly quarter mile intervals. As a result of this mapping program, Carter (1988) attempted an interpretation of the fault movement along some of the faults. No supporting structural information was included in Carter (1988), so it is assumed that the fault movement interpretation was derived from aerial photographs. Carter (1988) interpreted the Sox Lake fault and the Schreiber Point fault as dextral strike-slip faults; the Cook Lake fault and Syenite Lake fault as dip-slip faults; and the Worthington Bay fault as a sinistral strike-slip fault.

2.5 Quaternary Geology

Quaternary geology in the Schreiber area was interpreted and updated for the Schreiber area as part of the Phase 1 Terrain and Remote Sensing Study by AECOM (2013b) and is summarized here. The Northern Ontario Engineering Geology Terrain Study (MRD 160) and updated AECOM interpretation are shown in Figure 3.

The Quaternary sediments in the Schreiber area are glacial and post-glacial materials which overlie the bedrock. All glacial landforms and related materials are associated with the Wisconsinan glaciation, which began approximately 115 Ka before present (BP) (Barnett, 1992).

As shown in Figure 3, most of the Schreiber area is mapped as exposed bedrock, with thin discontinuous drift cover. Quaternary sediments consist mainly of outwash deposits and ground moraine (till). In the Phase 2 assessment areas, limited outwash deposits are mapped along some of the valleys (Figure 3).

Outwash deposits are believed to range from a few to several metres in thickness and occur in several of the larger fault controlled valleys that transect the Crossman lake batholith. These deposits are generally well-sorted and comprised of stratified sand, gravel, and local boulders. The ground moraine (till) deposits have a silty-sand matrix and contain abundant clasts in the pebble to cobble size range. The thickness of the till in these areas, based on exploration borehole records and surficial mapping, is generally on the order of 1 to 3 m (AECOM, 2013b).

Morris (2000) reports bedrock erosional features (e.g., striae, roche moutonnée) and landforms that indicate a regional ice flow direction of 194° with a range of measured directions, due to local topographic conditions, of between 165 to 238°.

Bogs and organic-rich alluvial deposits are present along water courses in the Schreiber area and in rock floored basins. These deposits tend to have a limited thickness, as determined by regional studies, and areal extent.

3 Methodology

The structural interpretation of the Schreiber area was based on high-resolution remote sensing data sets, including a high-resolution airborne magnetic survey contracted by the NWMO to Sander Geophysics Limited (SGL, 2015), topographic data collected during the airborne magnetic survey, and high-resolution World View-2 satellite imagery procured from Digital Globe.

3.1 Source Data Description

All data were assessed for quality, processed, and reviewed before use in the lineament interpretation. The geophysical data were used to evaluate deeper bedrock structures and proved invaluable to identifying potential bedrock structures beneath areas of surficial cover and aiding in establishing the age relationships among the different lineament sets. Topography (DEM) and satellite imagery (World View-2) data sets were used to identify surficial lineaments expressed in the topography, drainage, and vegetation. Throughout this study, the best resolution data available was used for the lineament interpretation

3.1.1 High-Resolution Magnetic Data

Sander Geophysics Limited (SGL) completed a fixed-wing, high-resolution airborne magnetic survey in the Schreiber area between April 12 and April 24, 2014 (SGL, 2015). The survey area included Blocks (A) and (B) shown in Figure 4.

The airborne survey in the Schreiber area included a total of 3,397 km of flight lines covering a surface area of approximately 174 km^2. Flight operations were conducted out of the Greenstone Regional Airport, in Geraldton, Ontario using a Britten-Norman BN-2 Islander. Data were acquired along traverse lines flown in an east-west direction spaced at 100 m, and control lines flown north-south spaced at 500 m. The survey was flown at a target altitude of 80 m above ground level, with an average ground speed of 100 knots (185 km/h). Airborne magnetic data were acquired using a magnetometer sensor mounted in a fibreglass stinger extending from the tail of the aircraft. The survey acquisition parameters are listed below:

- Traverse line spacing of 100 m
- Traverse line azimuth of 090 - 270°
- Control line spacing of 500 m
- Control line azimuth of 000 - 180°
- Grid cell size of 25 m
- Targeted sensor height of 80 m
- Acquisition date of April 12 to April 24, 2014

Acquired data was processed by the Sander Geophysics Limited (SGL, 2015) and provided to SRK as GRD files. The following products of the high resolution airborne magnetic survey were available for this structural lineament interpretation:

- Total magnetic intensity
- First vertical derivative of the total magnetic intensity
- Second vertical derivative of the total magnetic intensity
- Reduction to the pole of the total magnetic intensity

- First vertical derivative of the reduction to the pole of the total magnetic intensity
- Second vertical derivative of the reduction to the pole of the total magnetic intensity
- Tilt derivative of the reduction to the pole of the total magnetic intensity
- Analytic signal of the total magnetic intensity
- Total horizontal derivative of total magnetic intensity
- Total horizontal derivative of reduction to the pole of the total magnetic intensity
- Total magnetic intensity with high-pass Butterworth filter applied
- Total magnetic intensity with low-pass Butterworth filter applied
- Reduction to pole of total magnetic intensity with high-pass Butterworth filter applied
- Reduction to pole of total magnetic intensity with low-pass Butterworth filter applied

The first and second vertical derivatives, and tilt derivative grids were converted to ERS images that had data ranges, shading, and colour ranges enhanced in ERMapper to outline the structures present. A series of compressed raster images was created in ERMapper for use in ArcGIS.

3.1.2 Digital Elevation Model

Topographic data was collected during the magnetic survey conducted by Sander Geophysics Limited (SGL, 2015). The survey acquisition parameters are identical to those described for the high-resolution magnetic data in Section 3.1.1.

Topographic data was processed by Sander Geophysics Limited and provided to SRK as GRD files. The data grid was then converted to an ERS image, and the data ranges, shading (including hill shade and shaded relief), and colour ranges of the digital elevation model (DEM) were enhanced in ERMapper to highlight the structures present (Figure 5). Compressed raster images were created in ERMapper for use in ArcGIS.

3.1.3 High-Resolution Satellite Imagery

High-resolution World View-2 satellite imagery was procured by SRK on behalf of the NWMO from Digital Globe Incorporated via ESRI Canada.

Imagery was collected by the World View-2 GeoEye sensor. The spectral ranges and spatial resolution of each band are listed in Table 3. World View-2 also collects 4 additional visible and near infrared bands not used in the construction of imagery for the Schreiber area, and not listed below.

Table 3: Spectral Ranges and Spatial Resolution for the Primary World View-2 Visible Bands

Band	Range (nm)	Resolution (m)
Panchromatic	450 – 800	0.46
Blue	450 – 510	1.80
Green	510 – 580	1.80
Red	655 – 690	1.80

A natural colour composite of the World View-2 satellite imagery was provided for the majority of the assessment area as a georeferenced TIFF file from ESRI Canada / Digital Globe Incorporated, and utilized in this format for the lineament interpretations. For the northern part of Block (A), only the panchromatic data was available and provided by ESRI Canada / Digital Globe Incorporated (Figure 6).

3.2 Lineament Interpretation Workflow

A structural lineament interpretation of each of the two Phase 2 assessment areas (Blocks (A) and (B)) was conducted to identify the location and orientation of potential individual fractures or fracture zones and to evaluate their relative timing relationships within the context of the local and regional geological setting.

Lineaments were interpreted using a workflow designed to address issues of subjectivity and reproducibility that are inherent to any lineament interpretation. The workflow follows a set of detailed guidelines using the high resolution airborne geophysical (magnetic), and high resolution surficial (DEM, World View-2 satellite imagery) data sets described above. The interpretation guidelines involved three steps:

- Step 1: Independent lineament interpretation by two individual interpreters for each data set and assignment of certainty level (1, 2, or 3 representing low, medium and high certainty).
- Step 2: Integration of lineament interpretations for each individual data set and first determination of reproducibility.
- Step 3: Integration of lineament interpretations for the surficial data sets (DEM and satellite imagery) followed by integration of the combined surficial data set with the magnetic data set, with determination of coincidence in each integration step.

Each identified lineament feature was classified in an attribute table in ArcGIS. The description of the attribute fields used is included in Table 4. Fields 1 to 9 are populated during Step 1. Fields 10 and 11 are populated during Step 2. Fields 12 to 20 are populated during Step 3.

The interpreted features were classified into three general categories based on a working knowledge of the structural history and bedrock geology of the Schreiber area. These categories include ductile, brittle and dyke lineaments, described as follows:

- **Ductile lineaments**: Features which were interpreted as being associated with the internal fabric of the rock units (including sedimentary or volcanic layering, tectonic foliation or gneissosity, and magmatic foliation) were classified as ductile lineaments. This category also includes recognizable penetrative shear zone fabric. See Figure A1 for example.
- **Brittle lineaments:** Features interpreted as fractures (joints or joint sets, faults or fault zones, and veins or vein sets) were classified as brittle lineaments. This category also includes brittle-ductile shear zones, and brittle partings interpreted to represent discontinuous re-activation parallel to the ductile fabric. Brittle lineaments are commonly characterized by continuous magnetic lows, offsets of magnetic highs and ductile lineaments (as described above), and breaks in topography and vegetation. At the desktop stage of the investigation, this category also includes features of unknown affinity. See Figure A2 for example.
- **Dyke lineaments**: Features which were interpreted, on the basis of their distinct character, (e.g., scale and composition of fracture in-fill, orientation, geophysical signature and topographic expression), were classified as dykes. Dykes were largely interpreted from the magnetic data set, and are commonly characterized by continuous linear magnetic highs. The interpretation of dykes is often combined with pre-existing knowledge of the bedrock geology of the study area. See Figure A3 for example.

A detailed description of the three workflow steps, as well as the way each associated attribute field is populated for interpreted lineament, is provided below.

Table 4: Attribute Table Fields Populated for the Lineament interpretation

ID	Attribute	Brief Description
1	Rev_ID	Reviewer initials
2	Feat_ID	Feature identifier
3	Data_typ	Data set used (MAG, DEM, SAT)
4	Feat_typ	Type of feature used to identify each lineament Satellite Imagery: A. Lineaments drawn along straight or curved lake shorelines B. Lineaments drawn along straight or curved changes in intensity or texture (i.e., vegetation) C. Lineaments drawn down centre of thin rivers or streams D. Lineaments drawn along a linear chain of lakes E. Other (if other, define in comments) Digital Elevation Model: A. Lineaments drawn along straight or curved topographic valleys B. Lineaments drawn along straight or curved slope walls C. Other (if other, define in comments) Airborne Geophysics (magnetic and electromagnetic data): A. Lineaments drawn along straight or curved magnetic high B. Lineaments drawn along straight or curved magnetic low C. Lineaments drawn along straight or curved steep gradient D. Other (if other, define in comments)
5	Name	Name of feature (if known)
6	Certain	Value describing the interpreters confidence in the feature being related to bedrock structure (1-low, 2-medium or 3-high)
7	Length*	Length of feature is the sum of individual lengths of mapped polylines and is expressed in kilometres
8	Width**	Width of feature; this assessment is categorized into 5 bin classes: A. < 100 m B. 100 – 250 m C. 250 – 500 m D. 500 – 1,000 m E. > 1,000 m
9	Azimuth	Lineament orientation expressed as degree rotation between 0 and 180 degrees
10	Buffer_RA_1	Buffer zone width for first reproducibility assessment (in metres)
11	RA_1	Feature value (1 or 2) based on reproducibility assessment
12	Buffer_RA_2	Buffer zone width for coincidence assessment (in metres)
13	RA_2	Feature value (1, 2 or 3) based on coincidence assessment
14	MAG	Feature identified in geophysical data set (Yes or No)
15	DEM	Feature identified in DEM data set (Yes or No)
16	SAT	Feature identified in satellite imagery data set (Yes or No)
17	F_Width	Final interpretation of the width of feature
18	Rel_age	Interpretation of relative age of feature, in accord with regional structural history
19	Comment	Comment field for additional relevant information on a feature
20	Object	Geological element identified, e.g., dyke, fault, joint, contact

* The length of each interpreted feature is calculated based on the sum of all segment lengths that make up that lineament.

** The width of each interpreted feature is determined by expert judgment and utilization of a GIS-based measurement tool. Width determination takes into account the nature of the feature as assigned in the Feature type (Feat_typ) attribute.

3.2.1 Step 1: Lineament Interpretation and Certainty Level

To accommodate the generation of the best possible, unbiased lineament interpretation, two individual interpreters followed an identical process for structural lineament analysis during Step 1. The first step of the lineament interpretation was to have each individual interpreter independently produce GIS lineament maps and detailed attribute tables for each of the three data sets. Step 1 of the

structural lineament analysis is conducted up to a scale of 1:25,000 and follows a designated workflow.

The interpretation of magnetic data follows a two-step process. The first step involves the drawing of ductile features interpreted as tectono-stratigraphic form lines using high-resolution first vertical derivative magnetic data (Figure 7). Additionally, tilt angle magnetic data was used for enhancement of areas of low magnetic contrast. The form lines trace the geometry of magnetic high lineaments and may represent the geometry of stratigraphy within metavolcanic and metasedimentary rocks or the internal fabric (foliation) within granitoid batholiths and gneissic rocks. Magnetic highs associated with dykes (i.e. linear crosscutting magnetic highs in orientations identified in the literature as dyke orientations) are not included in this process. This process highlights discontinuities between form lines, particularly in stratigraphic form lines (e.g., form lines intersecting) that represent structures (faults, folds), unconformities, or intrusive contacts. The process of drawing form lines is instrumental in highlighting lineaments in the magnetic data.

The second step involves drawing a structural base layer that represents all interpreted lineaments regardless of interpreted age, type (e.g., ductile, brittle or dyke), or kinematics. Evidence for interpreted lineaments can be derived from several sources in the magnetic data, including discontinuities between form lines, offset of magnetic units, or the presence of linear magnetic lows or highs. The first vertical derivative magnetic data is used mainly with the tilt angle grid to further enhance this interpretation.

The lineament interpretation of topographic data involved tracing linear or curvi-linear features along topographic valleys, slope walls and any other structurally related features that are visible in a colour mosaic constructed from the digital elevation model (DEM) derived from the airborne geophysical survey. Similarly, the lineament interpretation of satellite imagery involved tracing linear or curvi-linear features along visible shore lines, changes in colour intensity or texture (e.g., vegetation), linear rivers and streams, and along linear chains of features associated with lakes that are visible in World View-2 satellite imagery.

Lineaments from each of the data sets were assigned attributes by each interpreter to characterize what type of feature the lineament was drawn along, the interpreters certainty that the lineament represents a bedrock structure, and the general width of the topographic feature.
Lineaments identified in the DEM and/or in the satellite imagery that were interpreted to be due to glacial transport were excluded from the lineament interpretation data set. The following criteria were utilized to decide whether a DEM or satellite imagery lineament should be excluded:

- The lineament coincides with a mapped ice-flow feature, moraine, or esker
- The lineament is parallel to known eskers or moraines and is marked by narrow, curving ridges
- The lineament is parallel to the local ice flow direction and is accompanies by drumlin-shaped hills in the topographic data set
- The lineament in the satellite imagery is parallel to the local ice flow direction and coincides with a lineament from the topography interpreted that has been identified as glacial
- The lineament was considered to be representative of a magmatic foliation, and not of tectonic origin

The Step 1 lineament analysis resulted in the generation of one interpretation for each data set (e.g., magnetic, DEM, satellite imagery) for each interpreter, resulting in a total of six individual GIS layer-based interpretations. Within these data sets, cross-cutting relationships between individual lineaments were assessed. Following this assessment, based on the expert judgement of each

interpreter, lineament segments were merged, resulting in lineament lengths that correspond to the sum of all parts.

During Step 1, identified lineaments were attributed with fields one to nine as listed in Table 4.

3.2.2 Step 2: Lineament Reproducibility Assessment 1 (RA_1)

During Step 2, individual lineament interpretations produced by each interpreter were compared for each data set. This included a reproducibility assessment based on the coincidence, or lack thereof, of interpreted lineaments within a data set-specific buffer zone. The two individual lineament interpretations for each data set were then integrated and a single interpretation was generated for each data set (Figures 8 to 10). A discussion of the parameters used during this step follows.

Buffer Size Selection

Buffer sizes for lineaments in each data set were based on the magnetic grid resolution. It was determined using trial-and-error over a selected portion of the lineament interpretation that buffer sizes of five times the grid cell resolution provided a balanced result for assessing reproducibility.

A buffer of 125 m (either side of the lineament) was generated for the magnetic data. This value is equivalent to five times the data set grid cell resolution (25 m) of the high resolution magnetic data. Given that the DEM data was extracted from the same survey, the same buffer size was applied to the DEM data.

A 125 m buffer was applied to the satellite imagery data in order to be consistent with the magnetic and DEM buffer size.

The buffer size widths were included in the attribute fields of each interpretation file (Table 4). The buffers were used as an initial guide to determine coincidence between lineaments, with the expert judgement of the interpreter ultimately determining which lineaments were coincident.

Reproducibility Assessment

The generation of an integrated lineament interpretation for each data set, including the reproducibility assessment, followed a three-step process:

- Lineament buffers generated for the Step 1 interpretation were overlain on top of the buffers generated for the lead Step 1 interpretation for each data set. The lead interpretation Step 1 lineaments were then overlain on top of these buffers, and all lineaments that occurred within overlapping buffers were carried forward and copied into a new file for Step 2. These lineaments were attributed with a reproducibility value (RA_1; Table 4) of two in the Step 2 attribute table.
- The remaining lineaments in the lead Step 1 interpretation were then manually analyzed by both interpreters on the basis of the available imagery for each data set. In some instances, this included adapting the shape and extent of individual lineaments to increase the accuracy of spatial location or length of the lineament, and carrying the adapted lineament forward into the Step 2 interpretation file. These lineaments were attributed a RA_1 value of one in the Step 2 attribute table. Where it was determined by the two interpreters that these features were not representative of potential bedrock structure, they were removed from the data set.
- Finally, the lineament interpretation of the second Step 1 interpretation was overlain on top of the Step 2 integrated file, and all remaining lineaments in the second interpreter's Step 1 interpretation were then manually analyzed by both interpreters on the basis of the available imagery for each data set. In some instances, this included adapting the shape and extent of

individual lineaments to increase the accuracy of spatial location or length of the lineament, and carrying the adapted lineament forward into the Step 2 interpretation file. These lineaments were attributed a RA_1 value of one in the Step 2 attribute table. All remaining lineaments that were attributed a certainty value of one were removed, if it was determined by the two lineament interpreters that these features were not representative of potential lineaments.

As specified above, the decision on whether or not to adapt the shape and extent of an individual lineament and (or) whether the lineament was carried forward to the next step followed analysis of the specified lineament with the available imagery and a discussion between the two interpreters. The following guidelines were applied:

- If a lineament was drawn continuously by one interpreter but as individual, spaced or disconnected segments by the other interpreter, the lineament was carried forward to the Step 2 interpretation with a RA_1 value of two.
- If more than two thirds of a lineament were identified by one interpreter compared to the other interpreter, the lineament was carried forward to the Step 2 interpretation with a RA_1 value of two. If less than two thirds of a lineament were identified by one interpreter compared to the other interpreter, the longer lineament was cut, and each portion was attributed with RA_1 values accordingly.

The resulting Step 2 interpretations for each data set (e.g., magnetics, topography, and satellite imagery) were then refined using expert judgement to avoid any structurally inconsistent relationships. This included adapting the lineaments within the limits of the assigned buffer zone to avoid any mutually crosscutting relationships, and updating the attribute fields.

3.2.3 Step 3: Coincidence Assessment (RA_2)

During Step 3, the integrated lineament interpretations for each data set were amalgamated into one final interpretation. First, lineaments derived from the DEM and satellite data were merged to produce an integrated surficial lineament data set. Subsequently, the geophysical lineaments were integrated with the integrated surficial lineaments to produce a final amalgamated interpretation. A discussion of the parameters used during this step follows below.

Surficial Integration

The World View-2 satellite data have a resolution of 46 centimetres (cm) whilst the DEM data has a resolution of approximately 25 m. Furthermore, the orientation of minor and intermediate topographic features as identified in the DEM can be ambiguous due to the resolution of the data, while these features could be drawn with high confidence from the World View-2 satellite data. Therefore, lineaments derived from the satellite data were used as the lead data set, and lineaments drawn from DEM data were used as the secondary data set.

A buffer of 125 m (five times the resolution of the DEM) was generated around the DEM lineaments and the satellite lineaments were overlain on top of this buffer. Similar to the procedure in RA_1, all lineaments that occurred within overlapping buffers were carried forward and copied into a new file. These lineaments were attributed with a RA_2 coincidence value of two (RA_2; Table 4). The remaining satellite and DEM lineaments were then manually analyzed by both interpreters on the basis of the available imagery for each data set. In some instances, this included adapting the shape and extent of individual lineaments to increase the accuracy of spatial location or length of the lineament. These lineaments were attributed a RA_2 value of one in the attribute table (RA_2; Table 4).

Final Integration

The geophysical data supplies important information about structures in the subsurface. Therefore, for this step of the interpretation, the lineaments derived from geophysical data were given precedence over lineaments derived from surficial data, since the latter only provide information about the surface expression of structures.

On this premise, all lineaments derived from the magnetic data were included in the final interpretation. A buffer of 125 m (five times the resolution of the geophysical data and DEM) was generated around the integrated surficial lineaments, and the geophysical lineaments were overlain on top of this buffer. This buffer size was included as an attribute field for all interpreted lineaments (Buffer RA_2; Table 4). As part of this comparison, coincident lines were identified and attributed. Next, non-coincident lineaments were evaluated against the magnetic data by both interpreters, and if required, were adapted and carried forward to the final Step 3 data set. This resulted in a combined interpretation with lineaments derived from the magnetic and surficial data sets.

The following rules were applied for determining coincidence between the data set-specific lineament maps:

- If any coincidence of lineaments occurred between two lineament data sets, the longest lineament was carried forward to the Step 3 interpretation and attributed as derived from two (or more) data sets, regardless of the length of overlap between the lineaments. This meant that if any part of a lineament derived from one data set was identified in another data set, it was considered that this lineament was reproduced.
- In the case that a lineament derived from topographic or satellite imagery data was longer than a coincident lineament derived from geophysical data, the former lineament was cut and the non-coincident portion was carried forward into the final Step 3 interpretation as a single entity. Both the lineament in the geophysical data and the non-coincident portion derived from another data set were then attributed accordingly in terms of coincidence.
- A lineament derived from topographic and (or) satellite imagery data that would fall within the buffer of a lineament derived from geophysical data would be attributed as reproduced in the relevant data sets if the orientation of the lineaments did not deviate significantly.
- Short (less than 500 m) discontinuous topographic and satellite imagery data lineaments that are at low angles to geophysical data lineaments but extending outside the geophysical lineament buffer were considered to be coincident.
- Short (less than 500 m) topographic and satellite imagery data lineaments that are at high angles to geophysical data lineaments, largely overlapped with the buffer zone from the geophysical data lineament, and had no further continuity (i.e., singular elements), were not carried forward to the final interpretation. This was done on the basis that these short segments represent a subsidiary lineament that is related to a broader fault zone already included as a fault lineament in the final interpretation based on identification in the geophysical data.

During this process, each lineament was attributed with a text field highlighting in which data sets it was identified. The final coincidence value (RA_2; Table 4) was then calculated as the sum of the number of data sets in which each lineament was identified, i.e., a value of 1 to 3.

The resulting lineament interpretation, representing the integration of all data sets, was then evaluated and modified (within the limits of relevant buffers) in order to develop a final lineament interpretation that is consistent with the known structural history of the Schreiber region. This included defining the age relationships of the interpreted lineaments on the basis of cross-cutting relationships between different generations of fault lineaments and populating the attribute field for each lineament for the relative age (Rel_Age; Table 4). This incorporated a working knowledge of

the structural history of the Schreiber area, combined with an understanding of the lineament characteristics in each lineament population (e.g., brittle versus ductile). The structural history of the area is described in Section 2.4, based on the existing literature.

The interpreted crosscutting and age relationships between different families of fault lineaments and within individual families of fault lineaments were refined using the available data. Crosscutting relationships were evaluated based on the through-going nature and termination of fault lineaments and evaluated against the regional structural history as described in Section 2.4.

3.2.4 Lineament Length

Lineament lengths were calculated using a simple geometrical calculation of the total length of the polyline in ArcGIS.

The length distribution of the various integrated data sets was analyzed through a comparison of summary statistics, frequency histograms, log-log plots and boxplots. Histograms and summary statistics were computed using Microsoft Excel's Data Analysis add-in. Histogram bins were computed using arbitrary 500 m bins.

There is no information available on the depth extent into the bedrock of the lineaments interpreted for the Schreiber area. In the absence of available information, the interpreted length can be used as a proxy for the depth extent of the identified structures. However, this is highly dependent on the style and structural history of a given fault. A preliminary assumption may be that the longer interpreted lineaments in the Schreiber area may extend to greater depths than the shorter interpreted lineaments.

3.2.5 Lineament Trends

An analysis of lineament trends is an essential part of the structural lineament interpretation, as it allows the interpreter to identify different sets of structures and to relate those sets to the known structural history of the area. Lineament orientations were assessed for each data set within Block (A) and Block (B) in the Schreiber area to determine the dominant lineament trends, and potential conjugate sets.

Lineament orientations (azimuth) were calculated using ET EasyCalculate 10, an add-in extension to ArcGIS. This add-in provides a function (polyline_GetAzimuth.cal) that calculates the azimuth of each polyline at a user-specified point and populates an assigned attribute field. SRK used the mid-point of each interpreted lineament to calculate the azimuth.

Rose diagrams are circular or semi-circular histograms that depict orientation (azimuthal) data and frequency for each data bin. The histogram peaks show the frequency of occurrence of lineament orientations within each bin. Rose diagrams were produced in Spheristat, with frequencies divided into 5° bins in order to avoid oversimplification of the lineament orientations. Lineament lengths are also used as a weight factor for computing rose diagrams that display the lineament trends.

3.2.6 Lineament Density

Analyses of lineament density were conducted for the Schreiber area. The lineament density analysis was conducted using the ArcGIS Analysis and Spatial Analyst toolsets, and included creating lineament density plots, lineament intersection points, and conducting an intersection point density analysis for the magnetic, surficial, and final integrated lineament data sets.

Lineament line density of all interpreted lineaments in the Schreiber area was determined by examining the statistical density of individual lineaments using ArcGIS Spatial Analyst. A grid cell size of 50 m and a search radius of 1.25 km (equivalent to half the size of the longest boundary of the minimum area size of a potential siting area) were used for this analysis. The spatial analysis used a circular search radius examining the lengths of polylines intersected within the circular search radius around each grid cell.

Lineament intersections were calculated using the ArcGIS Analysis Tools Intersect function. To improve visualization of the lineament intersection points, SRK gridded their density using the ArcGIS Spatial Analyst function. Spatial Analyst calculates point density conceptually by defining a neighbourhood around each raster cell centre, and the number of points that fall within the neighbourhood is totalled and divided by the area of the neighbourhood. A grid cell size of 50 m and a search radius of 1.25 km (equivalent to half the size of the longest boundary of the minimum area size of a potential siting area) were used.

4 Lineament Interpretation Results

The following sections describe the results of the lineament interpretation for the Schreiber area based on analysis of the geophysical and surficial (DEM, Satellite) data sets. This includes discussion of the RA_1 assessment of reproducibility. In addition, the RA_2 results are discussed for the integration of the two surficial data sets and for the final integration of the magnetic data set with the surficial data sets.

4.1 Geophysical Lineaments

An interpretation of magnetic data allows for the distinction between ductile, dyke, and brittle lineaments. Ductile features traced from the magnetic data set are shown on Figures A1, 7, 7a, 7b, and are interpreted as traces of the geometry of stratigraphy within the greenstone belts or the internal fabric (foliation) within plutonic and gneissic rocks. Discontinuities between ductile features highlight structures (potential fractures, and fold structures), unconformities, or intrusive contacts. Therefore, they constitute an essential data component that should be used along with the first vertical derivative of the magnetic data for interpreting brittle and dyke lineaments. Ductile features are included in this report to provide context to the lineament interpretation, but they were not included in the statistical analyses of the lineament data sets.

Within the Schreiber area a total of 497 geophysical lineaments were interpreted. These data comprise lineaments that were identified and merged by the two interpreters based on interpretation from the geophysical data (Figure 8). The geophysical lineaments range in length from 0.12 to 10.12 km, having a median length of 1.22 km and a mean length of 1.7 km. From the total number of geophysical lineaments, 462 were characterized by discrete linear magnetic lows and interpreted as brittle lineaments and 35 were characterized by discrete linear magnetic highs and interpreted as dyke lineaments. An example of both of these types of features can be seen in Figures A2 and A3. Figure A2 shows a series of northwest and east-southeast trending lineaments defined in geophysical data by linear magnetic lows. Figure A3 shows a series of northwest to northeast trending linear magnetic highs in the geophysical data interpreted as dykes. Azimuth data weighted by length for the interpreted geophysical lineaments display a dominant diffuse northwest (300-340°) trend, with subordinate west northwest (280-290°), north northeast (010-025°), and east-west (080-095°) trends (Figure 8 inset).

Of the total geophysical lineaments, the reproducibility assessment identified coincidence for 202 lineaments (41%; RA_1 = 2) and a lack of coincidence for 295 lineaments (59 %; RA_1 = 1). For dyke lineaments, the reproducibility assessment identified coincidence between interpreters for 17 lineaments (46 %; RA_1 = 2), and a lack of coincidence for 18 lineaments (54 %; RA_1 = 1). Of the 497 total lineaments interpreted, 145 (29 %) were assigned the highest level of certainty (three), while 245 (50 %) were assigned certainty values of two, and 107 (20 %) were assigned certainty values of one.

Block (A) includes a total of 259 geophysical lineaments (Figure 8a). Of these, 251 were interpreted as brittle lineaments and 8 were interpreted as dyke lineaments. The lengths of geophysical lineaments within this block have a range from 0.16 to 10.18 km, with a median length of 1.05 km and a mean length of 1.53 km. Of the 259 geophysical lineaments interpreted in Block (A), 88 (33 %) were assigned the highest level of certainty (three), while 135 (53 %) were assigned medium certainty, and the remaining 36 (14 %) were assigned lower certainty. Of the 8 dyke lineaments identified in Block (A), 4 (40 %) were assigned certainty values of three, and 4 (60 %) were assigned

certainty values of two. None of the dyke lineaments was assigned a certainty value of one. The assessment of reproducibility indicates that 113 (43 %; RA_1 = 2) of the geophysical lineaments in Block (A) are coincident between both interpreters, whereas the remaining 146 (57 %; RA_1 = 1) were identified by one interpreter only. Reproducibility of the dyke lineaments indicate that no dyke lineaments were coincident between both interpreters, with all dyke lineaments being interpreted by a single interpreter only (100 %; RA_1=1). Azimuth data weighted by length for the geophysical lineaments interpreted in Block (A) exhibit a broad spread of trend orientations between 290° and 335°, with the most frequent orientation between 300° and 305° and a second frequent orientation between 325° and 335° (Figure 8a inset). Also, within this block the interpreted dyke lineaments show three discrete trends towards 330-335°, 000-010°, and 020-035°.

Block (B) includes a total of 238 geophysical lineaments (Figure 8b). Of these, 211 were interpreted as brittle lineaments and 27 were interpreted as dyke lineaments. These lineaments show a range in length from 0.12 to 9.85 km, with a median of 1.34 km and a mean of 1.88 km. Of the 238 lineaments interpreted in Block (B), 57 (24 %) were assigned the highest level of certainty (three), while 110 (46 %) were assigned medium certainty, and 71 (30 %) were assigned a lower certainty level. Of the dyke lineaments, 20 (74 %) of them were assigned the highest certainty value (three); whereas two lineaments (7 %) were attributed medium certainty, and five lineaments (18 %) were assigned a lower certainty. The assessment of reproducibility indicates that 89 (37 %; RA_1 = 2) of the geophysical lineaments within Block (B) are coincident between both interpreters, whereas the remaining 149 (63 %; RA_1 = 1) were identified by one interpreter. Reproducibility of the dyke lineaments indicate that 17 dyke lineaments (63%; RA_1=2) were coincident between both interpreters, with the remaining 10 (37 %; RA_1=1) dyke lineaments being interpreted by a single interpreter only. Azimuth data weighted by length for the geophysical lineaments interpreted in Block (B) exhibit a broad spread of orientations between 280 and 355°, with the greatest frequency in the 290 to 295° bin (Figure 8b inset). Within this block the 27 lineaments identified as dykes occur along one main trend of roughly 015° to 030°, and secondary 305° to 315° trend. In many instances, the northwest-trending lineaments cause breaks in west-northwest lineaments but do not show a clear offset (Figure 8, and Appendix Figures A9 and A10). An example of this can be seen in Block (B) at approximately 469505 mE 5421158 mN.

4.2 Surficial Lineaments

Surficial lineaments include lineaments interpreted from the DEM topography and satellite imagery data sets, and are each shown on Figures 9 and 10, respectively. An overview of the lineament interpretation based on these surface-based data sets is provided below.

4.2.1 DEM lineaments

A total of 958 lineaments were integrated based on lineaments identified from the DEM topography data by the two interpreters (Figure 9). Lineaments interpreted along sharp changes in topography in the DEM data are shown in Figure A2b. The DEM lineaments show a range in length from 0.08 to 9.74 km, with a median length of 0.73 km, and a mean length of 1.09 km. Of the 958 interpreted lineaments, 407 (42 %) were assigned the highest level of certainty (three), while 377 (39 %) were assigned certainty values of two, and 174 (18 %) were assigned certainty values of one. An assessment of reproducibility showed that of the total lineaments, 434 (45 %; RA_1 = 2) of the lineaments were coincident between two interpreters, and 524 lineaments (55 %; RA_1 = 1) were not coincident. Dyke lineaments were not interpreted in this data set. Azimuth data weighted by length for all DEM lineaments exhibit a broad diffuse northwest to north trend (290° to 005°; Figure 9 inset).

Block (A) includes a total of 479 DEM lineaments (Figure 9a). The length of DEM lineaments in Block (A) ranges from 0.14 to 9.11 km, with a median of 0.81 km, and a mean of 1.11 km. Of the 479 lineaments interpreted in this block, 202 (42 %) were assigned the highest level of certainty (three), with 209 (44 %) being assigned medium certainty, and 68 (14 %) assigned a lower certainty. The assessment of reproducibility for DEM lineaments identified in Block (A) showed that 218 (46 %; RA_1 = 2) lineaments have coincidence between the two interpreters, and that the remaining 261 (54 %; RA_1 = 2) lineaments were interpreted by a single interpreter only. Azimuth data weighted by length for the DEM lineaments interpreted in Block (A) exhibit a spread of data between 305° and 335°, with the most frequent orientation in the 310° to 315° bin. An additional data peak is present between 345° to 005° (Figure 9a inset).

Block (B) shows a total of 479 DEM lineaments (Figure 9b). The lengths of these lineaments range from 0.08 to 9.74 km, with a median length of 0.64 km, and a mean length of 1.06 km. Of the 479 lineaments interpreted in this block, 205 (43 %) were assigned the highest level of certainty (three), while 168 (35 %) were assigned a medium certainty, and 106 (22 %) were assigned a lower certainty. The reproducibility assessment for DEM lineaments identified in Block (B) shows coincidence for 216 (45 %; RA_1 = 1) lineaments between two interpreters, and a lack of coincidence for 263 (55 %; RA_1 = 1) of the total lineaments. Azimuth data weighted by length for the DEM lineaments interpreted in Block (B) exhibit a broad spread of orientations between 290° and 355° with the most prominent orientations in the 330° to 335° bin (Figure 9b inset).

4.2.2 Satellite Imagery Lineaments

A total of 986 lineaments were identified by the two interpreters from the satellite imagery data (Figure 10). Lineaments interpreted along linear streams and chains of lakes, and subtle variations in vegetation in the satellite imagery are shown in Figure A2c. Satellite lineaments show a range in length from 0.10 km to 10.1 km, with a median length of 0.8 km, and a mean length of 0.54 km. Of the 986 interpreted lineaments, 397 (40 %) were assigned the highest level of certainty (three), while 289 (30 %) were assigned certainty values of two, and 300 (30 %) were assigned certainty values of one. The reproducibility assessment identified coincidence between the two interpreters for 436 (44%; RA_1 = 2) lineaments, with the remaining 550 (56 %; RA_1 = 1) lineaments being identified by a single interpreter. Dyke lineaments were not interpreted in the satellite data set. Azimuth data weighted by length for all satellite lineaments exhibit a spread of data with peaks in the 270° to 275° and 285° to 290° bins (Figure 10 inset).

Block (A) includes a total of 504 satellite lineaments (Figure 10a). The lengths of the interpreted satellite lineaments range from 0.12 to 9.09 km long, with a median length of 0.80 m, and a mean length of 1.08 m. Of the satellite lineaments in Block (A), 202 (40 %) were assigned the highest level of certainty (three), 156 (31 %) were assigned medium certainty values, and 146 (29 %) were assigned a lower certainty. The reproducibility assessment identified coincidence between the two interpreters for 203 (40 %; RA_1 = 2) lineaments, with the remaining 301 (60 %; RA_1 = 2) lineaments being identified by a single interpreter only. Azimuth data weighted by length for the satellite lineaments interpreted in Block (A) exhibit a broad spread of orientations dominating from 270° to 340°, and more frequently, 020° to 085° (Figure 10a inset).

Within Block (B), a total of 482 satellite lineaments were identified (Figure 10b). The lengths of the interpreted satellite lineaments range from 0.10 km to 10.10 km, with a median length of 0.78 km, and a mean length of 1.10 km. The highest certainty value was attributed to 195 (40 %) of the satellite-based lineaments, while 133 (28 %) were assigned medium certainty, and the remaining 154 (32 %) were assigned lower certainty. An assessment of the reproducibility shows that 233 (48 %; RA_1 = 1) lineaments coincide well between the two interpreters, with the remaining 249 (52 %; RA_1 = 1) lineaments being identified by a single interpreter only. Azimuth data weighted by length

for the satellite lineaments interpreted in Block (B) exhibit a single dominant orientation in the 285° to 290° bin (Figure 10b inset).

4.3 Integrated Surficial Lineaments (RA_2)

The lineaments interpreted based on DEM and satellite imagery data were integrated to form the surficial lineament data set. This integration resulted in a total of 1,472 surficial lineaments (Figure 11).

The merging of lineaments interpreted based on DEM and satellite imagery resulted in lineaments of new lengths. Overall, lineaments interpreted from the satellite data are shorter compared to those interpreted from the DEM data. As a result, lineaments interpreted from both DEM and satellite data are longer than lineaments interpreted from a single surficial data set. The lengths of all surficial lineaments range from 0.09 to 10.4 km, with a median length of 0.596 km, and a mean length of 0.874 km.

Of the 1,472 lineaments, 654 (44 %) were assigned the highest level of certainty (three), while 513 (35 %) were assigned certainty values of two, and 305 (21 %) were assigned certainty values of one. The coincidence assessment between lineaments interpreted from the two surficial data sets identified coincidence for 670 (45 %) lineaments and a lack of coincidence for 802 (55 %) of the total integrated surficial lineaments. Azimuth data weighted by length for the integrated surficial lineaments exhibit a spread of data with the highest frequency in the 305° to 325° bins (Figure 11 inset).

Within Block (A) a total of 766 surficial lineaments were interpreted (Figure 11a). Their lengths range from 0.09 to 9.12 km, with a median length of 0.66 km, and a mean length of 0.96 km. Of the 767 surficial lineaments, 338 (44 %) were assigned the highest level of certainty (three), while 285 (37 %) were assigned certainty values of two, and 143 (19 %) were assigned certainty values of one. The coincidence assessment for Block (A) identified coincidence between the two surficial data sets for 320 (42 %) lineaments, with the remaining 446 (58 %) lineaments being identified in a single data set only. Azimuth data weighted by length for the integrated surficial lineaments interpreted in Block (A) exhibit a broad spread of orientations ranging from 300 to 080° with the highest frequency of lineaments within the 300° to 335° range (Figure 11a inset).

Within Block (B) a total of 706 surficial lineaments were interpreted (Figure 11b). Their lengths range from 0.1 to 10.42 km, with a median length of 0.6 km, and a mean length of 0.99 km. The highest certainty values were assigned to 316 (45 %) of the surficial lineaments, while 228 (32 %) were assigned medium certainty values, and 162 (23%) were assigned lower certainty values. The coincidence assessment for Block (B) identified coincidence between the two surficial data sets for 350 (50 %) lineaments, with the remaining 356 (50 %) lineaments being identified in a single data set only. Azimuth data weighted by length for the integrated surficial lineaments interpreted in Block (B) exhibit a spread of orientations from 270 to 340° with the highest frequency of lineaments oriented between 290° and 305° (Figure 11b inset).

4.4 Integrated Final Lineaments (RA_2)

The integrated lineament data set produced by merging all lineaments interpreted from the geophysical (Figures 12, 12a, 12b) and surficial (DEM and satellite imagery, Figures 11, 11a, 11b) data is presented on Figure 13.

The integrated lineament data set contains a total of 1,493 lineaments (including 1,458 brittle and 35 dyke lineaments). The length of all lineaments ranges from 0.11 to 10.17 km, with a median of 0.74 km and a mean of 1.11 km. Of all integrated lineaments, 25 lineaments are greater than 5 km in length (2 %), 111 lineaments are between 2.5 and 5 km in length (7 %), 409 lineaments are between 1 and 2.5 km in length (27 %), and 948 lineaments are less than 1 km in length (64 %).

Of the 1,493 integrated lineaments, 616 (41 %) were assigned the highest level of certainty (three), while 597 (40 %) were assigned certainty values of two, and 280 (19 %) were assigned certainty values of one. The coincidence assessment identified coincidence in all three data sets (RA_2 = 3) for 206 (14 %) lineaments, and 359 (24 %) lineaments were coincident with a lineament from one other data set (RA_2 = 2). A total of 928 (62 %) lineaments were not coincident with any other data set (RA_2 = 1). Furthermore, a total of 327 lineaments observed in magnetic data were coincident with an interpreted surficial lineament (represents 66 % of all geophysical lineaments). Azimuth data for the integrated lineament data set exhibit a dominant diffuse northwest trend (Figure 13 inset).

Within Block (A), the integrated lineament data set contains a total of 769 lineaments (Figure 13a). They have a length range of 0.11 to 10.17 km, with a median length of 0.78 km and a mean length of 1.10 km. Of all integrated lineaments within Block (A), 9 lineaments are greater than 5 km in length (1 %), 53 lineaments are between 2.5 and 5 km in length (7 %), 236 lineaments are between 1 and 2.5 km in length (31 %), and 471 lineaments are less than 1 km in length (61 %). Of the 769 integrated lineaments identified in Block (A), 334 (44 %) were assigned the highest level of certainty (three), while 322 (42 %) were assigned certainty values of two, and 113 (15 %) were assigned certainty values of one. The coincidence assessment identified coincidence in all three data sets (RA_2 = 3) for 103 (13 %) lineaments, and 187 (24 %) lineaments were coincident with a lineament from one other data set (RA_2 = 2). A total of 479 (63 %) lineaments were not coincident with any other data set (RA_2 = 1). Azimuth data weighted by length for the integrated final lineaments in Block (A) exhibit a diffuse northwest trend with the highest frequency of lineaments in the 300° to 335° bins (Figure 13a inset).

Within Block (B), the integrated lineament data set contains a total of 724 lineaments (Figure 13b). They have a length range of 0.11 to 9.79 km, with a median length of 0.70 km, and a mean length of 1.13 km. Of all integrated lineaments within Block (B), 16 lineaments are greater than 5 km in length (2 %), 58 lineaments are between 2.5 and 5 km in length (8 %), 174 lineaments are between 1 and 2.5 km in length (24 %), and 476 lineaments are less than 1 km in length (66 %). Of the 724 integrated lineaments identified in Block (B), 282 (39 %) were assigned the highest level of certainty (three), while 275 (38 %) were assigned certainty values of two, and 167 (23 %) were assigned certainty values of one. The coincidence assessment identified coincidence in all three data sets (RA_2 = 3) for 103 (14 %) lineaments, and 172 (24 %) lineaments were coincident with a lineament from one other data set (RA_2 = 2). A total of 449 (62 %) lineaments were not coincident with any other data set (RA_2 = 1). Azimuth data weighted by length for the integrated final lineaments in Block (B) exhibit a diffuse northwest trend with the highest frequency of lineaments in the 275° to 320° bins (Figure 13b inset).

5 Discussion

Lineament reproducibility, lineament trend, lineament length and the density of lineaments and their intersections are discussed below. In addition, the integration of the final lineament data set into the regional structural history and the relative age of lineament sets in the Schreiber area are discussed.

5.1 Lineament Reproducibility (RA_1) and Coincidence (RA_2)

Lineament reproducibility and coincidence are assessed in several steps during the analysis. First, the two individual interpretations for each data set are integrated to produce single data set specific RA_1 interpretations. Secondly, the individual data set interpretations are integrated to produce the final RA_2 data set. Reproducibility and coincidence values are presented in detail in Section 4.

The RA_1 data presented in Section 4 indicate a moderate reproducibility between interpreters for all three data sets. Reproducibility between interpreters is comparable for all data sets with between 41 and 45 % of total lineaments in each data set identified by both interpreters. Differences in the individual lineament interpretations from each interpreter for the same data set can be attributed to the judgement and subjectivity of the expert carrying out the interpretation. The total number of lineaments identified in the DEM and satellite data was similar (958 and 986, respectively) despite the differences in resolution for the data sets. This may be due to the variable topography in the Schreiber area, which enhances the ability to identify lineaments using DEM data. In contrast, fewer total lineaments were identified in the magnetic data set (497). To evaluate differences between features identified in the various data sets, coincidence assessment (RA_2) was carried out. Coincidence values between data sets (RA_2) may provide a measure of the confidence in the interpretation and may also highlight significance bedrock structures expressed in these different data sets.

Despite their similar total number of lineaments, only 45% of the total integrated surficial lineaments are coincident in both DEM and satellite imagery data (Section 4.3). Lack of lineament coincidence in the two surficial data sets may be attributed to structures observed in the DEM data that are obscured by vegetation and other surficial elements in the satellite data. Furthermore, the high resolution of the satellite imagery allowed for the interpretation of lineaments in areas of low resolution DEM data. Where coincidence occurs in the two surficial data sets, it is assumed to represent surficial expressions of the same bedrock feature. This can occur for example when a lineament drawn along a stream channel shown on the satellite imagery is coincident with a lineament that captures the trend of the associated topographic valley expressed in the digital elevation data.

Approximately 66% of all the geophysical lineaments interpreted were coincident with an interpreted surficial lineament (Section 4.4). Lack of coincidence between some geophysical and surficial lineaments may be the result of various factors such as: deep structures that are identified in the magnetic data may not have a surface expression; surficial features may not extend to great depth; certain structural features identified in the surficial data may not possess sufficient magnetic susceptibility contrast to be recognized in the magnetic data; and surface expressions of geophysical lineaments may be masked by the presence of overburden. An example of this is in the area around Bath Lake in Block (A), where low magnetic susceptibility only allows for identification of northwest trending structures while interpretation of the surficial data identifies a complex network of crosscutting structures (approximate location of this observation is at 466562 mE, 5427352 mN (NAD 83, UTM zone 16N)). Therefore, it is necessary to objectively analyze the results of the RA_2

assessment with the understanding that RA_2 = 1 does not necessarily imply a low degree of confidence that the specified lineament represents a true structural feature.

Examining coincidence values indicate that the most reproducible lineaments are typically long lineaments, occasionally extending throughout the entire assessment areas, and typically northwest trending. In the magnetic data, these lineaments are typically characterized by continuous magnetic lows, or by multiple breaks in the magnetic grain defining a continuous lineament. In surficial data, these lineaments are typically characterized by a combination of continuous sharp breaks in topography, vegetation and bedrock, elongated lakes, and relatively linear streams.

5.2 Lineament Trends

Length weighted lineament trends within the Schreiber area provide strong indication of sets of structures with preferred azimuths. An analysis of lineament orientations reveal an overall consistency between the orientations of lineaments identified in the various different data sets, which suggests that lineaments interpreted from all three data sets are identifying the same sets of structures. However, it should be noted that lineaments identified in the satellite imagery are typically west-northwest trending, while lineaments identified in the DEM data set are typically northwest trending. The greater number of west-northwest trending lineaments identified in the satellite data appears to be due to lineaments being defined by breaks in vegetation, in addition to the trends of elongated lakes and streams, while lineaments defined in the DEM data are exclusively defined by breaks in topography. Similar subtle differences occur between surficial lineament orientations within the Crossman Lake batholith in Block (A) and Block (B). Within Block (A), surficial lineaments are commonly northwest trending, with minor north and northeast trends also evident. In Block (B) surficial lineament orientations are dominantly northwest and west northwest trending, with the minor north and northeast trends less pronounced. Figure A4 summarizes the orientation of lineaments for all data sets.

Lineament trends observed in the magnetic data set show a wide spread of orientations trending towards the west-northwest to northwest directions, with evidence of minor but discrete peaks trending north-northeast and east-northeast (Figures 8, 12, and A3). The northwest oriented lineaments exhibit the same range in orientations as the Ross Lake, and Sox Creek faults, while the northeast oriented lineaments exhibit the same range in orientations as the Syenite Lake fault (Figure 12). In addition, the north trending lineaments are sub-parallel to mapped north trending faults such as the unnamed fault at the western margin of Block (B). However, the corresponding north trending lineament at the western margin of Block (B), interpreted from the geophysical data, is interpreted to be segmented by northwest trending faults that have not been mapped.

The surficial lineament trends tend to exhibit a similar broad northwesterly trend as observed in the geophysical lineaments, in addition to a minor east-northeast trend that is more pronounced than in the magnetic data. No dykes were recorded in the surficial lineament interpretation, however the northeast trend observed in the surficial data appears to be sub-parallel to the trend of the Marathon dyke swarm, in addition to being sub-parallel to the mapped Syenite Lake Fault. An example of this can be seen at approximately 487894 mE, 5420532 mN (NAD83, UTM zone 16N), where short segmented lineaments observed in the DEM data set are parallel to a northeast trending dyke observed in the geophysics data set. This observation suggests the existence of a set of potential structures that parallels the dyke lineaments. In addition, numerous surficial lineaments are proximal and parallel to a northwest trending mapped fault in the northern part of Block (B). Although, this mapped fault is defined as a single through-going structure, the surficial lineaments may define a more complex anastomosing network of structures along the same trend.

As expected, the integrated lineaments exhibit similar trends (northwest trend, with subordinate north and northeast trends) as seen in the magnetic and surficial data sets.

5.2.1 Relationship between Lineament Trends and Regional Stress Field

The principal neotectonic stress orientation in central North America is generally oriented approximately east-northeast (63° ± 28°; Zoback, 1992), although anomalous stress orientations have also been reported in the mid-continent that include a 90-degree change in azimuth of the maximum compressive stress axis (Brown et al. 1995) and a north-south maximum horizontal compressive stress (Haimson, 1990). Local variations, and other potential complicating factors involved in characterizing crustal stresses, including the effect of shear stress by mantle flow at the base of the lithosphere (Bokelmann, 2002; Bokelmann and Silver, 2002), the degree of coupling between the North American plate and the underlying mantle (Forte et al., 2010), the effects of crustal depression and Holocene rebound, and the influence of the thick lithospheric mantle root under the Canadian Shield, make it premature to correlate the regional neotectonic stress orientation with the orientation of interpreted lineaments.

However, it is possible to broadly speculate on the potential behavior of the identified lineaments if they were to be reactivated by the regional east-northeaster neotectonic stress regime. Roughly four orientations of lineaments were interpreted: northwest, west northwest to east-west, north, and northeast. Should the identified lineaments be reactivated under the current stress regime, the northwest oriented lineaments would likely reactivate as reverse dip-slip to oblique-slip faults, the west-northwest- and north-oriented lineaments would likely reactivate as oblique-slip faults, and the northeast-oriented lineaments would likely reactivate as normal dip-slip to oblique-slip faults. This would imply that the northwest, west-northwest and north lineaments would be reactivated under shear stress and northeast lineaments would be reactivated under tensile stress. It is also possible that under the current stress regime, northwest and northeast oriented lineaments could simultaneously reactivate as conjugate sets of structures.

5.3 Lineament Length

Interpreted geophysical (RA_1), surficial (RA_2) and final integrated (RA_2) lineaments classified by length are presented in Figures 14 and 15 (geophysical lineaments by length), Figures 16 and 17 (surficial lineaments by length), and Figures 18 and 19 (final integrated lineaments by length). Statistical analysis of the lineament lengths, including box-plots, cumulative log-log plots, and histograms of the geophysical, surficial, and final integrated lineaments graphically display the distribution of lineament length for each data set (shown on Figures 14 to 19, and Figures A5 and A6). It is important to keep in mind that the reported lengths may not necessarily reflect the full length of the lineament. Lineaments were traced within the assessment areas and could extend beyond its borders.

Evaluating lineament lengths within the assessment area reveal that a correlation exists between lineament length and RA_1 for all data sets. In both Block (A) and Block (B), a significantly greater number of geophysical, DEM, and satellite imagery lineaments, longer than 2.5 km showed coincidence between the two interpreters than did not. The same correlation was observed in the merged surficial and final data sets. In addition, the average and median lengths of surficial lineaments identified by both interpreters (RA_1 = 2) are 1.43 and 0.98 km, respectively, whilst the average and median lengths of surficial lineament identified by a single interpreter (RA_1 = 1) are 0.76 and 0.54 km, respectively. The same applies for the integrated geophysical data, whereby the average and median lengths of geophysical lineaments identified by both interpreters (RA_1 = 2) are 2.42 and 1.84 km, respectively, whist the average and median lengths of geophysical lineaments identified by a single interpreter (RA_1 = 1) are 1.20 and 0.92 km, respectively.

The histograms and cumulative log-log plots for the lineament data sets show that length ranges are generally similar between the different data sets and skewed towards shorter lineaments (Figure A5 and A6). The histograms and cumulative log-log plots for the integrated geophysical, surficial and final lineament data sets show that the surficial lineaments comprise a greater number of lineaments less than 1 km in length, compared to the geophysical and final integrated lineament data sets.

The box-plot results show that the geophysical lineaments have a significantly broader length range compared to the DEM and satellite lineaments (Figures A5 and A6). In general, the geophysical lineaments tend to be more continuous, resulting in longer lineaments in the Schreiber area. The longer length is most likely due to the geophysical lineaments typically being characterized by continuous linear magnetic lows or highs, or by multiple breaks in the magnetic grain defining a continuous lineament. Conversely, surficial lineaments in the Schreiber area are typically characterized by a combination of breaks in topography, vegetation and bedrock, and elongated lakes. These surficial features tend not to be as continuous as the magnetic features, resulting in the interpretation of shorter surficial lineaments relative to the geophysical lineaments.

The results indicate that lineaments that are identified in all data sets (i.e. RA_2 = 3) have mean length of 2.3 km with a median length of 1.73 km. These values are significantly greater than the mean and median lengths from each individual data set. This indicates that the most reproducible lineaments are typically longer, and may extend throughout an entire block. The long lineament lengths observed in the final data set is to be expected, as this data set resulted from the integration of the geophysical and surficial data sets. During this process, the most continuous lineaments, which are typically attributed with a high certainty, and were often coincident with portions of other lineaments observed in the other data sets. Integrating these lineaments resulted in even longer continuous lineaments.

Examining the final integrated lineaments per bin size reveals a small percentage of the lineaments are greater than 5 km (2 %), and between 2.5 and 5 km (7 %). A higher percentage of lineaments have lineament lengths between 1 and 2.5 km (27 %), and less than 1 km (64 %). Although there are some differences in length statistics observed between the two blocks; their differences are minor. In Block (A), a small fraction of the lineaments have lengths that are greater than 5 km (1%) or range between 2.5 and 5 km (7 %). In this block, upwards of 31 % of lineaments are between 1 and 2.5 km, with 61 % of lineaments with lengths less than 1 km. Similarly, in Block (B), only 2 % of lineaments have lengths that are greater than 5 km, and 8 % of lineaments have lengths between 2.5 and 5 km. The majority of the lineaments have lengths that range between 1 and 2.5 km (24 %), and less than 1 km (66 %). Overall, the longer lineaments trend predominantly northwest, and the shorter lineaments trend predominantly north (Figures 18 and 19).

Although there is no information available on the depth extent of the lineaments interpreted for the Schreiber area; the length information described above can be used as a proxy for the depth extent of the identified structures. Therefore, a preliminary assumption may be that the longer interpreted lineaments in the Schreiber area may extend to greater depths than the shorter interpreted lineaments.

5.4 Density

Analyses of lineament and intersection density were conducted for the two surveyed blocks (Block (A) and (B)) in the Schreiber area, as described in Section 3.2.6.

5.4.1 Lineament Density

Even though the density of interpreted lineaments is relatively uniform in the Schreiber area, some variations are noted within the Crossman Lake batholith. Lineament density is discussed for each data set below. It should also be noted that since interpreted lineaments are only traced to the margins of the Phase 2 assessment area, there will in many cases be a border of apparent low lineament density around the margins of both Block (A) and Block (B).

In general, the geophysical lineament densities observed in Block (A) and Block (B) show a similar uniform lineament density, with some areas showing decreased density (Figures 20 and 21). The highest geophysical lineament density within Block (A) is located in the eastern half of the block (Figure 20). The zones of relatively high density appear to be associated with the east margin of the Crossman Lake batholith in the area, where a greater number of lineaments are sub-parallel to, and define the batholith margin. In addition, a relatively higher density of lineaments is present in the southeast corner of the block, where a large northwest trending fault zone intersects the Crossman Lake batholith (Figure 2). An area of relatively lower lineament density occurs in the northwest portion of the block (Figure 20). The lower density area is associated with spacing between lineaments in the range of 1 km in the area around Bath Lake. This lower density area, however, may simply be related to the high topographic variability and its effect on airborne acquisition of magnetic data. As a result, there is some uncertainty in the calculated geophysical lineament density in this area.

The geophysical lineaments within Block (B) show a uniform density throughout in the eastern portion of the Crossman Lake batholith (Figure 21). The highest lineament density in Block (B) occurs in the central area of the block, proximal to Guy Lake. This zone of high lineament density is immediately south of a major northwest trending fault zone that extends across the entire block (Figure 2). The lowest lineament density occurs immediately southwest of the zone of highest lineament density, and north/northwest of Robbie Lake.

The integrated surficial lineament density is generally uniform throughout the Schreiber area (Figures 22 and 23), however there are some differences compared to the geophysical lineament density. Surficial lineaments interpreted in Block (A) are relatively high due to the use of high-resolution satellite imagery and extensive bedrock exposure, which makes surficial lineaments readily interpretable (Figure 22). This is particularly evident in the east half of the block, proximal to the margin of the Crossman Lake Batholith. The highest density areas in Block (A) are associated with very tight lineament spacing, whereas lower density areas, for example, southeast of Beavertrap Lake, exhibit slightly wider average lineament spacing.

Similarly, surficial lineaments in Block (B) show a generally uniform density, with some local variation (Figure 23). The highest density areas in Block (B) are located towards the north of the block, near Guy Lake, and proximal to a major northwest trending fault zone that extends across the entire block (Figure 2). An additional zone of relatively higher lineament density occurs towards the southeast part of the block, near Spoke Lake, and is associated with the intersection of a series of laterally extensive northwest and north trending faults near the margin of the Schreiber – Hemlo Greenstone Belt (Figure 2). The lower density areas occur in the centre of the block, northeast of Leader Lake. These areas' lineaments exhibit slightly wider lineament spacings.

The final integrated lineament density shows a similar distribution as the magnetic and surficial lineament density throughout the Schreiber area (Figures 24 and 25). In Block (A), slightly lower densities occur southeast of Beavertrap Lake and around Bath Lake (Figure 24) and the areas of highest density are associated with the eastern margin of the Crossman lake batholith, and in the southeast corner of the block. In Block (B), the lineament density is generally uniform throughout

(Figure 25). Similar to the geophysical and surficial lineament density, the areas of highest density in Block (B) are located in the north of the block where the major fault zone crosscuts the block, and towards the southeast of the block, near the margin of the Schreiber – Hemlo Greenstone Belt, while the lowest density occurs northeast of Leader Lake (Figure 25).

5.4.2 Intersection Density

The distribution of lineament intersections within the two survey blocks in the Schreiber area was analyzed. Similar to the lineament density, the intersection density is relatively uniform in the two surveyed blocks, with some spatial variability.

In general, the geophysical intersection densities observed in Block (A) and Block (B) is similar to the geophysical lineament density patterns with some minor differences. The geophysical intersection density within Block (A) is elevated in the area around Winston Lake and is located near the margin of the Crossman Lake batholiths (Figure 26). Further to the west, near Beavertrap and Bath lakes, the intersection density is relatively lower despite the area being transected by a number of lineaments (Figure 26). Around Beavertrap Lake and Bath Lake lineaments are predominantly northwest trending, which are only sporadically cross-cut by northeast trending lineaments, resulting in a lower intersection density. This area of low intersection density coincides with area of low magnetic intensity within the Crossman Lake batholith (SGL, 2015), as well as the area of lower geophysical lineament density described above. The intersections between geophysical lineaments within Block (B) show a relatively uniform density throughout, with several pockets of low intersection density (Figure 27).

Similar distributions are observed in the surficial intersection densities plots in Block (A) and Block (B) as were observed in the surficial lineament density plots. An area east of Beavertrap Lake in Block (A) exhibits a relatively lower intersection density that coincides with an area of lower lineament density, despite there being good bedrock exposure (Figure 28). In Block (B) the central portion of the block shows a slightly lower density (Figure 29) which also coincides with an area of lower lineament density.

The integrated lineament intersection densities are shown on Figures 30 and 31. Relatively lower lineament intersection densities occur near Beavertrap Lake and Bath Lake in Block (A) and throughout the central portion of Block (B). Overall, two general observations can be made between lineaments and their intersection densities. In particular, areas of lower lineament density are likely to result in lower intersection densities because there are fewer lineaments to intersect. In addition, areas that may have a higher number of lineaments, but all trending in the same orientation can also lead to lower intersection densities. This observation is apparent in the geophysical lineament densities near Bath Lake, where the lineaments are predominantly trending northwest. In this area there is a lack of cross-cutting lineaments, resulting in few intersections.

5.5 Lineament Truncation and Relative Age Relationships

The structural history of the Schreiber area, outlined in Section 2.4, provides a framework that may aid in constraining the relative age relationships of the interpreted bedrock lineaments. In summary, six main regionally distinguishable deformation episodes (D_1 to D_6) are inferred to have overprinted the bedrock geological units of the Schreiber area.

The D_1 to D_4 events produced F_1 isoclinal folds, and D_1 thrust faults, kilometre-scale F_2 asymmetric folds, mineral flattening and (or) elongation, a crenulation S_2 foliation, local D_3 S-C fabrics with a dextral sense of shear, F_4 kink folds, and D_4 small-scale faults. D_1 to D_4 is summarized as a protracted period of brittle-ductile deformation comprising elements of compression, and sinistral

and dextral transpression. D_1 to D_4 occurred between ca. 2.719 and ca. 2.679 Ga and may have partially overlapped with emplacement of the Crossman Lake batholith.

Two phases of post-D_4 brittle deformation are identified within the Schreiber area (Figure 32). D_5 produced a set of approximately east-west to west-northwest trending faults that are subparallel to the regional S_2 foliation. D_6 produced a set of approximately northwest to north, and northeast trending faults that typically display a dextral sense of shear, though locally may display a sinistral sense of shear that is particularly associated with south-trending faults (Figures A9 and A10). No estimates for the timing of D_5 or D_6 brittle deformation are present in literature.

Excluding dyke lineaments, the final integrated lineaments identified in the Schreiber area are interpreted to represent successive stages of brittle-ductile to brittle deformation. These lineaments can be classified into three main stages based on relative age and in accord with the structural history described above including (from oldest to youngest): 83 D_1-D_4 (brittle-ductile) lineaments; 311 D_5 (brittle) lineaments; and 1,064 D_6 (brittle) lineaments. Thirty-five dyke lineaments were also identified (Figure 32).

Of the 83 D_1-D_4 brittle-ductile lineaments, 65 are interpreted in Block (A) and 18 are interpreted in Block (B). In Block (A) the D_1-D_4 lineaments are typically curvilinear to arcuate shape at the northern and eastern margins of the Crossman Lake batholith (Figure A7). In Block (B) the D_1-D_4 lineaments are exclusively located in the southeast corner of the study area within the rocks of the Schreiber – Hemlo greenstone belt and trend approximately east-west (Figure A8). The sense of motion of the early brittle-ductile D_1-D_4 lineaments cannot be conclusively inferred from the lineament interpretations. However, literature suggests that the D_1-D_4 lineaments within the Schreiber – Hemlo greenstone belt (located in the southeast corner of Block (B)) were developed during a period of compression and transpression that varied from north to northwest directed, and south to southeast directed (as described in Section 2). In Block (A), the D_1-D_4 lineaments are located parallel to, and at the margins of the Crossman Lake batholith, and may be related to emplacement of the batholith (Figure A9). Since no D_1-D_4 lineaments crosscut the interior of the Crossman Lake batholith, this suggests that the batholith was emplaced during the waning stages of D_1-D_4 deformation.

The D_5 brittle lineaments have a dominantly east-west to west-northwest trend in both Blocks (A) and (B). The most continuous D_5 brittle lineaments have a complex geometry defined by pronounced, magnetic lows in the magnetic data set, and a series of narrow valleys and (or) streams in the surficial data sets. D_5 lineaments truncate D_1-D_4 brittle-ductile lineaments, and are typically observed to be truncated by D_6 lineaments. Locally, D_5 lineaments may offset minor D_6 lineaments, which is most likely attributed to fault reactivation during D_6. The sense of motion along D_5 lineaments is uncertain, however, where visible, a sinistral strike-separation is typically observed (Figure A9). The sinistral strike-separation suggests that D_5 lineaments may have formed as strike-slip faults, within a regional stress regime where the maximum principle stress may have been oriented northeast-southwest.

In both Block (A) and Block (B), the D_6 brittle lineaments have a dominantly southeast to south trend with sporadic, typically shorter, segmented northeast-trending lineaments. The northwest and northeast trending lineaments may form a conjugate pair. These lineaments truncate the D_1-D_4 brittle-ductile lineaments, and typically truncate or offset D_5 lineaments. The D_6 lineaments are interpreted to display both dextral and sinistral strike-separations (Figure A10).

5.5.1 Mapped Fault and Lineament Relationships

The bedrock geology shown in Figure 2 identified two unnamed and two named (Sox Creek and Ross Lake faults) northwest trending faults, one northeast-trending fault (Syenite Lake Fault), and two unnamed north trending faults in the Schreiber area that extend into the two blocks. These faults are interpreted as D_6 structures in Section 3.2 (Carter, 1998) (discussed above in Section 5.5 and shown in Figure 2, and overlain with the final interpreted lineaments classified by relative age in Figure 32). In, addition, one Matachewan-age dyke is identified in Block (A).

The lineament analysis interpreted a total of 1,493 brittle and dyke lineaments. It should be noted that all of the mapped (and named) faults shown on Figure 3 that intersect the two blocks were reproduced during the lineament analysis. Only the north trending unnamed fault towards the north of Block (B) was not identified during the lineament interpretation. All of the observed lineaments correlating with the mapped faults were interpreted in at least two of the data sets (RA_2 $\geq$ 2). The unnamed west-northwest trending faults toward the northwest of Block (A), and toward the north of Block (B), and the north trending fault near the western margin of Block (B) were observed in all data sets (RA_2 = 3), even though the traces of the observed lineaments may diverge slightly from the mapped faults. The west-northwest trending fault in the north of Block (B) shows evidence of dextrally offsets at the contact between the Crossman Lake batholith and the greenstone belt rocks. In addition, the magnetic data shows that two parallel north-northeast trending interpreted dyke lineaments are also offset dextrally across this same mapped unnamed fault. All but one of the mapped faults were assigned a certainty of three, with a small section of the Ross Lake Fault having a certainty of two.

The relationships between mapped faults and lineaments forms much of the basis for defining the lineament relative age relationships, as described in detail in Section 5.5 above.

6 Summary of Results

This report documents the source data, workflow, and results from a lineament interpretation of geophysical (magnetic) and surficial (satellite imagery, DEM topography) data sets acquired as part of Phase 2 Preliminary Assessment for two blocks in the Schreiber area. The lineament analysis provides an interpretation of the location and orientation of possible ductile, brittle and dyke lineaments on the basis of remotely sensed data, and helps to evaluate their relative timing relationships within the context of the regional geological setting. The workflow involves a three step process that was designed to address the issues of subjectivity and reproducibility. The distribution of lineaments in the Schreiber area reflects the bedrock structure, resolution of the data sets used, and surficial cover.

Within the Schreiber area, a total of 497 geophysical lineaments, 958 DEM lineaments, and 986 satellite lineaments were interpreted by the two interpreters (RA_1) from their respective data sets. Merging the lineaments derived from the DEM and satellite data resulted in a total of a 1,472 surficial lineaments (RA_2). Merging the surficial lineaments with those derived from the geophysical data resulted in a total of 1,493 final integrated lineaments (RA_2).

The findings from the RA_1 data integration reveal a moderate reproducibility between interpreters for all three data sets (i.e. 41 % to 45% lineaments in each data set were identified by both interpreters). The variability between interpreters could be attributed to the resolution of the data sets and the judgement and subjectivity of the expert carrying out the interpretation. In general, longer lineaments were identified more often by both interpreters. The findings from the RA_2 data integration reveal a moderate coincidence between lineaments interpreted from the three data sets (i.e. 38 % of lineaments were coincident in at least one other data set and 62 % of lineaments lacked coincidence with other data sets). The variability between lineaments derived from the different data sets could be attributed to multiple variables, including deep structures identified in the magnetic data that may not have a surface expression, surficial features that may not extend to depth, features identified in the surficial data that may not possess sufficient magnetic susceptibility contrast to be recognized in the magnetic data. Evaluating lineament lengths of the final integrated lineaments reveal that longer lineaments were identified more often in the various data sets.

An analysis of lineament orientations reveal an overall consistency between the orientations of lineaments identified in the various different data sets, which suggests that lineaments interpreted from all three data sets are identifying the same sets of structures. Examining all data sets reveal dominant northwest to west northwest trends, in addition to minor north and northeast trends. The northwest to west-northwest oriented lineaments define a pervasive regional brittle-ductile fabric.

Evaluation of lineaments by length revealed relatively few lineaments longer than 2.5 km (i.e. 9 % of lineaments are greater than 2.5 km) and 64% of lineaments are less than 1 km in length. Overall, the longer lineaments trend predominantly northwest, and the shorter lineaments trend predominantly north.

Analyzing lineament density provides insight on the distribution of bedrock structures. Overall lineament density is generally uniform throughout the Schreiber area, however some variations exist. In Block (A), slightly lower densities occur southeast of Beavertrap Lake and around Bath Lake. In Block (B), an area of relatively lower density occurs northeast of Leader Lake.

In Block (A) lower lineament densities are observed in an area of lower magnetic intensity around Bath Lake, and also southeast of Beavertrap Lake. Within Block (B) a lower lineament density zone is observed northwest of Leader Lake.

The final interpreted lineaments can be classified within the structural history into three successive stages of brittle-ductile and brittle deformation, including: 83 D_1-D_4 (ductile to brittle-ductile) lineaments; 331 D_5 (brittle) lineaments; and 1,064 D_6 (brittle) lineaments. Thirty-five dyke lineaments were also identified.

In Block (A) the D_1-D_4 lineaments typically are curvilinear to arcuate in shape, and occur at the northern and eastern margins of the Crossman Lake batholith. In Block (B) the D_1-D_4 lineaments are exclusively located in the southeast corner of the assessment area within the rocks of the Schreiber – Hemlo greenstone belt and trend approximately east-west. Across both areas, the D_5 brittle lineaments exhibit a dominant east-west orientation, and a minor west-northwest orientation. These lineaments are interpreted to truncate D_1-D_4 brittle-ductile lineaments, and are typically observed to be truncated or offset by D_6 lineaments. Locally, D_5 lineaements may offset minor D_6 lineaments. The D_6 brittle lineaments have a dominantly northwest trend with minor, typically shorter, segmented, north and northeast trending lineaments also observed. D_6 lineaments are interpreted to truncate D_1-D_4 brittle-ductile lineaments, and typically truncate or offset the D_5 lineaments. In many cases, D_6 lineaments display some evidence of both sinistral and dextral strike-separation.

7 References

AECOM (AECOM Canada Ltd.), 2013a. Phase 1 Geoscientific Desktop Preliminary Assessment of Potential Suitability for Siting a Deep Geological Repository for Canada's Used Nuclear Fuel, Township of Schreiber, Ontario. Prepared for Nuclear Waste Management Organization (NWMO). NWMO Report Number: APM-REP-06144-0035.

AECOM Canada Ltd., 2013b. Phase 1 Geoscientific Desktop Preliminary Assessment, Terrain and Remote Sensing Study, Township of Schreiber, Ontario. Prepared for Nuclear Waste Management Organization (NWMO). NWMO Report Number: APM-REP-06144-0036.

Barnett, P.J. 1992. Quaternary Geology of Ontario. *In* Geology of Ontario, Ontario Geological Survey, Special Volume 4, Part 2, p. 1010-1088.

Berman, R.G., Easton, R.M. and Nadeau, L. 2000. A New Tectonometamorphic Map of the Canadian Shield: Introduction; The Canadian Mineralogist, v. 38, p. 277-285.

Berman, R.G., Sanborn-Barrie, M., Stern, R.A. and Carson, C.J. 2005. Tectonometamorphism at *ca.* 2.35 and 1.85 Ga *in* the Rae Domain, western Churchill Province, Nunavut, Canada: Insights from Structural, Metamorphic and *in situ* Geochronological Analysis of the Southwestern Committee Bay Belt; The Canadian Mineralogist, v. 43, p. 409-442.

Bleeker, W. and Hall, B. 2007. The Slave Craton: Geology and Metallogenic Evolution; *In* Goodfellow, W.D., ed., Mineral Deposits of Canada: A Synthesis of Major Deposit-Types, District Metallogeny, the Evolution of Geological Provinces, and Exploration Methods: Geological Association of Canada, Mineral Deposits Division, Special Publication No. 5, p. 849-879.

Bokelmann, G.H.R. 2002. Which Forces Drive North America?, Geology, v.30, p.1027-1030.

Bokelmann, G.H.R. and Silver, P.G. 2002. Shear Stress at the Base of Shield Lithosphere. Geophysical Research Letters, v. 29, p.61-64.

Breaks, F.W. and Bond, W.D. 1993. The English River Subprovince – An Archean Gneiss Belt: Geology, Geochemistry and Associated Mineralization; Ontario Geological Survey, Open File Report 5846, v. 1, p. 483.

Brown, A., Everitt, R.A., Martin C.D. and Davison, C.C. 1995. Past and Future Fracturing in AECL Research Areas in the Superior Province of the Canadian Precambrian Shield, with Emphasis on the Lac Du Bonnet Batholith; Whiteshell Laboratories, Pinawa, Manitoba.

Buchan, K.L., Halls, H.C. and Mortensen, J.K. 1996. Paleomagnetism, U-Pb Geochronology, and Geochemistry of Marathon dykes, Superior Province, and Comparison with the Fort Frances Swarm. Canadian Journal of Earth Sciences, v. 33, p. 1583-1595.

Buchan, K.L. and Ernst, R.E. 2004. Diabase Dyke Swarms and Related Units in Canada and Adjacent Regions. Geological Survey of Canada, Map 2022A, scale 1:5,000,000.

Carter, M.W. 1988. Geology of Schreiber-Terrace Bay area, District of Thunder Bay. Ontario Geological Survey, Open File Report 5692, p. 287.

Corfu, F. and Muir, T.L. 1989. The Hemlo-Heron Bay Greenstone Belt and Hemlo Au-Mo Deposit, Superior Province, Ontario, Canada: 1. Sequence of Igneous Activity Determined by Zircon U-Pb Geochronology. Chemical Geology, v. 79, p. 183-200.

Corfu, F., Stott, G.M. and Breaks, F.W. 1995. U-Pb Geochronology and Evolution of the English River Subprovince, an Archean low P – high T Metasedimentary Belt in the Superior Province; Tectonics, v.14, p. 1220-1233.

Corfu, F. and Stott, G.M. 1996. Hf Isotopic Composition and Age Constraints on the Evolution of the Archean central Uchi Subprovince, Ontario, Canada; Precambrian Research, v.78, p. 53-63.

Corrigan, D., Galley, A.G. and Pehrsson, S. 2007. Tectonic Evolution and Metallogeny of the Southwestern Trans-Hudson Orogen, *in* Goodfellow, W.D., ed., Mineral Deposits of Canada: A Synthesis of Major Deposit-Types, District Metallogeny, the Evolution of Geological Provinces, and Exploration Methods: Geological Association of Canada, Mineral Deposits Division, Special Publication No. 5, p. 881-902.

Davis, D.W., and Lin, S. 2003. Unraveling the Geologic History of the Hemlo Archean Gold Deposit, Superior Province, Canada; a U–Pb Geochronological Study. Economic Geology and the Bulletin of the Society of Economic Geologists 98, p. 51-67.

Easton, R.M. 2000a. Metamorphism of the Canadian Shield, Ontario, Canada. I. The Superior Province; The Canadian Mineralogist, v. 38, p. 287-317.

Easton, R.M. 2000b. Metamorphism of the Canadian Shield, Ontario, Canada. II. Proterozoic metamorphic history; The Canadian Mineralogist, v. 38, p. 319-344.

Forte, A., Moucha, R., Simmons, N., Grand, S., and Mitrovica, J., 2010. Deep-mantle Contributions to the Surface Dynamics of the North American Continent. Tectonophysics, v. 481, p. 3–15

Fralick P., Davis, D.W. and Kissin, S.A. 2002. The age of the Gunflint Formation, Ontario, Canada: Single zircon U-Pb Age Determinations from Reworked Volcanic Ash. Canadian Journal of Earth Sciences, v.39, p. 1085-1091.

Fraser, J.A. and Heywood, W.W. (editors) 1978. Metamorphism in the Canadian Shield; Geological Survey of Canada, Paper, p. 78-10, 367.

Geofirma (Geofirma Engineering Ltd.), 2015. Phase 2 Geoscientific Preliminary Assessment, Findings from Initial Field Studies, Township of Schreiber, Ontario. Prepared for the Nuclear Waste Management Organization (NWMO), NWMO Report Number: APM-REP-06145-0005.

Golder (Golder Associates Ltd.), 2011. Initial Screening for Siting a Deep Geological Repository for Canada's Used Nuclear Fuel, Township of Schreiber, Ontario. Prepared for Nuclear Waste Management Organization (NWMO). Report Number: 10-1152-0110 (5000).

Haimson, B.C. 1990. Scale Effects in Rock Stress Measurements. In Proceedings international workshop on scale effects in rock masses, Loen, AA Balkema, Rotterdam, p.89-101.

Hamilton, M.A., David, D.W., Buchan, K.L. and Halls H.C. 2002. Precise U-Pb Dating of Reversely Magnetized Marathon Diabase Dykes and Implications for Emplacement of Giant Dyke Swarms along the Southern Margin of the Superior Province, Ontario. Geological Survey of Canada, Current Research 2002-F6, p. 10.

Jackson, S.L. 1998. Stratigraphy, Structure and Metamorphism; Part 1, p.1--58, in S.L. Jackson, G.P. Beakhouse and D.W. Davis, Geological Setting of the Hemlo Gold Deposit; an Interim Progress Report, Ontario Geological Survey, Open File Report 5977, p. 121.

Johnson, M. D., Armstrong, D.K., Sanford, B.V., Telford, P.G. and Rutka, M.A. 1992. Paleozoic and Mesozoic Geology of Ontario. *In* Geology of Ontario, Ontario Geological Survey, Special Volume 4, Part 2, p. 907-1008.

Jolly, W.T. 1978. Metamorphic history of the Archean Abitibi Belt; *In* Metamorphism in the Canadian Shield; Geological Survey of Canada, Paper 78-10, p. 63-78.

Kraus, J. and Menard, T. 1997. A Thermal Gradient at Constant Pressure: Implications for Low- to Medium-pressure Metamorphism in a Compressional Tectonic Setting, Flin Flon and Kisseynew Domains, Trans-Hudson Orogen, Central Canada; The Canadian Mineralogist, v. 35, p. 1117-1136.

Lin, S. 2001. Stratigraphic and Structural Setting of the Hemlo Gold Deposit, Ontario, Canada. Economic Geology, v. 96, p. 477-507.

Menard, T. and Gordon, T.M. 1997. Metamorphic P-T paths from the Eastern Flin Flon Belt and Kisseynew Domain, Snow Lake, Manitoba; The Canadian Mineralogist, v. 35, p. 1093-1115.

Morris, T.F. 2000. Quaternary Geology Mapping and Overburden Sampling, Area of Schreiber, Northwestern Ontario; *In* Summary of Field Work and Other Activities 2000, Ontario Geological Survey, Open File Report 6032, p. 33-1 to 33-7.

Muir, T.L. 2003. Structural Evolution of the Hemlo Greenstone Belt in the Vicinity of the World-Class Hemlo Gold Deposit. Canadian Journal of Earth Sciences, vol. 40, p. 395-430.

NWMO (Nuclear Waste Management Organization), 2010. Moving Forward Together: Process for Selecting a Site for Canada's Deep Geological Repository for Used Nuclear Fuel. Nuclear Waste Management Organization, May 2010.

NWMO (Nuclear Waste Management Organization), 2013. Preliminary Assessment for Siting a Deep Geological Repository for Canada`s Used Nuclear Fuel – Township of Schreiber, Ontario – Findings from Phase One Studies. NWMO Report Number APM-REP-06144-0033.

OGS (Ontario Geological Survey), 2011. 1:250 000 Scale Bedrock Geology of Ontario; Ontario Geological Survey, Miscellaneous Release–Data 126 - Revision 1.

Osmani, I.A., 1991. Proterozoic Mafic Dyke Swarms in the Superior Province of Ontario. *In* Geology of Ontario, Ontario Geological Survey, Special Volume 4, Part 1, p. 661-681.

Pease, V., Percival, J., Smithies, H., Stevens, G. and Van Kranendonk, M. 2008. When did Plate Tectonics begin? Evidence from the orogenic record; *In* Condie, K.C. and Pease, V., eds.,

When Did Plate Tectonics Begin on Earth?; Geological Society of America Special Paper 440, p. 199-228.

Percival, J.A., Sanborn-Barrie, M., Skulski, T., Stott, G.M., Helmstaedt, H. and White, D.J. 2006. Tectonic Evolution of the Western Superior Province from NATMAP and Lithoprobe Studies; Can. J. Earth Sciences v.43, p. 1085-1117.

Peterman, Z.E. and Day, W. 1989. Early Proterozoic activity on Archean faults in the Western Superior Province – Evidence from Pseudotachylite. Geology, vol. 17, p. 1089-1092.

Polat, A. and Kerrich, R. 1999. Formation of an Archean tectonic mélange in the Schreiber-Hemlo greenstone belt, Superior Province, Canada: Implications for Archean subduction-accretion process. Tectonics, v. 18, p. 733-755.

Polat, A., Kerrich, R. and Wyman, D.A. 1998. The late Archean Schreiber–Hemlo and White River–Dayohessarah Greenstone Belts, Superior Province: Collages of Oceanic Plateaus, Oceanic Arcs, and Subduction–Accretion Complexes. Tectonophysics, v. 289, p. 295-326.

Powell, W.G., Carmichael, D.M. and Hodgson, C.J. 1993. Thermobarometry in a Subgreenschist to Greenschist Transition in Metabasites of the Abitibi Greenstone Belt, Superior Province, Canada; J. Metamorphic Geology, v.11, p.165-178.

Santaguida, F. 2002. Precambrian Geology Compilation Series – Schreiber Sheet; Ontario Geological Survey, Map 2665-revised, scale 1:250,000.

SGL (Sander Geophysics Limited), 2015. Phase 2 Geoscientific Preliminary Assessment, Acquisition, Processing and Interpretation of High-Resolution Airborne Geophysical Data, Township of Schreiber, Ontario. Prepared for Nuclear Waste Management Organization (NWMO). NWMO Report Number: APM-REP-06145-0006.

Smyk, M.C. and Schnieders, B.R. 1995. Geology of the Schreiber Greenstone Assemblage and its Gold and Base Metal Mineralization. Institute on Lake Superior Geology 41st Annual Meeting, Proceedings Volume 41, Field Trip Guidebook, p. 86.

Sutcliffe, R.H. 1991. Proterozoic Geology of the Lake Superior Area; *In* Geology of Ontario, Ontario Geological Survey, Special Volume 4, Part 1, p. 627-658.

Thurston, P.C. 1991. Archean Geology of Ontario: Introduction. *in* Geology of Ontario, Ontario Geological Survey, Special Volume 4, Part 1, p. 3-25.

Turek, A., Sage, R.P., and Van Schmus, W.R. 1992. Advances in the U–Pb Zircon Geochronology of the Michipicoten Greenstone Belt, Superior Province, Ontario. Canadian Journal of Earth Sciences, 29: 1154–1165.

Williams, H. R., G.M. Stott, K.B. Heather, T.L. Muir and R.P. Sage. 1991. Wawa Subprovince. *In* Geology of Ontario, Ontario Geological Survey, Special Volume 4, Part 1, p. 485-525.

Young, G.M., Long, D.G.F., Fedo, C.M., Nesbitt, H.W., 2001. Paleoproterozoic Huronian Basin: Product of a Wilson Cycle Punctuated by Glaciations and a Meteorite Impact. Sediment. Geol. 141–142, p. 233-254.

Zaleski, E., O. van Brennan and V.L. Peterson. 1999. Geological evolution of the Manitouwadge Greenstone Belt and Wawa-Quetico Subprovince Boundary, Superior Province, Ontario, Constrained by U-Pb Zircon Dates of Supracrustal and Plutonic Rocks. Can. J. Earth Sci. 36, 945-966.

Zoback, M.L., 1992. First- and Second-order Patterns of Stress in the Lithosphere: The World Stress Map Project; Journal of Geophysical. Research, 97, p.11, 703-11,728.

8 APPENDIX

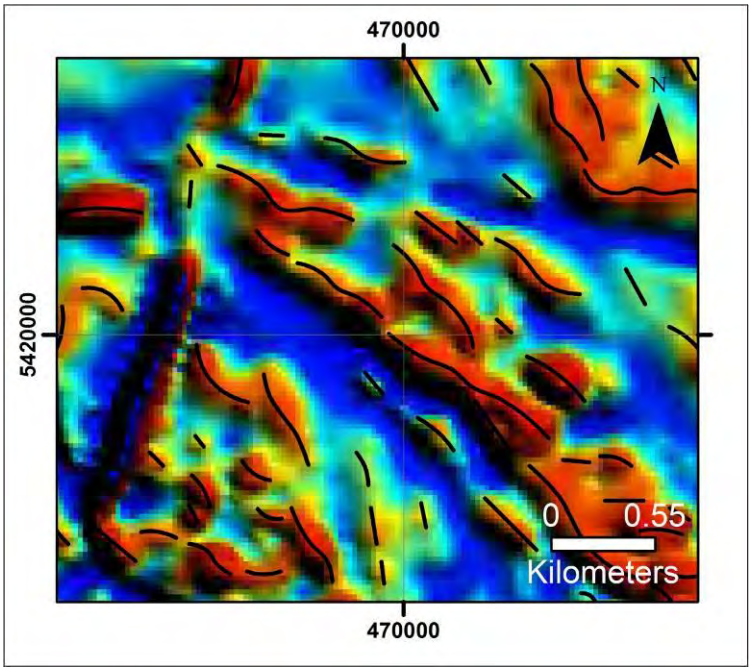


Figure A1: Example of Ductile Lineaments from the Schreiber Area Defined by Curvi-linear Magnetic Highs

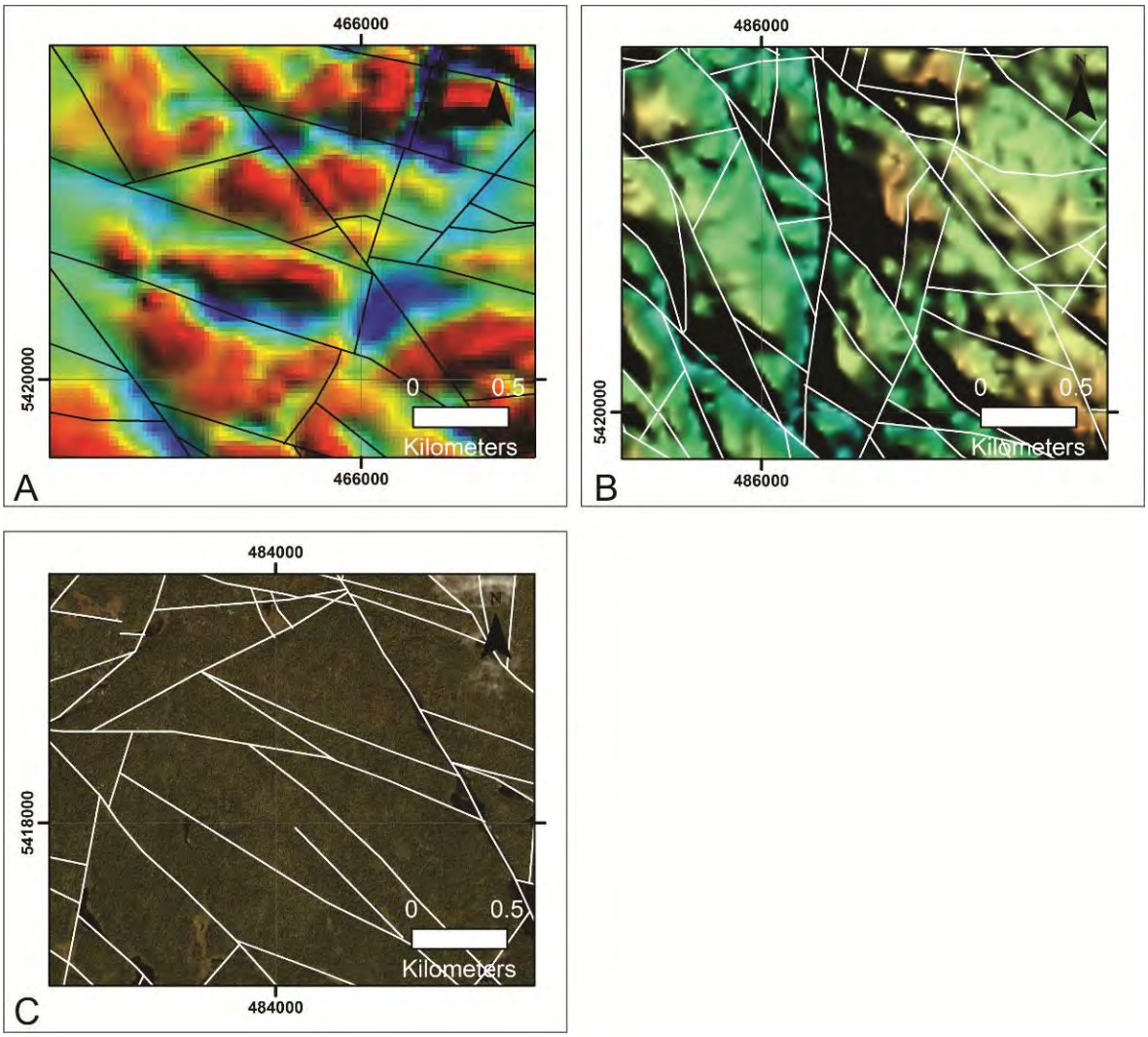


Figure A2: Example of Brittle Lineaments from the Schreiber Area

Defined by breaks in magnetic highs and curvi-linear magnetic lows in magnetic data (top left), breaks in topography in DEM data (top right), and curvi-linear breaks in exposed bedrock and vegetation in satellite data (bottom left).

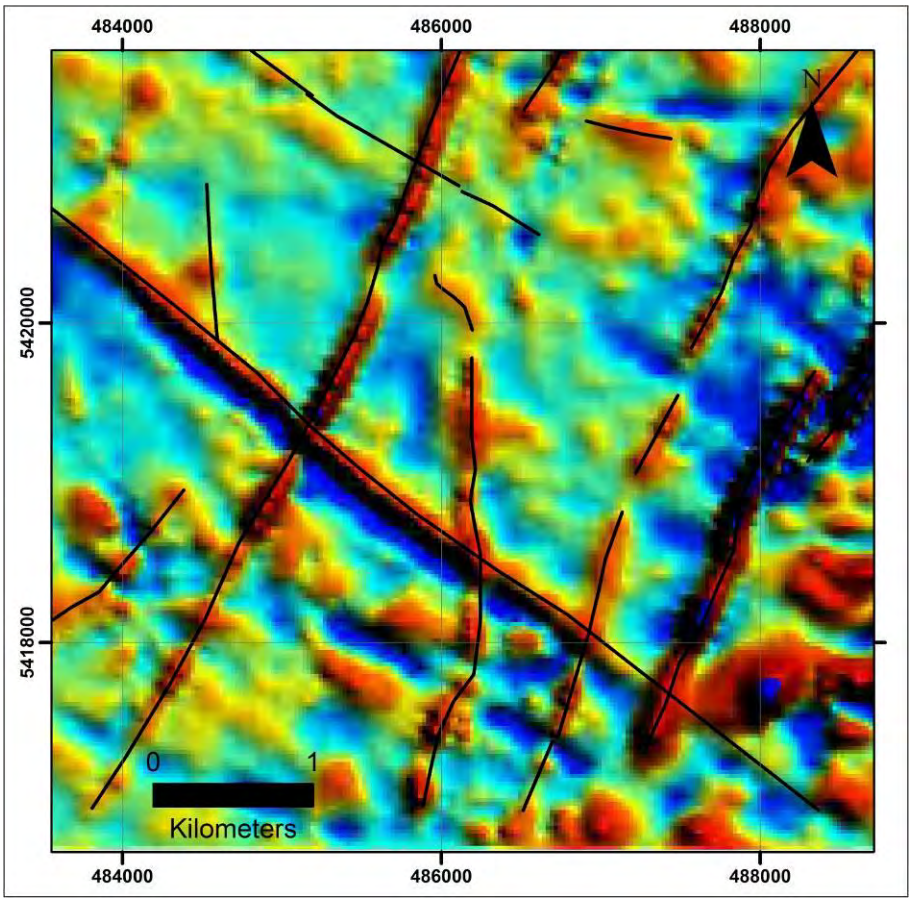
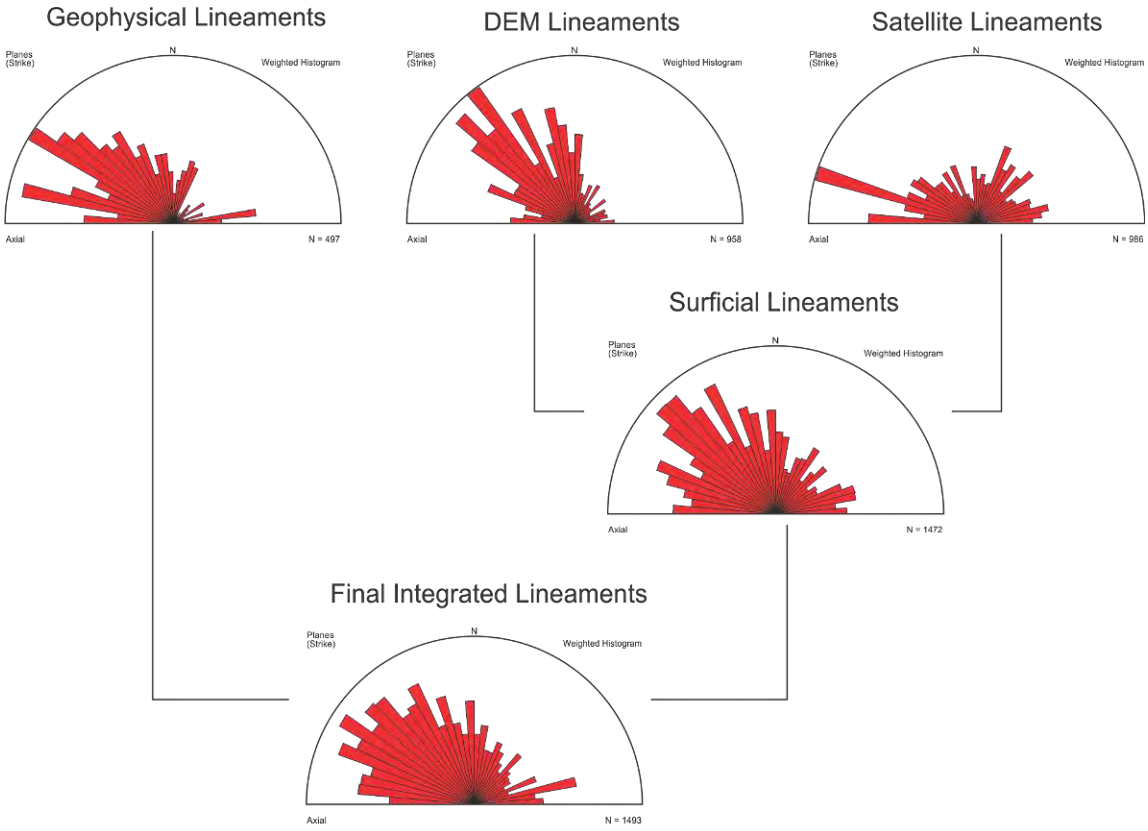


Figure A3: Example of Dyke Lineaments from the Schreiber Area Defined by Linear Magnetic Highs



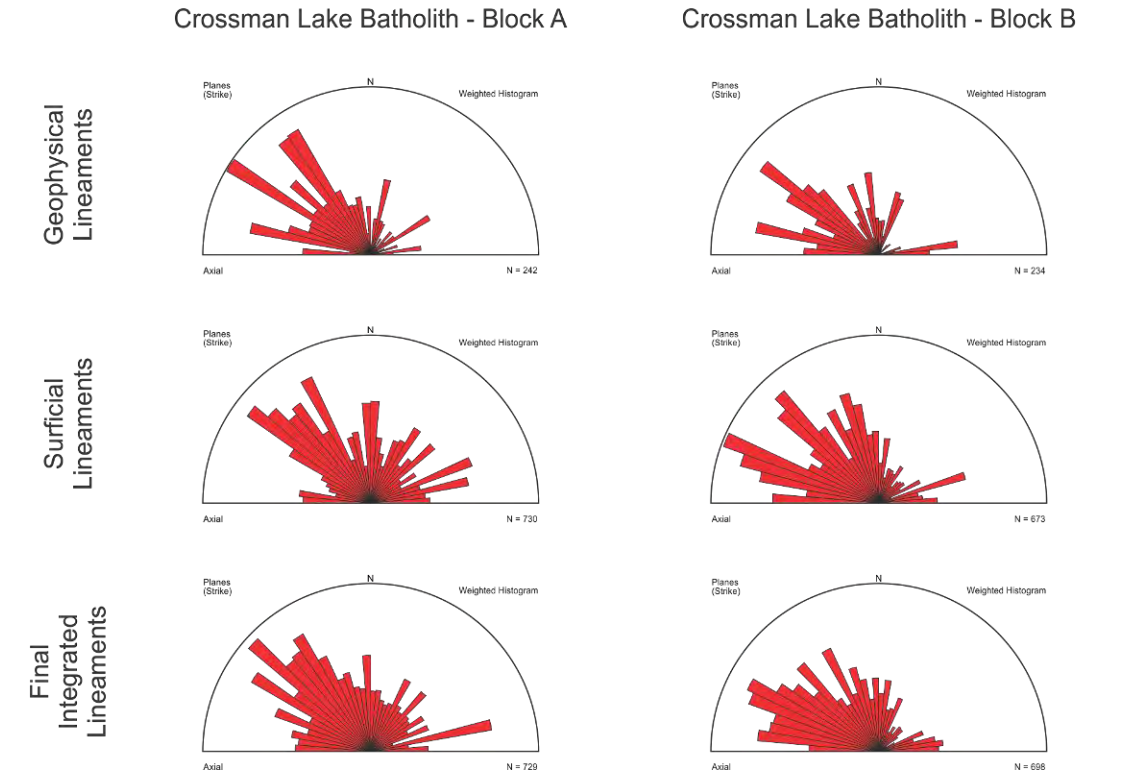


Figure A4: Summary of Lineament Orientations in the Crossman Lake batholith within the Schreiber Area

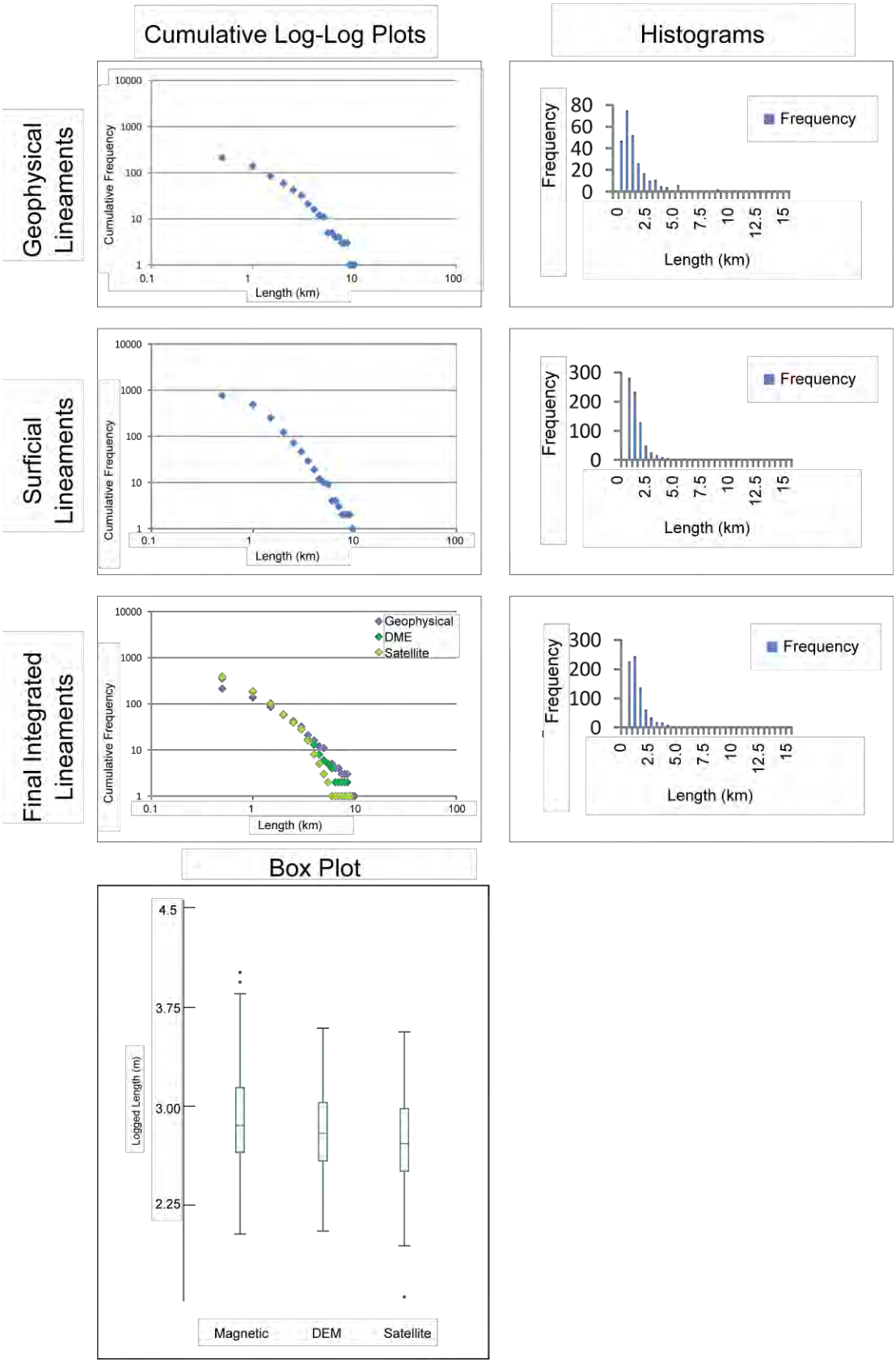


Figure A5: Summary of Length Statistics for Block (A)

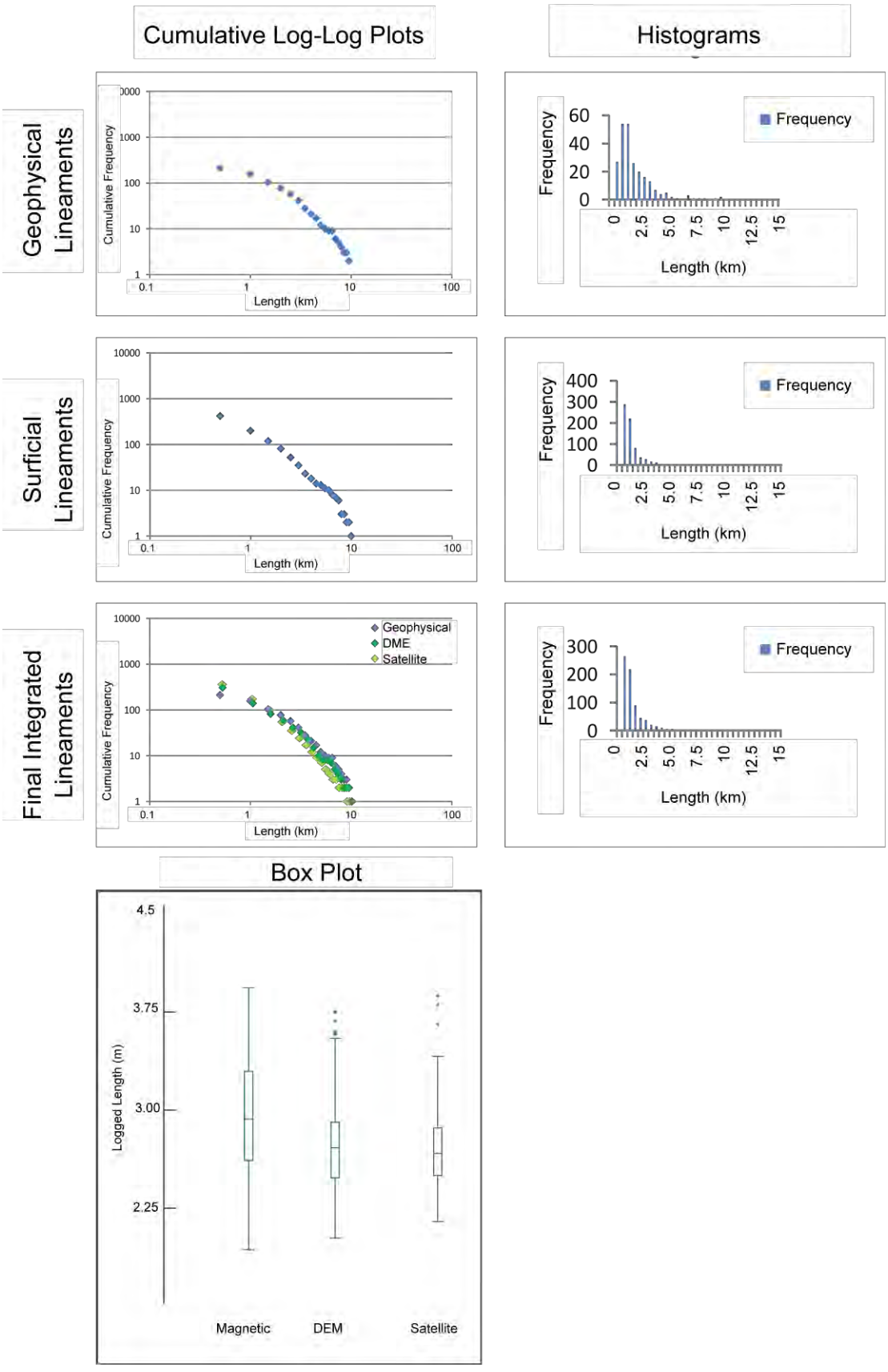


Figure A6: Summary of Length Statistics for Block (B)

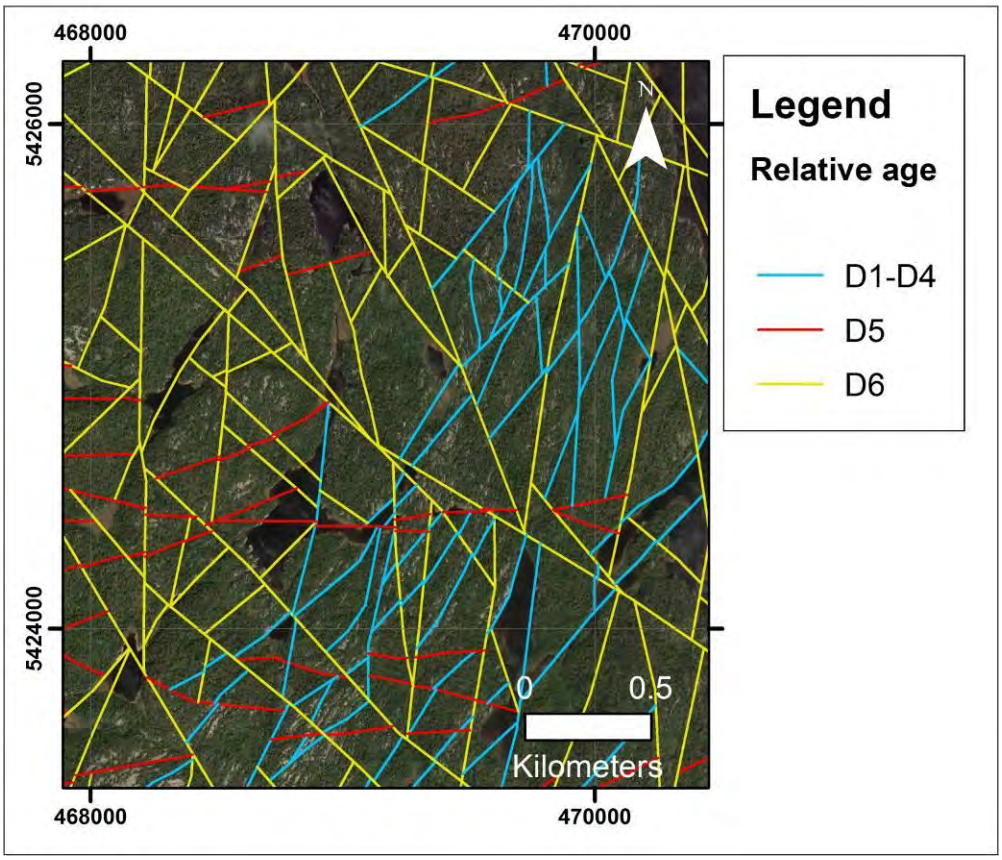


Figure A7: Final Integrated Lineaments Overlaid on Satellite Imagery Showing Northeast to North Trending D_1-D_4 Lineaments Defining faults and Shear Zones at the Eastern Margin of the Crossman Lake Batholith in Block (A)

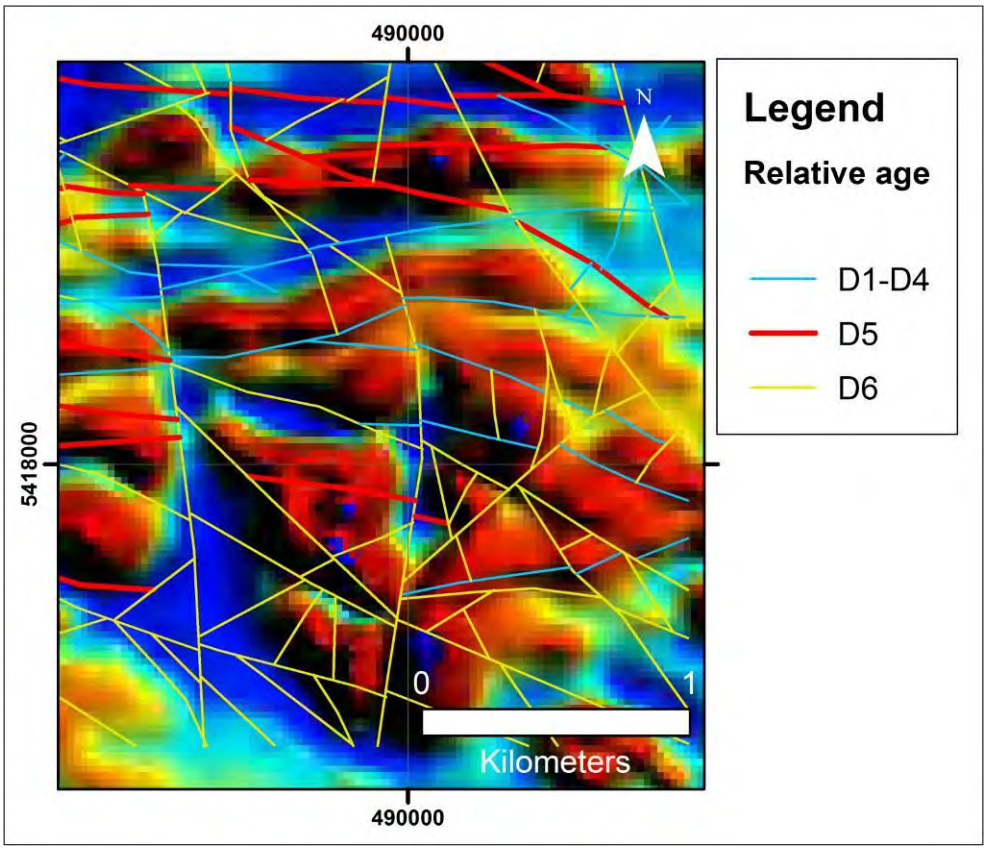


Figure A8: Final Integrated Lineaments Overlaid on Geophysics Data Showing Curvi-linear, Segmented D_1-D_4 in the Schreiber – Hemlo Greenstone Belt in Block (B)

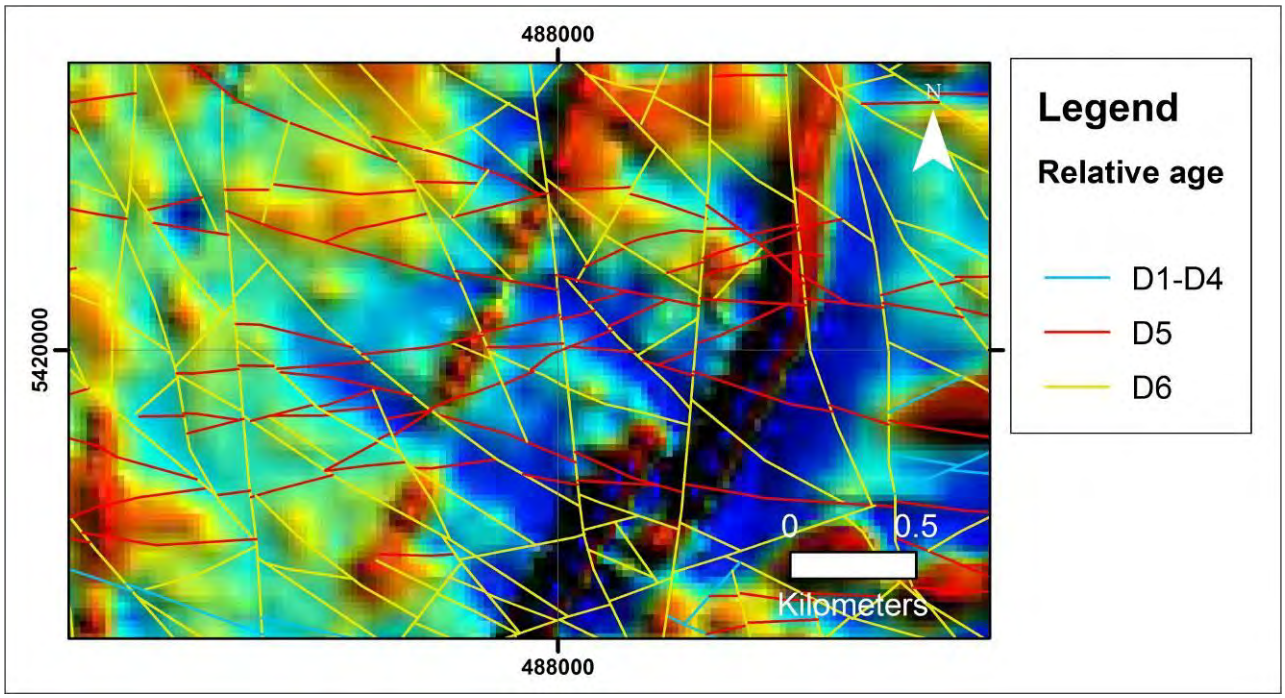


Figure A9: Final Integrated Lineaments Overlaid on Geophysics Data Showing East-West to North Northwest Trending D_5 Fault with Rare Sinistral Offset of D_6 Lineaments

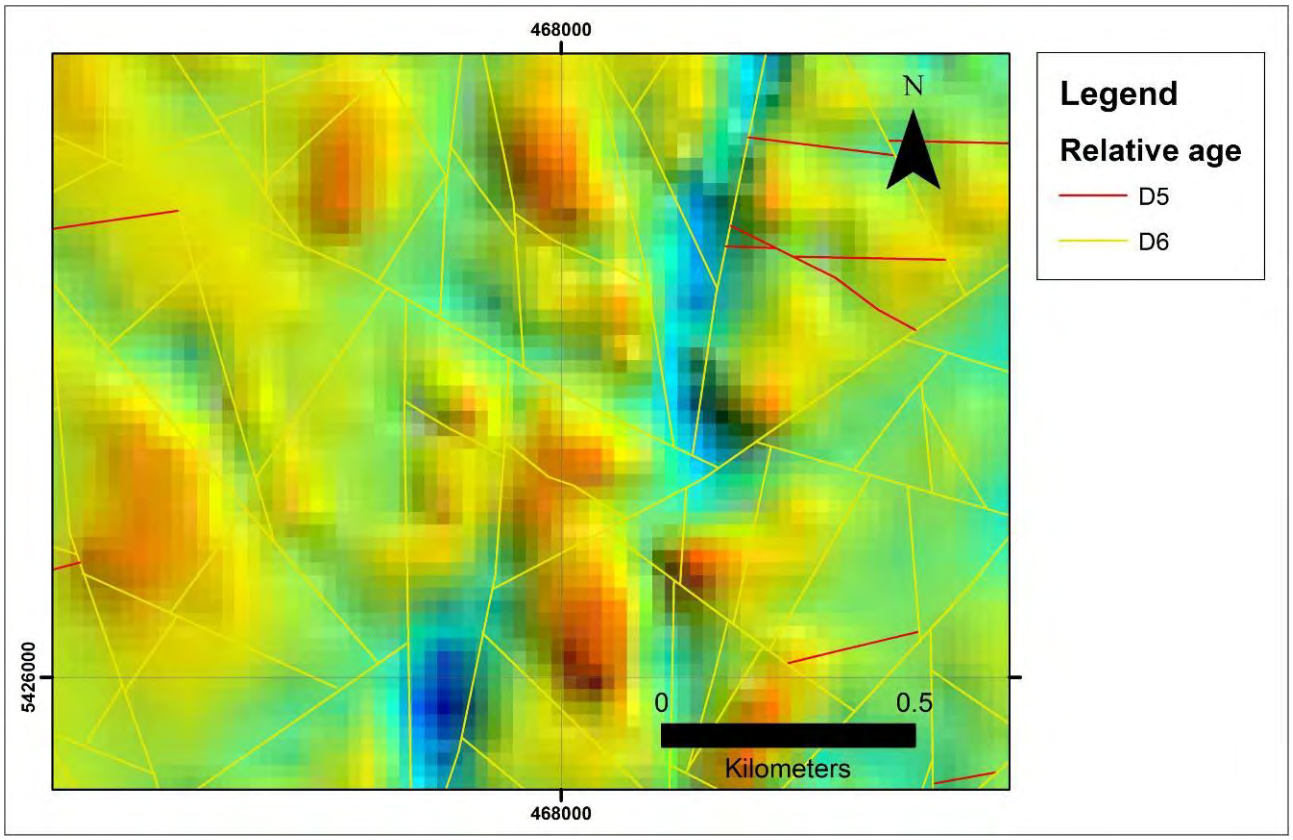
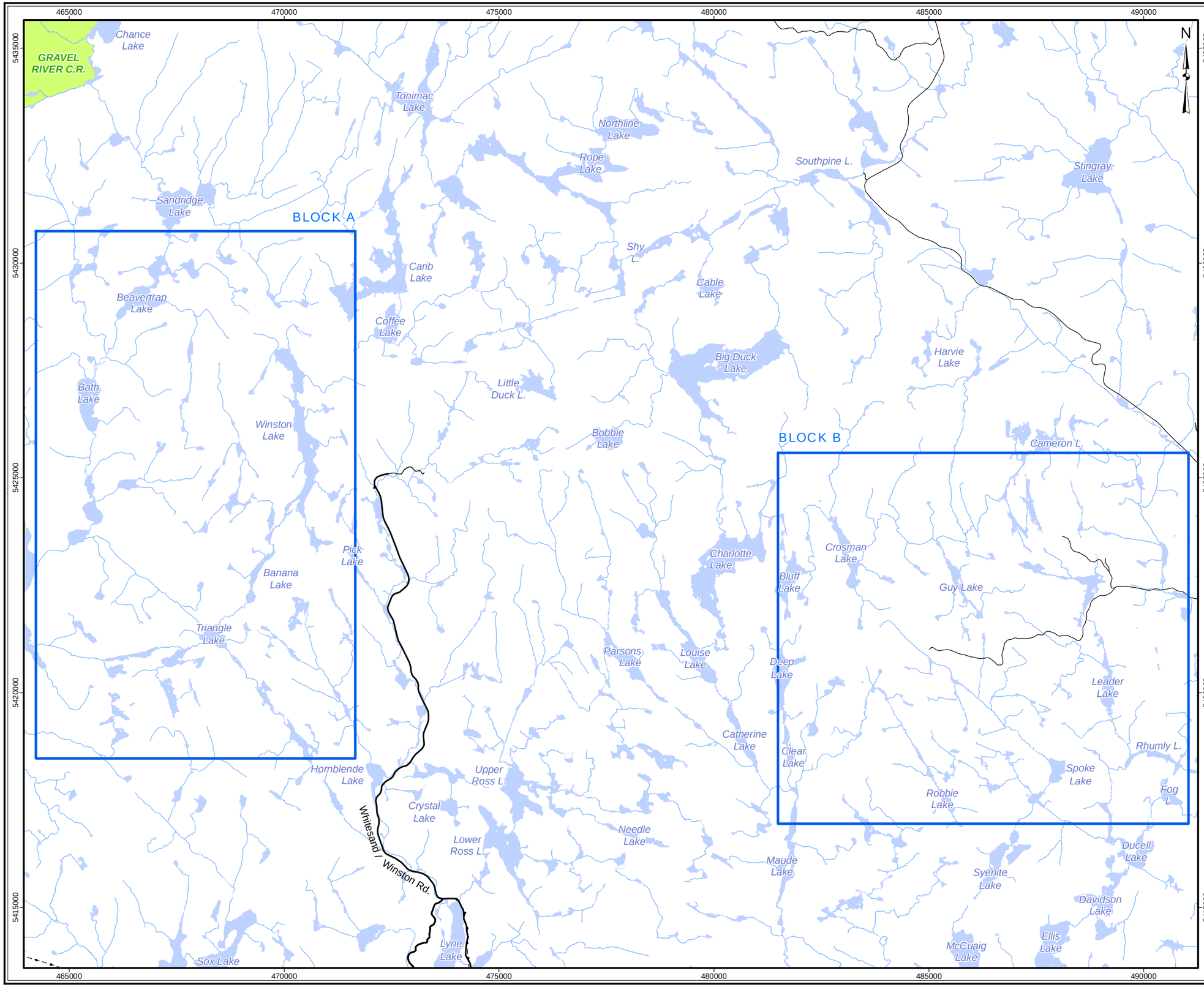


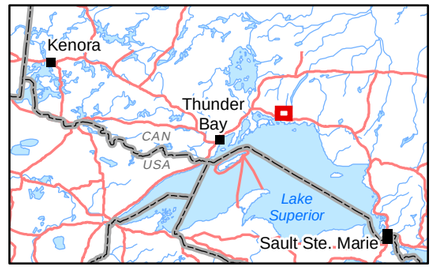
Figure A10: Final Integrated Lineaments Overlaid on Geophysics Data Showing Network of D_6 Northwest, North, and Northeast Trending. Northwest Trending Faults Show Dextral Strike-Separation, with Sporadic Sinistral Strike-Separation Also Observed

FIGURES



LEGEND

- Phase 2 Assessment Area
- Major Road
- Minor Road
- Powerline
- Watercourse
- Waterbody
- Conservation Reserve



REFERENCE

Base Data: MNR LIO, obtained 2009-2014, CanVec topography

5 km

srk consulting

PROJECT

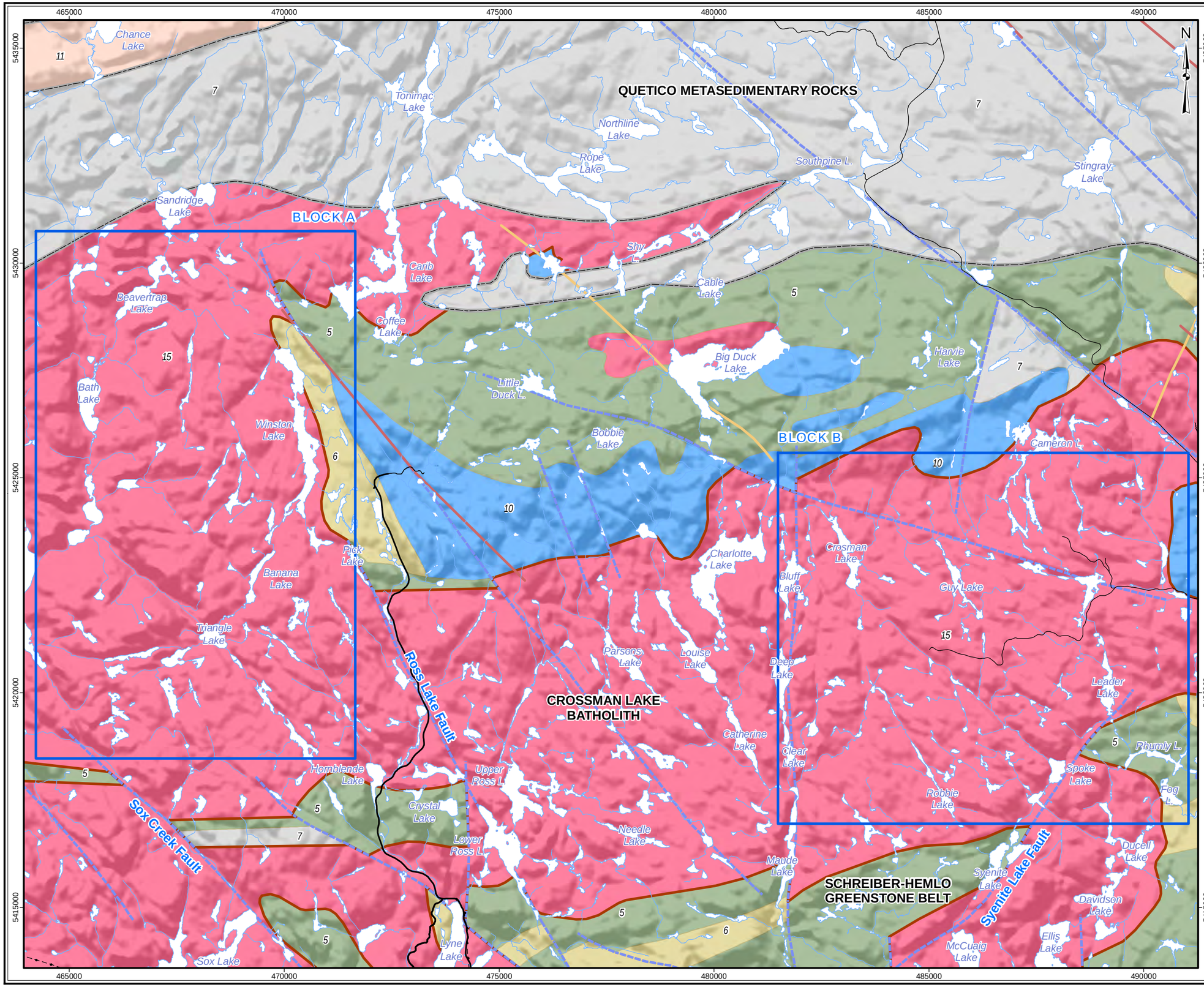
Phase 2 Structural Lineament Interpretation
Schreiber Area, Ontario

TITLE

Location and Overview of the Schreiber Area

DESIGN	KR	02 SEP 2014	**Figure 1**	REVISION 3
GIS	JA	04 FEB 2015		UTM ZONE 16N
CHECK	SDC	04 FEB 2015		NAD 1983
REVIEW	AF	04 FEB 2015		1:85,000

File: SRK_NWMO_SCH_Fig01_Locality

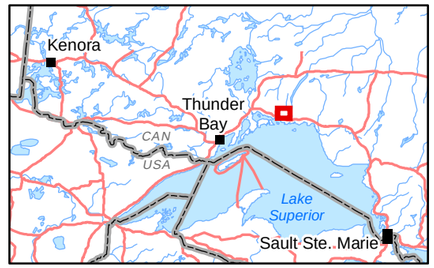


LEGEND

- Phase 2 Assessment Area
- Major Road
- Minor Road
- Powerline
- Watercourse
- Waterbody
- Matachewan mafic dike
- Dyke (Other)
- Mapped Fault
- Quetico/Wawa Subprovince boundary
- Batholith Contact

Bedrock Geology

- 10 Mafic suite
- 15 Biotite granite suite
- 7 Clastic metasedimentary rocks
- 6 Intermediate to felsic metavolcanic rocks
- 5 Mafic metavolcanic rocks
- 11 Tonalite gneiss suite



REFERENCE

Base Data: MNR LIO, obtained 2009-2014,
CanVec topography
Bedrock/Fault/Dyke: OGS MRD 126-REV1 (1:250,000)

5 km

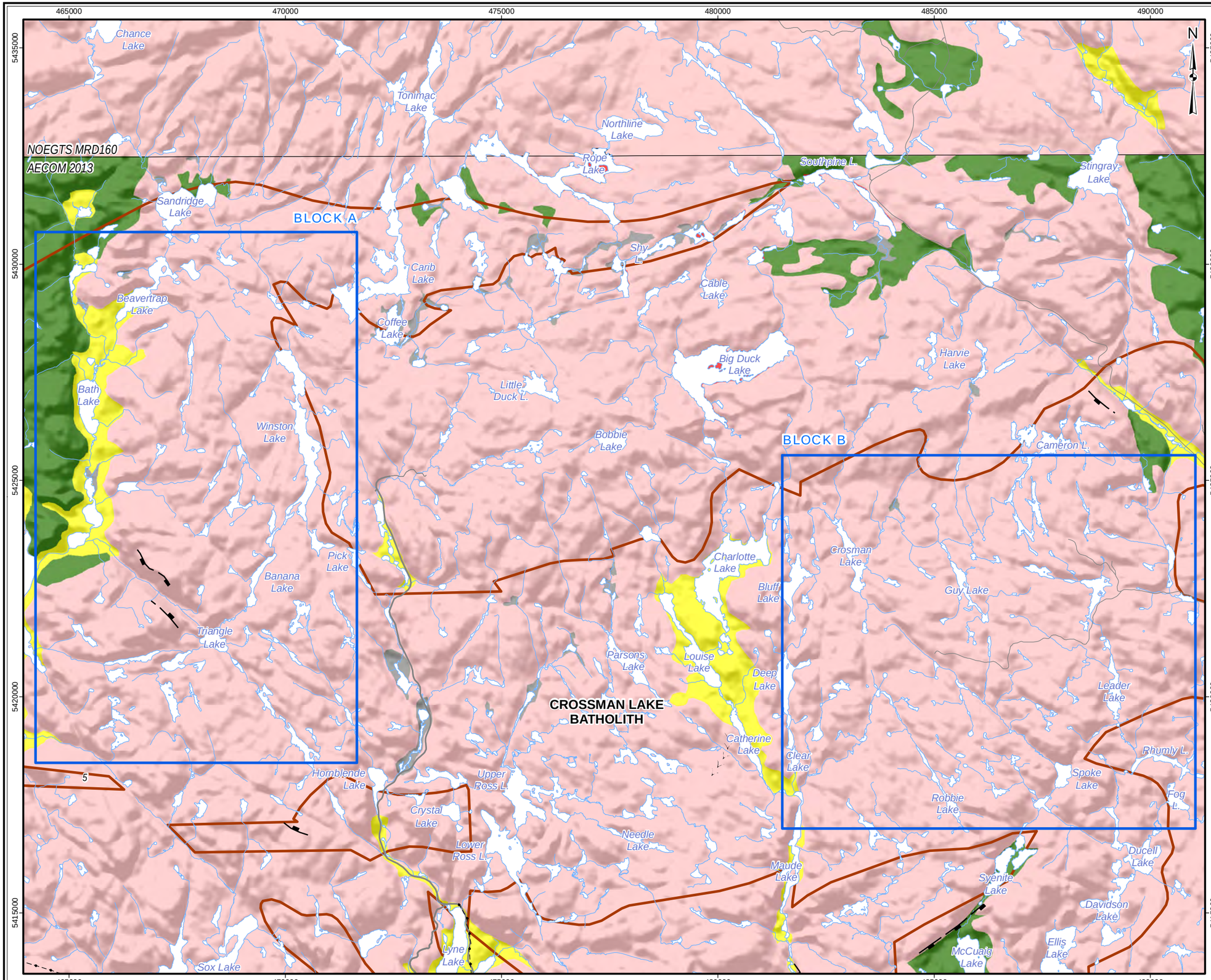
srk consulting

PROJECT
Phase 2 Structural Lineament Interpretation
Schreiber Area, Ontario

TITLE
Bedrock Geology of the Schreiber Area

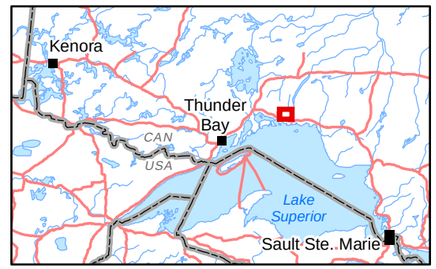
DESIGN	KR	02 SEP 2014	**Figure 2**	REVISION 3
GIS	JA	04 FEB 2015		UTM ZONE 16N
CHECK	SDC	04 FEB 2015		NAD 1983
REVIEW	AF	04 FEB 2015		1:85,000

File: SRK_NWMO_SCH_Fig02_Bedrock



LEGEND

- Phase 2 Assessment Area
- Major Road
- Minor Road
- Powerline
- Watercourse
- Waterbody
- Batholith Contact
- Escarpment
- Esker
- Morainal Terrain
- Glaciofluvial Terrain
- Glaciolacustrine Terrain
- Organic Terrain
- Bedrock Terrain



REFERENCE

Base Data: MNR LIO, obtained 2009-2014,
CanVec topography
Surficial Terrain: AECOM 2013, Digital Northern Ontario Engineering Geology Terrain Study (MRD160)

5 km

srk consulting

PROJECT

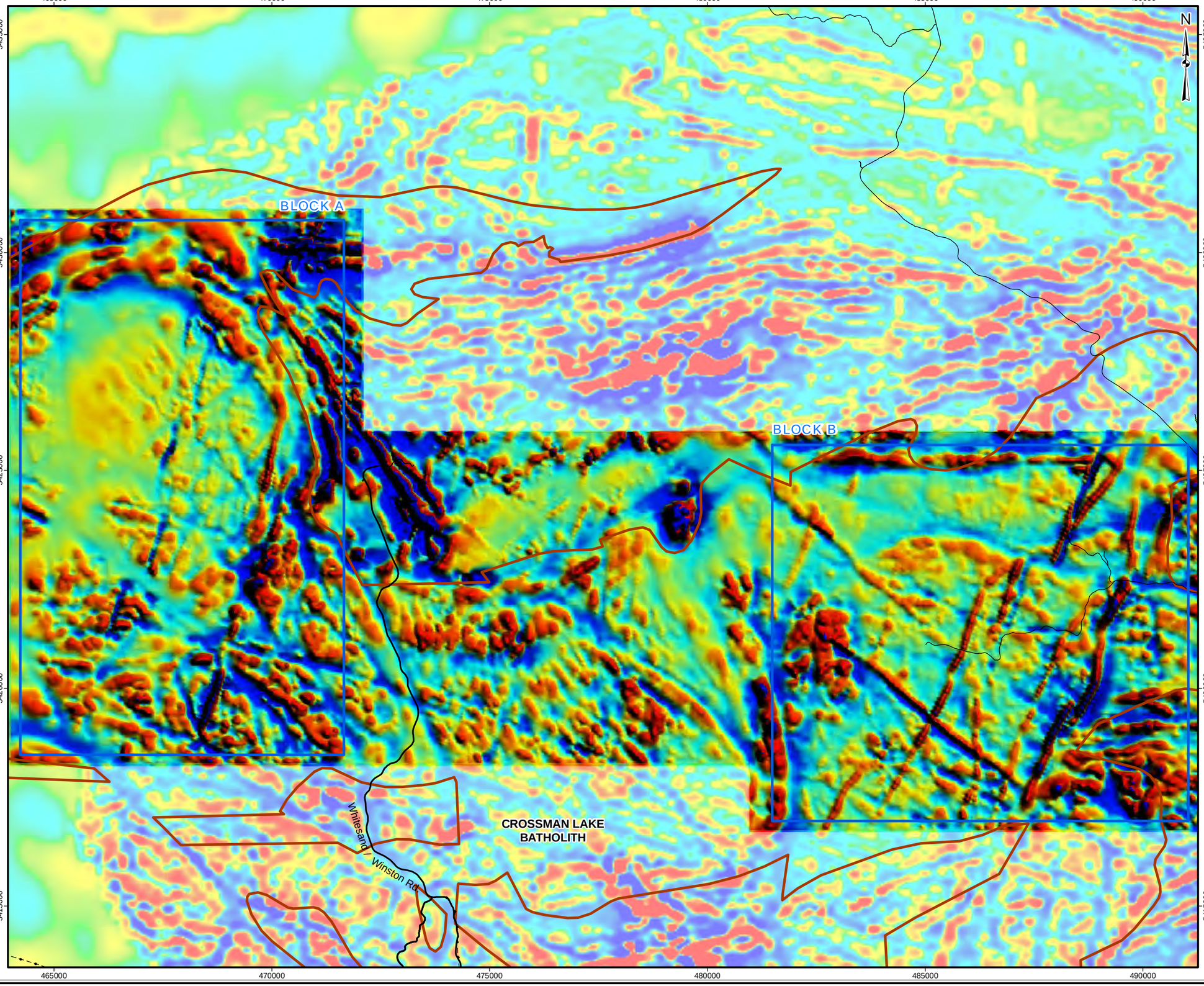
Phase 2 Structural Lineament Interpretation
Schreiber Area, Ontario

TITLE

Terrain Features of the Schreiber Area

DESIGN	KR	02 SEP 2014	**Figure 3**	REVISION 3
GIS	JA	11 FEB 2015		UTM ZONE 16N
CHECK	SDC	11 FEB 2015		NAD 1983
REVIEW	AF	11 FEB 2015		1:85,000

File: SRK_NWMO_SCH_Fig03_Surficial



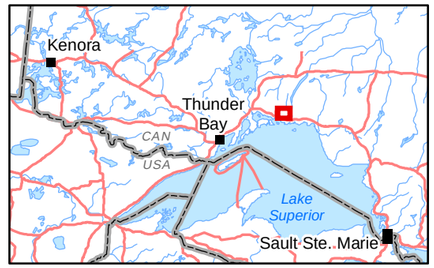
LEGEND

- Phase 2 Assessment Area
- Major Road
- Minor Road
- Powerline
- Batholith Contact

nT/km

High : 26869

Low : -4219



REFERENCE

Base Data: MNR LIO, obtained 2009-2014
Geophysics: OGS Schreiber Area survey GDS1104
GSC Magnetic Compilation
Detail: SGL 2015

5 km

srk consulting

PROJECT

Phase 2 Structural Lineament Interpretation
Schreiber Area, Ontario

TITLE

Pole Reduced Magnetic Data (First Vertical Derivative) of the Schreiber Area

DESIGN	KR	02 SEP 2014	**Figure 4**	REVISION 3
GIS	JA	04 FEB 2015		UTM ZONE 16N
CHECK	SDC	04 FEB 2015		NAD 1983
REVIEW	AF	04 FEB 2015		1:85,000

File: SRK_NWMO_SCH_Fig04_MAG

465000 470000 475000 480000 485000 490000

5435000 5430000 5425000 5420000 5415000

N

Chance Lake
Tonimac Lake
Northline Lake
Rope Lake
Southpine L.
Stingray Lake
Sandridge Lake
BLOCK A
Shy L.
Carib Lake
Cable Lake
Beavertrap Lake
Coffee Lake
Big Duck Lake
Harvie Lake
Bath Lake
Little Duck L.
Winston Lake
Bobbie Lake
BLOCK B
Cameron L.
Pick Lake
Crosman Lake
Charlotte Lake
Bluff Lake
Guy Lake
Banana Lake
Triangle Lake
Parsons Lake
Louise Lake
Deep Lake
Leader Lake
Catherine Lake
Clear Lake
Phumly L.
Hornblende Lake
Upper Ross L.
Spoke Lake
Fog L.
Crystal Lake
Robbie Lake
Whitesand
Lower Ross L.
CROSSMAN LAKE BATHOLITH
Needle Lake
Winston Rd
Maude Lake
Syenite Lake
Ducell Lake
Davidson Lake
Lyne Lake
McCuaig Lake
Ellis Lake
Sox Lake

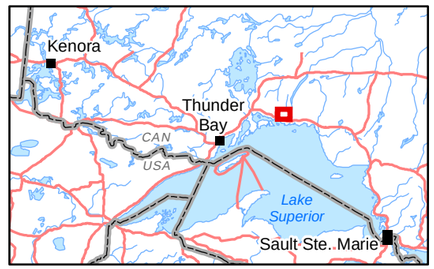
465000 470000 475000 480000 485000 490000

LEGEND

- Phase 2 Assessment Area
- Major Road
- Minor Road
- Powerline
- Waterbody
- Batholith Contact

Elevation (masl)

590
500
400
300
234



REFERENCE

Base Data: MNR LIO, obtained 2009-2014
Relief backdrop: CDSM (NRCAN)
DEM: SGL 2015

5 km

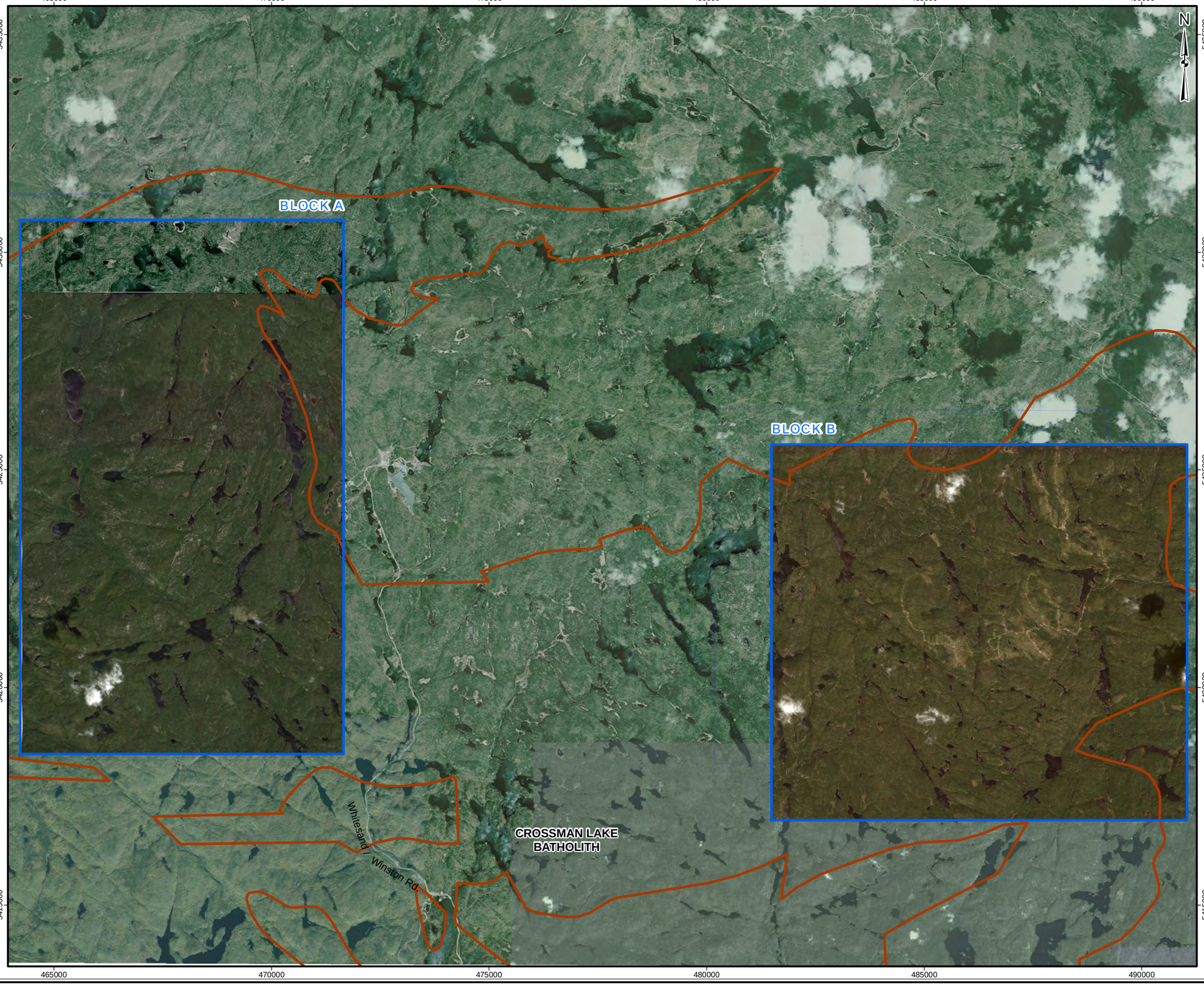
srk consulting

PROJECT
Phase 2 Structural Lineament Interpretation
Schreiber Area, Ontario

TITLE
Digital Elevation Data of the Schreiber Area

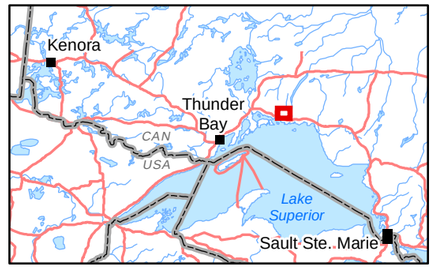
DESIGN	KR	02 SEP 2014	**Figure 5**	REVISION 3
GIS	JA	04 FEB 2015		UTM ZONE 16N
CHECK	SDC	04 FEB 2015		NAD 1983
REVIEW	AF	04 FEB 2015		1:85,000

File: SRK_NWMO_SCH_Fig05_DEM



LEGEND

- Phase 2 Assessment Area
- Batholith Contact



REFERENCE

Base Data: MNR LIO, obtained 2009-2014
Image backdrop: TerraMetrics 2014
Detail: World View 2 GeoEye

5 km

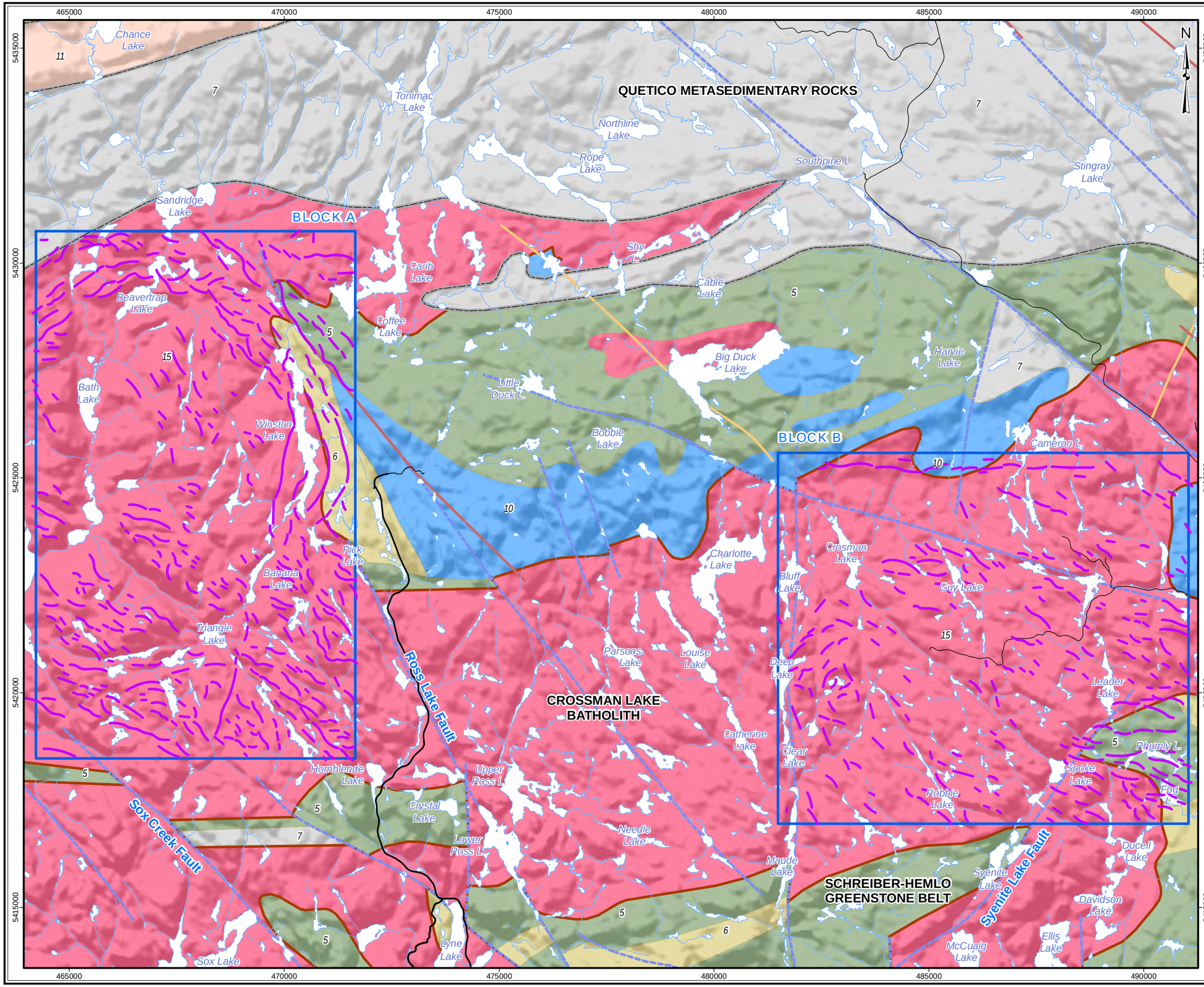
srk consulting

PROJECT
Phase 2 Structural Lineament Interpretation
Schreiber Area, Ontario

TITLE
Satellite Imagery Data of the Schreiber Area

DESIGN	KR	02 SEP 2014	**Figure 6**	REVISION 3
GIS	JA	04 FEB 2015		UTM ZONE 16N
CHECK	SDC	04 FEB 2015		NAD 1983
REVIEW	AF	04 FEB 2015		1:85,000

File: SRK_NWMO_SCH_Fig06_SAT

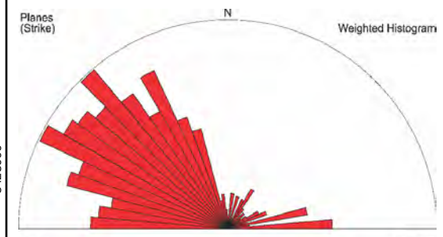


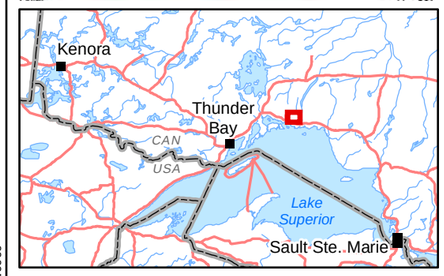
LEGEND

- Phase 2 Assessment Area
- Major Road
- Minor Road
- Watercourse
- Waterbody
- Matachewan mafic dike
- Dyke (Other)
- Mapped Fault
- Quetico/Wawa Subprovince boundary
- Batholith Contact
- Ductile lineament

Bedrock Geology

- 10 Mafic suite
- 15 Biotite granite suite
- 7 Clastic metasedimentary rocks
- 6 Intermediate to felsic metavolcanic rocks
- 5 Mafic metavolcanic rocks
- 11 Tonalite gneiss suite





REFERENCE

Base Data: MNR LIO, obtained 2009-2014,
CanVec topography
Bedrock/Fault/Dyke: OGS MRD 126-REV1 (1:250,000)

5 km

srk consulting

PROJECT
Phase 2 Structural Lineament Interpretation
Schreiber Area, Ontario

TITLE
Ductile Features of the Schreiber Area

DESIGN	KR	02 SEP 2014	**Figure 7**	REVISION 4
GIS	JA	04 FEB 2015		UTM ZONE 16N
CHECK	SDC	04 FEB 2015		NAD 1983
REVIEW	AF	04 FEB 2015		1:85,000

File: SRK_NWMO_SCH_Fig07_Formlines

462000 464000 466000 468000 470000 472000 474000

5430000 5428000 5426000 5424000 5422000 5420000

BLOCK A

Beavertrap Lake

Bath Lake

Winston Lake

Banana Lake

Triangle Lake

Pick Lake

Carib Lake

Coffee Lake

Little Duck L.

CROSSMAN LAKE BATHOLITH

Ross Lake Fault

15

5

6

10

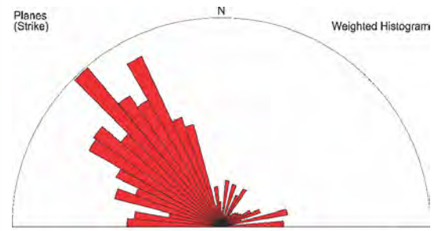
N

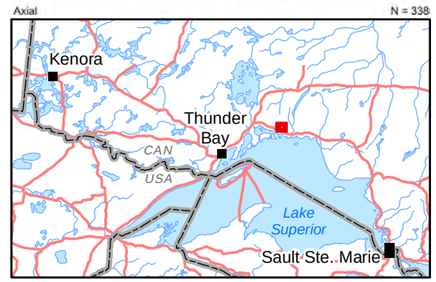
LEGEND

- Phase 2 Assessment Area
- Major Road
- Minor Road
- Watercourse
- Waterbody
- Matachewan mafic dike
- Dyke (Other)
- Mapped Fault
- Quetico/Wawa Subprovince boundary
- Batholith Contact
- Ductile lineament

Bedrock Geology

- 10 Mafic suite
- 15 Biotite granite suite
- 7 Clastic metasedimentary rocks
- 6 Intermediate to felsic metavolcanic rocks
- 5 Mafic metavolcanic rocks
- 11 Tonalite gneiss suite





REFERENCE

Base Data: MNR LIO, obtained 2009-2014,
CanVec topography
Bedrock/Fault/Dyke: OGS MRD 126-REV1 (1:250,000)

0 1 km

srk consulting

PROJECT
Phase 2 Structural Lineament Interpretation
Schreiber Area, Ontario

TITLE
Ductile Features of the Schreiber Area - Block A

DESIGN	KR	02 SEP 2014	**Figure 7a**	REVISION 2
GIS	JA	04 FEB 2015		UTM ZONE 16N
CHECK	SDC	04 FEB 2015		NAD 1983
REVIEW	AF	04 FEB 2015		1:48,000

File: SRK_NWMO_SCH_Fig07a_Formlines

480000 482000 484000 486000 488000 490000 492000

5426000 5424000 5422000 5420000 5418000 5416000

BLOCK B

Cameron L.

10

Charlotte Lake

Bluff Lake

Crosman Lake

Guy Lake

15

Louise Lake

Deep Lake

Leader Lake

Catherine Lake

Clear Lake

5

Rhumly L.

CROSSMAN LAKE BATHOLITH

Spoke Lake

Fog L.

Robbie Lake

Ducell Lake

Maude Lake

SCHREIBER-HEMLO GREENSTONE BELT

Syenite Lake

Syenite Lake Fault

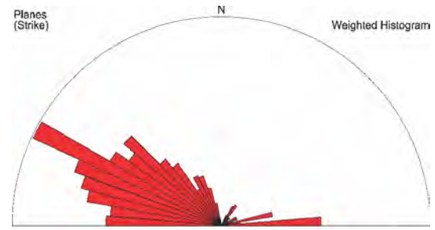
N

LEGEND

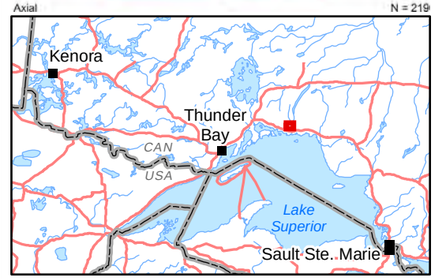
- Phase 2 Assessment Area
- Major Road
- Minor Road
- Watercourse
- Waterbody
- Matachewan mafic dike
- Dyke (Other)
- Mapped Fault
- Quetico/Wawa Subprovince boundary
- Batholith Contact
- Ductile lineament

Bedrock Geology

- 10 Mafic suite
- 15 Biotite granite suite
- 7 Clastic metasedimentary rocks
- 6 Intermediate to felsic metavolcanic rocks
- 5 Mafic metavolcanic rocks
- 11 Tonalite gneiss suite



Axial N = 219



REFERENCE

Base Data: MNR LIO, obtained 2009-2014,
CanVec topography
Bedrock/Fault/Dyke: OGS MRD 126-REV1 (1:250,000)

2 km

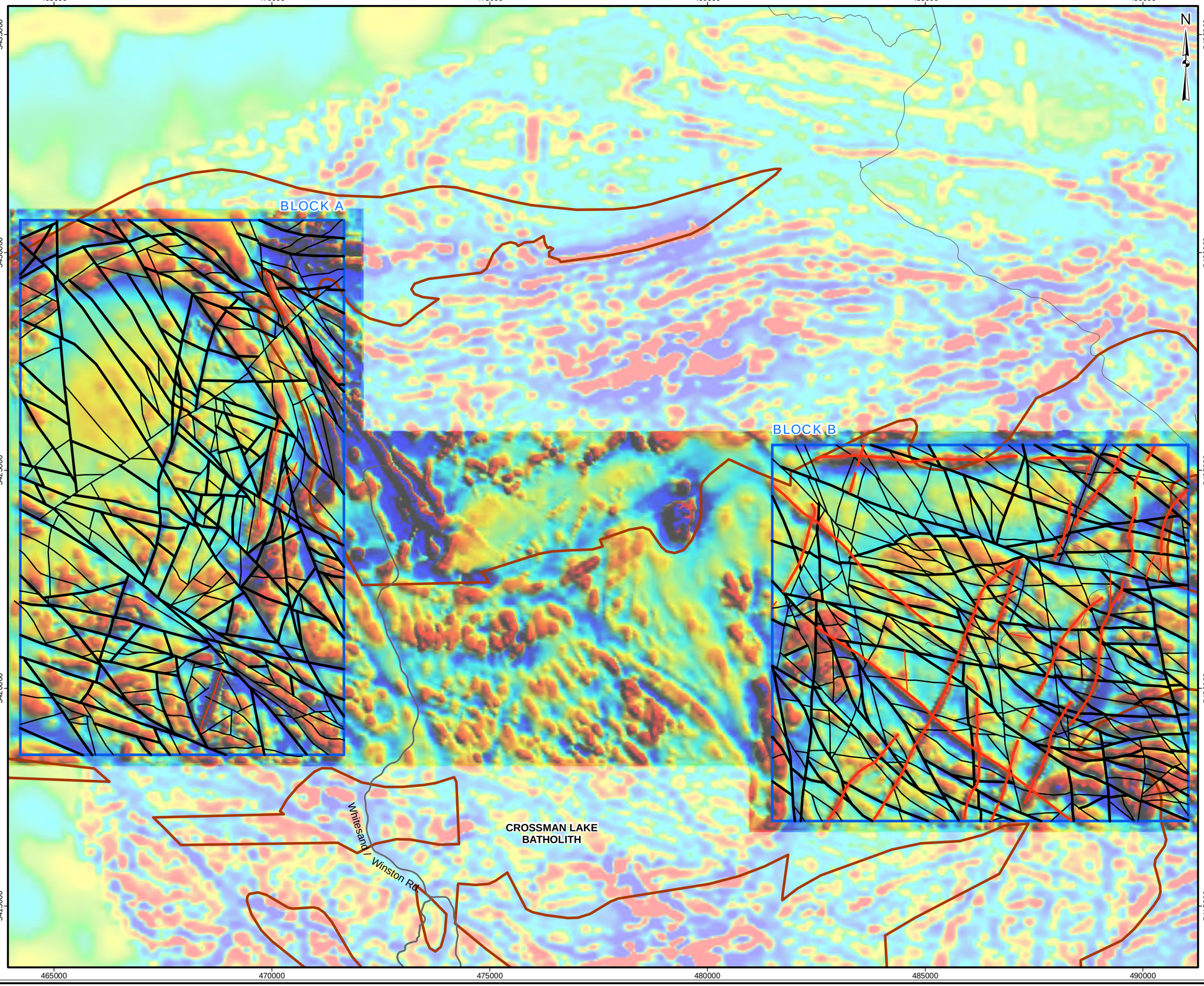
srk consulting

PROJECT
Phase 2 Structural Lineament Interpretation
Schreiber Area, Ontario

TITLE
Ductile Features of the Schreiber Area - Block B

DESIGN	KR	02 SEP 2014	**Figure 7b**	REVISION 2
GIS	JA	04 FEB 2015		UTM ZONE 16N
CHECK	SDC	04 FEB 2015		NAD 1983
REVIEW	AF	04 FEB 2015		1:48,000

File: SRK_NWMO_SCH_Fig07b_Formlines



LEGEND

- Phase 2 Assessment Area
- Major Road
- Minor Road
- Batholith Contact

Dyke, Reproducibility (RA_1)

- 1
- 2

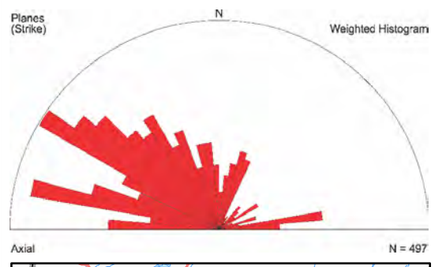
Lineament, Reproducibility (RA_1)

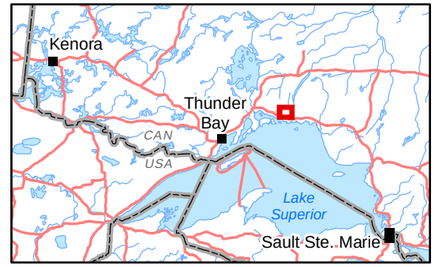
- 1
- 2

nT/km

High : 26869

Low : -4219





REFERENCE

Base Data: MNR LIO, obtained 2009-2014
Geophysics: OGS Schreiber Area survey GDS1104
GSC Magnetic Compilation
Detail: SGL 2015

5 km

srk consulting

PROJECT

Phase 2 Structural Lineament Interpretation
Schreiber Area, Ontario

TITLE

**Interpreted Lineaments (RA-1)
from Pole Reduced Magnetic Data (1VD)
of the Schreiber Area**

DESIGN	KR	02 SEP 2014	**Figure 8**	REVISION 3
GIS	JA	04 FEB 2015		UTM ZONE 16N
CHECK	SDC	04 FEB 2015		NAD 1983
REVIEW	AF	04 FEB 2015		1:85,000

File: SRK_NWMO_SCH_Fig08_MAGra1

462000 464000 466000 468000 470000 472000 474000

5430000 5428000 5426000 5424000 5422000 5420000

BLOCK A

N

CROSSMAN LAKE BATHOLITH

Ross Lake Fault

LEGEND

- Phase 2 Assessment Area
- Major Road
- Minor Road
- Matachewan mafic dike
- Dyke (Other)
- Mapped Fault
- Quetico/Wawa Subprovince boundary
- Batholith Contact

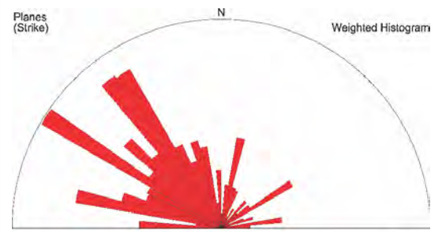
Reproducibility (RA_1)

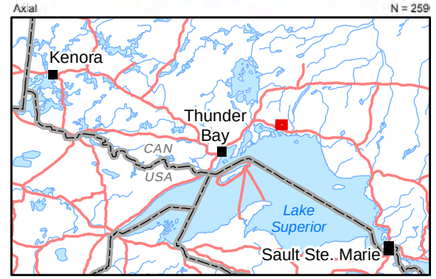
Dyke	Lineament
1	1
2	2

nT/km

High : 26869

Low : -4219





REFERENCE

Base Data: MNR LIO, obtained 2009-2014
Geophysics: OGS Schreiber Area survey GDS1104
GSC Magnetic Compilation
Detail: SGL 2015

0 1 km

srk consulting

PROJECT

Phase 2 Structural Lineament Interpretation
Schreiber Area, Ontario

TITLE

Interpreted Lineaments (RA-1) from Pole Reduced Magnetic Data (1VD) of the Schreiber Area Area – Block A

DESIGN	KR	02 SEP 2014	**Figure 8a**	REVISION 2
GIS	JA	04 FEB 2015		UTM ZONE 16N
CHECK	SDC	04 FEB 2015		NAD 1983
REVIEW	AF	04 FEB 2015		1:48,000

File: SRK_NWMO_SCH_Fig08a_MAGRA1

480000 482000 484000 486000 488000 490000 492000

5426000 5424000 5422000 5420000 5418000 5416000

BLOCK B

CROSSMAN LAKE BATHOLITH

SCHREIBER-HEMLO GREENSTONE BELT

Syenite Lake Fault

N

LEGEND

- Phase 2 Assessment Area
- Major Road
- Minor Road
- Matachewan mafic dike
- Dyke (Other)
- Mapped Fault
- Batholith Contact

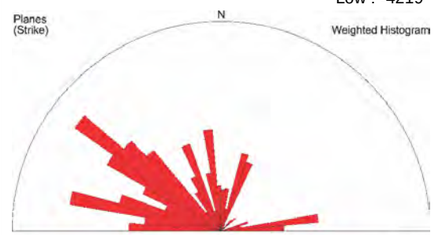
Reproducibility (RA_1)

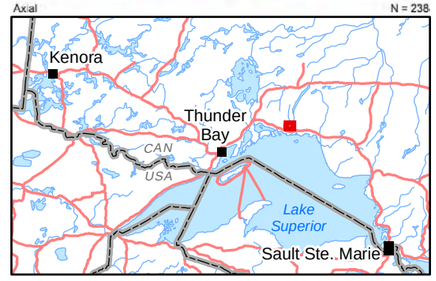
Dyke	Lineament
1	1
2	2

nT/km

High : 26869

Low : -4219





REFERENCE

Base Data: MNR LIO, obtained 2009-2014
Geophysics: OGS Schreiber Area survey GDS1104
GSC Magnetic Compilation
Detail: SGL 2015

2 km

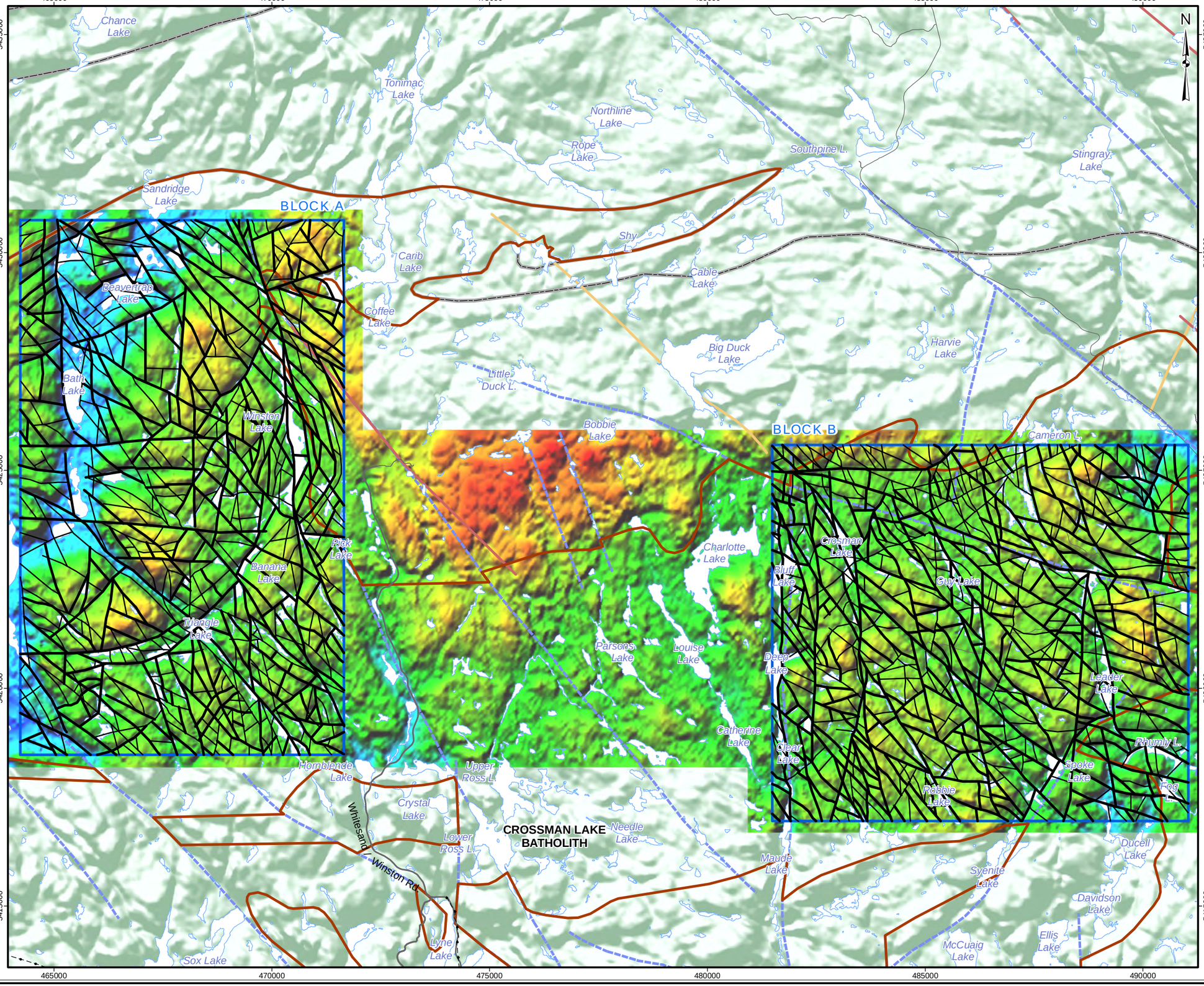
srk consulting

PROJECT: Phase 2 Structural Lineament Interpretation
Schreiber Area, Ontario

TITLE: **Interpreted Lineaments (RA-1) from Pole Reduced Magnetic Data (1VD) of the Schreiber Area - Block B**

DESIGN	KR	02 SEP 2014	**Figure 8b**	REVISION 3
GIS	JA	04 FEB 2015		UTM ZONE 16N
CHECK	SDC	04 FEB 2015		NAD 1983
REVIEW	AF	04 FEB 2015		1:48,000

File: SRK_NWMO_SCH_Fig08b_MAGRA1



LEGEND

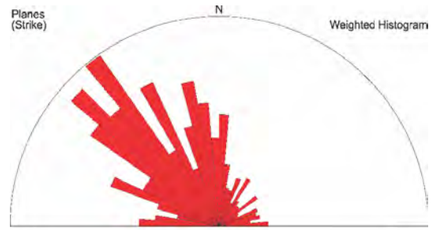
- Phase 2 Assessment Area
- Major Road
- Minor Road
- Powerline
- Waterbody
- Matachewan mafic dike
- Dyke (Other)
- Mapped Fault
- Quetico/Wawa Subprovince boundary
- Batholith Contact

Reproducibility (RA_1)

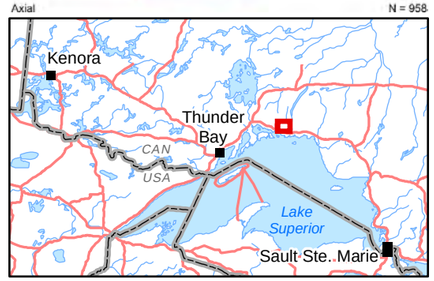
- 1
- 2

Elevation (masl)

590
500
400
300
234



Axial N = 958



REFERENCE

Base Data: MNR LIO, obtained 2009-2014
Relief backdrop: CDSM (NRCAN)
DEM: SGL 2015

5 km

srk consulting

PROJECT
Phase 2 Structural Lineament Interpretation
Schreiber Area, Ontario

TITLE
Interpreted Lineaments from Digital Elevation Data of the Schreiber Area

DESIGN	KR	02 SEP 2014	**Figure 9**	REVISION 3
GIS	JA	04 FEB 2015		UTM ZONE 16N
CHECK	SDC	04 FEB 2015		NAD 1983
REVIEW	AF	04 FEB 2015		1:85,000

File: SRK_NWMO_SCH_Fig09_DEMra1

462000 464000 466000 468000 470000 472000 474000

5430000 5428000 5426000 5424000 5422000 5420000

BLOCK A

Beavertrap Lake

Bath Lake

Winston Lake

Banana Lake

Triangle Lake

Pick Lake

Carib Lake

Coffee Lake

Little Duck L.

CROSSMAN LAKE BATHOLITH

Ross Lake Fault

5

15

6

10

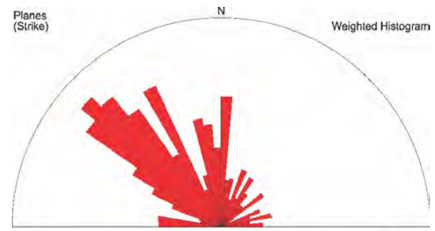
N

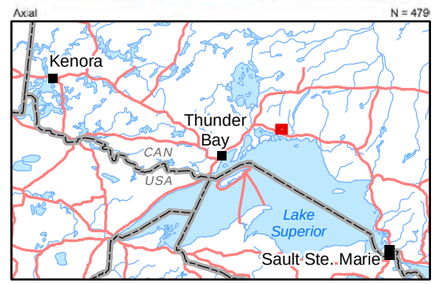
LEGEND

- Phase 2 Assessment Area
- Major Road
- Minor Road
- Watercourse
- Waterbody
- Matachewan mafic dike
- Dyke (Other)
- Mapped Fault
- Quetico/Wawa Subprovince boundary
- Batholith Contact

Reproducibility (RA_1)

- 1
- 2





REFERENCE

Base Data: MNR LIO, obtained 2009-2014
Relief backdrop: CDSM (NRCAN)
DEM: SGL 2015

2 km

srk consulting

PROJECT

Phase 2 Structural Lineament Interpretation
Schreiber Area, Ontario

TITLE

Interpreted Lineaments from Digital Elevation Data of the Schreiber Area - Block A

DESIGN	KR	02 SEP 2014	**Figure 9a**	REVISION 3
GIS	JA	04 FEB 2015		UTM ZONE 16N
CHECK	SDC	04 FEB 2015		NAD 1983
REVIEW	AF	04 FEB 2015		1:48,000

File: SRK_NWMO_SCH_Fig09a_DEMra1

480000 482000 484000 486000 488000 490000 492000

5426000 5424000 5422000 5420000 5418000 5416000

BLOCK B

Cameron L.

Charlotte Lake

Crossman Lake

Bluff Lake

Guy Lake

Louise Lake

Deep Lake

Catherine Lake

Clear Lake

Leader Lake

Rhumly L.

Spoke Lake

Robbie Lake

Fog L.

CROSSMAN LAKE BATHOLITH

Maude Lake

Syenite Lake

Syenite Lake Fault

Ducell Lake

SCHREIBER-HEMLO GREENSTONE BELT

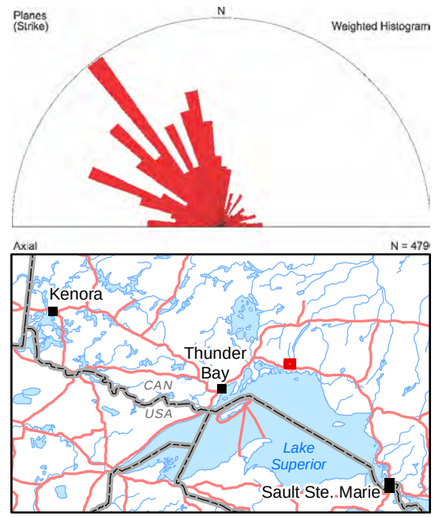
N

LEGEND

- Phase 2 Assessment Area
- Major Road
- Minor Road
- Watercourse
- Waterbody
- Matachewan mafic dyke
- Dyke (Other)
- Mapped Fault
- Quetico/Wawa Subprovince boundary
- Batholith Contact

Reproducibility (RA_1)

- 1
- 2



REFERENCE

Base Data: MNR LIO, obtained 2009-2014
Relief backdrop: CDSM (NRCAN)
DEM: SGL 2015

2 km

srk consulting

PROJECT

Phase 2 Structural Lineament Interpretation
Schreiber Area, Ontario

TITLE

Interpreted Lineaments from Digital Elevation Data of the Schreiber Area - Block B

DESIGN	KR	02 SEP 2014	**Figure 9b**	REVISION 3
GIS	JA	04 FEB 2015		UTM ZONE 16N
CHECK	SDC	04 FEB 2015		NAD 1983
REVIEW	AF	04 FEB 2015		1:48,000

File: SRK_NWMO_SCH_Fig09b_DEMra1

465000 470000 475000 480000 485000 490000

5435000 5430000 5425000 5420000 5415000

N

BLOCK A

BLOCK B

CROSSMAN LAKE
BATHOLITH

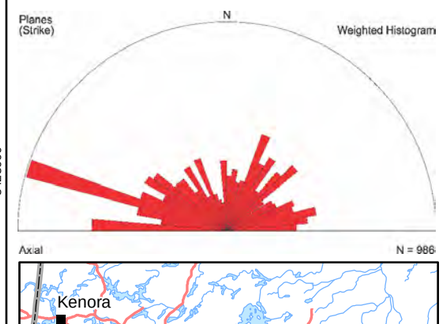
Whitesand – Winston Rd.

LEGEND

- Phase 2 Assessment Area
- Matachewan mafic dyke
- Dyke (Other)
- Mapped Fault
- Quetico/Wawa Subprovince boundary
- Batholith Contact

Reproducibility (RA_1)

- 1
- 2





REFERENCE

Base Data: MNR LIO, obtained 2009-2014
Image backdrop: TerraMetrics 2014
Detail: World View 2 GeoEye

5 km

srk consulting

PROJECT
Phase 2 Structural Lineament Interpretation
Schreiber Area, Ontario

TITLE
Interpreted Lineaments from Satellite Imagery Data of the Schreiber Area

DESIGN	KR	02 SEP 2014	**Figure 10**	REVISION 3
GIS	JA	04 FEB 2015		UTM ZONE 16N
CHECK	SDC	04 FEB 2015		NAD 1983
REVIEW	AF	04 FEB 2015		1:85,000

File: SRK_NWMO_SCH_Fig10_SATra1

462000 464000 466000 468000 470000 472000 474000

5430000 5428000 5426000 5424000 5422000 5420000

BLOCK A

Beavertrap Lake

Bath Lake

Winston Lake

Banana Lake

Triangle Lake

Pick Lake

Carb Lake

Coffee Lake

Little Duck L.

CROSSMAN LAKE BATHOLITH

Ross Lake Fault

5

15

6

10

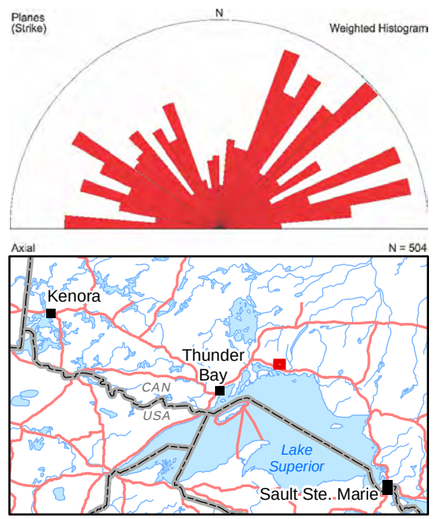
N

LEGEND

- Phase 2 Assessment Area
- Matachewan mafic dyke
- Dyke (Other)
- Mapped Fault
- Quetico/Wawa Subprovince boundary
- Batholith Contact

Reproducibility (RA_1)

- 1
- 2



REFERENCE

Base Data: MNR LIO, obtained 2009-2014
Image backdrop: TerraMetrics 2014
Detail: World View 2 GeoEye

0 1 km

srk consulting

PROJECT
Phase 2 Structural Lineament Interpretation
Schreiber Area, Ontario

TITLE
Interpreted Lineaments from Satellite Imagery Data of the Schreiber Area - Block A

DESIGN	KR	02 SEP 2014	**Figure 10a**	REVISION 3
GIS	JA	04 FEB 2015		UTM ZONE 16N
CHECK	SDC	04 FEB 2015		NAD 1983
REVIEW	AF	04 FEB 2015		1:48,000

File: SRK_NWMO_SCH_Fig10a_SATra1

480000 482000 484000 486000 488000 490000 492000

5426000 5424000 5422000 5420000 5418000 5416000

BLOCK B

CROSSMAN LAKE BATHOLITH

SCHREIBER-HEMLO GREENSTONE BELT

Syenite Lake Fault

5

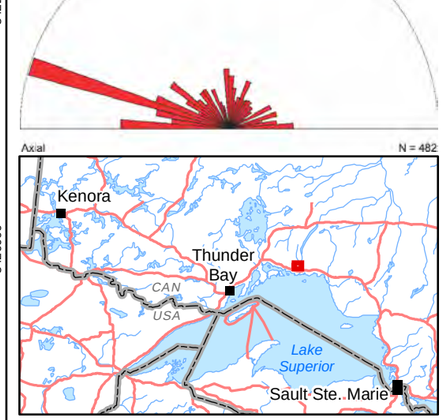
N

LEGEND

- Phase 2 Assessment Area
- Matachewan mafic dyke
- Dyke (Other)
- Mapped Fault
- Batholith Contact

Reproducibility (RA_1)

- 1
- 2



REFERENCE

Base Data: MNR LIO, obtained 2009-2014
Image backdrop: TerraMetrics 2014
Detail: World View 2 GeoEye

2 km

srk consulting

PROJECT
Phase 2 Structural Lineament Interpretation
Schreiber Area, Ontario

TITLE
Interpreted Lineaments from Satellite Imagery Data of the Schreiber Area - Block B

DESIGN	KR	02 SEP 2014	**Figure 10b**	REVISION 3
GIS	JA	04 FEB 2015		UTM ZONE 16N
CHECK	SDC	04 FEB 2015		NAD 1983
REVIEW	AF	04 FEB 2015		1:48,000

File: SRK_NWMO_SCH_Fig10b_SATra1

465000 470000 475000 480000 485000 490000

5435000 5430000 5425000 5420000 5415000

N

QUETICO METASEDIMENTARY ROCKS

CROSSMAN LAKE BATHOLITH

SCHREIBER-HEMLO GREENSTONE BELT

BLOCK A

BLOCK B

Chance Lake
Tonimac Lake
Northline Lake
Rope Lake
Southpine L.
Stingray Lake
Sandridge Lake
Shy L.
Carib Lake
Cable Lake
Coffee Lake
Beavertrap Lake
Bath Lake
Winston Lake
Big Duck Lake
Harvie Lake
Little Duck L.
Bobbie Lake
Cameron L.
Pick Lake
Banana Lake
Triangle Lake
Charlotte Lake
Crosman Lake
Bluff Lake
Guy Lake
Parsons Lake
Louise Lake
Deep Lake
Leader Lake
Catherine Lake
Clear Lake
Phumly L.
Spoke Lake
Fog L.
Robbie Lake
Ross Lake Fault
Sox Creek Fault
Syenite Lake Fault
Hornblende Lake
Upper Ross L.
Crystal Lake
Lower Ross L.
Needle Lake
Maude Lake
Syenite Lake
Ducell Lake
Davidson Lake
McCuaig Lake
Ellis Lake
Lyne Lake
Sox Lake

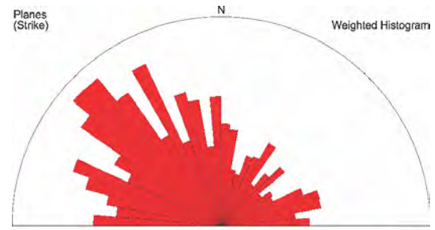
11 7 5 15 6 10

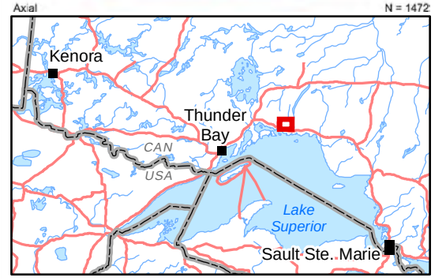
LEGEND

- Phase 2 Assessment Area
- Major Road
- Minor Road
- Watercourse
- Waterbody
- Matachewan mafic dyke
- Dyke (Other)
- Mapped Fault
- Quetico/Wawa Subprovince boundary
- Batholith Contact

Certainty
1
2
3

Bedrock Geology
- 10 Mafic suite
- 15 Biotite granite suite
- 7 Clastic metasedimentary rocks
- 6 Intermediate to felsic metavolcanic rocks
- 5 Mafic metavolcanic rocks
- 11 Tonalite gneiss suite





REFERENCE

Base Data: MNR LIO, obtained 2009-2014,
CanVec topography
Bedrock/Fault/Dyke: OGS MRD 126-REV1 (1:250,000)

5 km

srk consulting

PROJECT
Phase 2 Structural Lineament Interpretation
Schreiber Area, Ontario

TITLE
Interpreted Lineaments from Surficial Data of the Schreiber Area

DESIGN	KR	02 SEP 2014	**Figure 11**	REVISION 3
GIS	JA	04 FEB 2015		UTM ZONE 16N
CHECK	SDC	04 FEB 2015		NAD 1983
REVIEW	AF	04 FEB 2015		1:85,000

File: SRK_NWMO_SCH_Fig11_SurfRA1

462000 464000 466000 468000 470000 472000 474000

5430000 5428000 5426000 5424000 5422000 5420000

BLOCK A

Beavertrap Lake

Bath Lake

Pays Plat Lake

Winston Lake

Banana Lake

Triangle Lake

Carib Lake

Coffee Lake

Little Duck L.

Pick Lake

CROSSMAN LAKE BATHOLITH

Ross Lake Fault

15

5

6

10

N

LEGEND

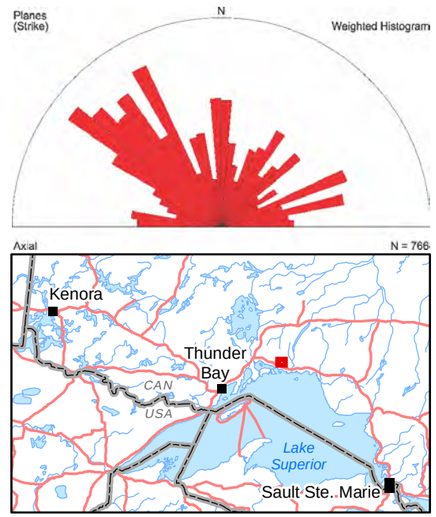
- Phase 2 Assessment Area
- Major Road
- Minor Road
- Watercourse
- Waterbody
- Matachewan mafic dyke
- Dyke (Other)
- Mapped Fault
- Quetico/Wawa Subprovince boundary
- Batholith Contact

Certainty

- 1
- 2
- 3

Bedrock Geology

- 10 Mafic suite
- 15 Biotite granite suite
- 7 Clastic metasedimentary rocks
- 6 Intermediate to felsic metavolcanic rocks
- 5 Mafic metavolcanic rocks
- 11 Tonalite gneiss suite



REFERENCE

Base Data: MNR LIO, obtained 2009-2014,
CanVec topography
Bedrock/Fault/Dyke: OGS MRD 126-REV1 (1:250,000)

0 1 km

srk consulting

PROJECT

Phase 2 Structural Lineament Interpretation
Schreiber Area, Ontario

TITLE

Interpreted Lineaments from Surficial Data of the Schreiber Area - Block A

DESIGN	KR	02 SEP 2014	**Figure 11a**	REVISION 2
GIS	JA	04 FEB 2015		UTM ZONE 16N
CHECK	SDC	04 FEB 2015		NAD 1983
REVIEW	AF	04 FEB 2015		1:48,000

File: SRK_NWMO_SCH_Fig11a_SurfRA1

480000 482000 484000 486000 488000 490000 492000

5426000 5424000 5422000 5420000 5418000 5416000

BLOCK B

Cameron L.

10

Crosman Lake

Guy Lake

15

Charlotte Lake

Bluff Lake

Louise Lake

Deep Lake

Catherine Lake

Clear Lake

CROSSMAN LAKE BATHOLITH

Leader Lake

5

Rhumly L.

Spoke Lake

Fog L.

Robbie Lake

Ducell Lake

Maude Lake

Syenite Lake

SCHREIBER-HEMLO GREENSTONE BELT

Syenite Lake Fault

N

LEGEND

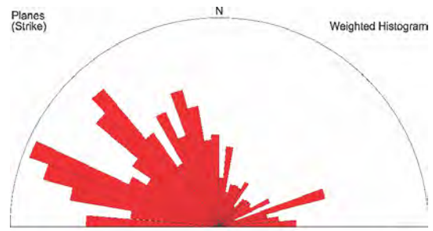
- Phase 2 Assessment Area
- Major Road
- Minor Road
- Watercourse
- Waterbody
- Matachewan mafic dyke
- Dyke (Other)
- Mapped Fault
- Quetico/Wawa Subprovince boundary
- Batholith Contact

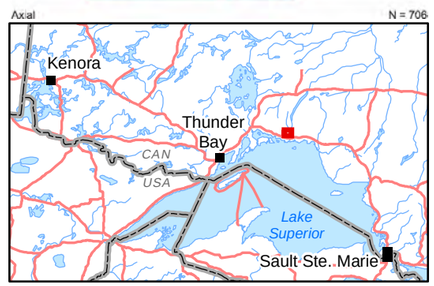
Certainty

- 1
- 2
- 3

Bedrock Geology

- 10 Mafic suite
- 15 Biotite granite suite
- 7 Clastic metasedimentary rocks
- 6 Intermediate to felsic metavolcanic rocks
- 5 Mafic metavolcanic rocks
- 11 Tonalite gneiss suite





REFERENCE

Base Data: MNR LIO, obtained 2009-2014,
CanVec topography
Bedrock/Fault/Dyke: OGS MRD 126-REV1 (1:250,000)

2 km

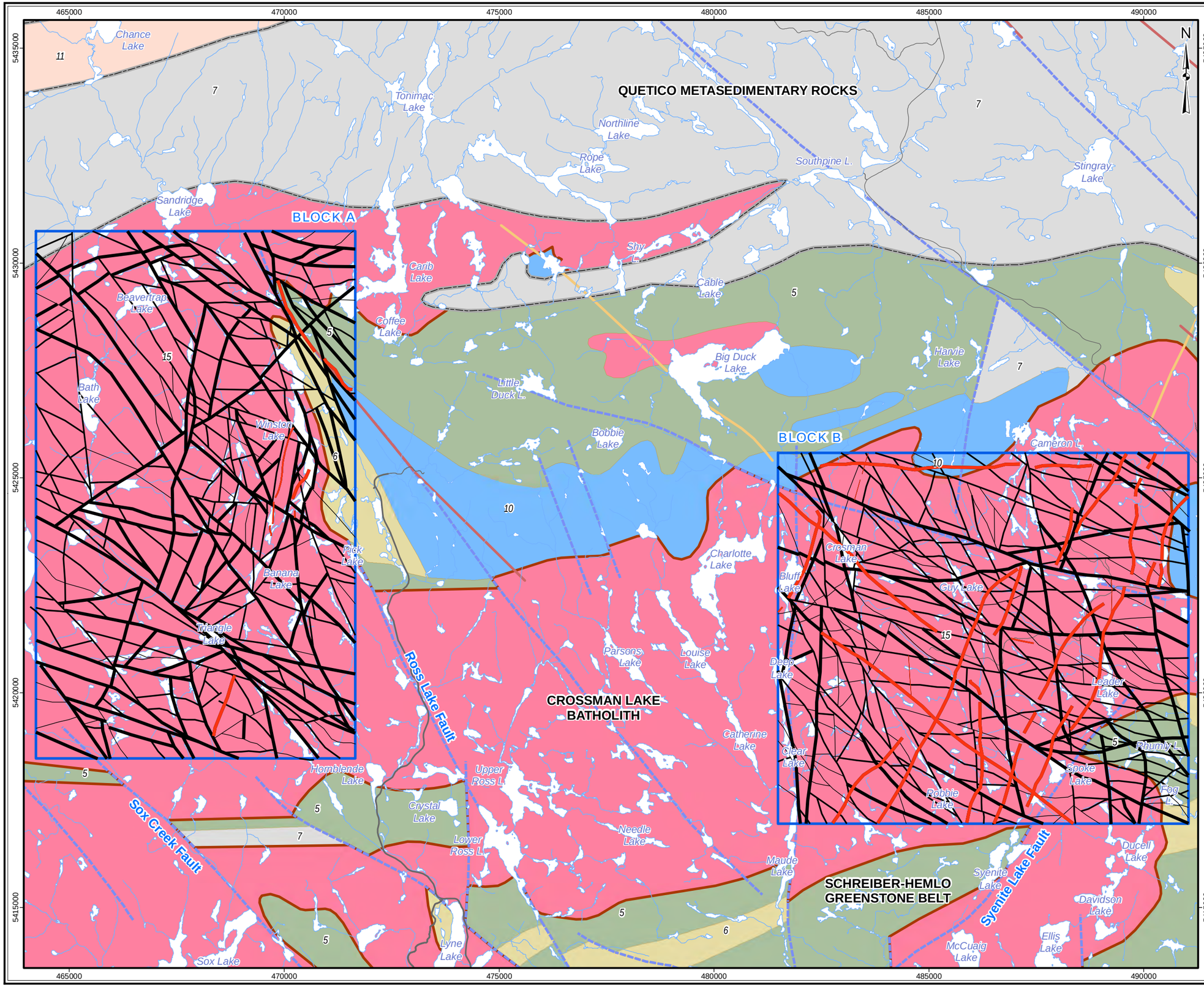
srk consulting

PROJECT
Phase 2 Structural Lineament Interpretation
Schreiber Area, Ontario

TITLE
Interpreted Lineaments from Surficial Data of the Schreiber Area - Block B

DESIGN	KR	02 SEP 2014	**Figure 11b**	REVISION 2
GIS	JA	04 FEB 2015		UTM ZONE 16N
CHECK	SDC	04 FEB 2015		NAD 1983
REVIEW	AF	04 FEB 2015		1:48,000

File: SRK_NWMO_SCH_Fig11b_SurfRA1



LEGEND

- Phase 2 Assessment Area
- Major Road
- Minor Road
- Watercourse
- Waterbody
- Matachewan mafic dyke
- Dyke (Other)
- Mapped Fault
- Quetico/Wawa Subprovince boundary
- Batholith Contact

Certainty

Lineament

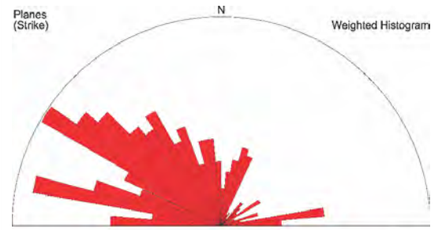
- 1
- 2
- 3

Dyke

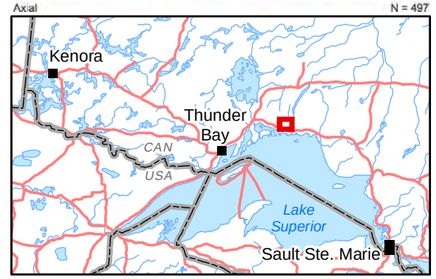
- 1
- 2
- 3

Bedrock Geology

- 10 Mafic suite
- 15 Biotite granite suite
- 7 Clastic metasedimentary rocks
- 6 Intermediate to felsic metavolcanic rocks
- 5 Mafic metavolcanic rocks
- 11 Tonalite gneiss suite



Axial N = 497



REFERENCE

Base Data: MNR LIO, obtained 2009-2014,
CanVec topography
Bedrock/Fault/Dyke: OGS MRD 126-REV1 (1:250,000)

5 km

srk consulting

PROJECT

Phase 2 Structural Lineament Interpretation
Schreiber Area, Ontario

TITLE

Interpreted Lineaments from Pole Reduced Magnetic Data of the Schreiber Area

DESIGN	KR	02 SEP 2014	**Figure 12**	REVISION 2
GIS	JA	04 FEB 2015		UTM ZONE 16N
CHECK	SDC	04 FEB 2015		NAD 1983
REVIEW	AF	04 FEB 2015		1:85,000

File: SRK_NWMO_SCH_Fig12_GeophRA1

462000 464000 466000 468000 470000 472000 474000

5430000 5428000 5426000 5424000 5422000 5420000

BLOCK A

Beavertrap Lake

Bath Lake

Pays Plat Lake

Winston Lake

Carib Lake

Coffee Lake

Little Duck L.

Pick Lake

Banana Lake

Triangle Lake

CROSSMAN LAKE BATHOLITH

Ross Lake Fault

15

5

6

10

N

LEGEND

- Phase 2 Assessment Area
- Major Road
- Minor Road
- Watercourse
- Waterbody
- Matachewan mafic dyke
- Dyke (Other)
- Mapped Fault
- Quetico/Wawa Subprovince boundary
- Batholith Contact

Certainty

Lineament

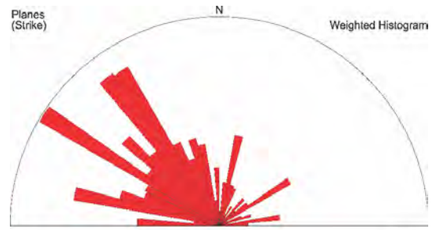
- 1
- 2
- 3

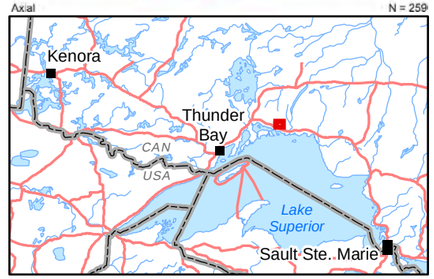
Dyke

- 1
- 2
- 3

Bedrock Geology

- 10 Mafic suite
- 15 Biotite granite suite
- 7 Clastic metasedimentary rocks
- 6 Intermediate to felsic metavolcanic rocks
- 5 Mafic metavolcanic rocks
- 11 Tonalite gneiss suite





REFERENCE

Base Data: MNR LIO, obtained 2009-2014,
CanVec topography
Bedrock/Fault/Dyke: OGS MRD 126-REV1 (1:250,000)

0 1 km

srk consulting

PROJECT

Phase 2 Structural Lineament Interpretation
Schreiber Area, Ontario

TITLE

Interpreted Lineaments from Pole Reduced Magnetic Data of the Schreiber Area - Block A

DESIGN	KR	02 SEP 2014	**Figure 12a**	REVISION 2
GIS	JA	04 FEB 2015		UTM ZONE 16N
CHECK	SDC	04 FEB 2015		NAD 1983
REVIEW	AF	04 FEB 2015		1:48,000

File: SRK_NWMO_SCH_Fig12a_GeophRA1

480000 482000 484000 486000 488000 490000 492000

5426000 5424000 5422000 5420000 5418000 5416000

BLOCK B

Cameron L.

Charlotte Lake

Bluff Lake

Crosman Lake

Guy Lake

Louise Lake

Deep Lake

Leader Lake

Catherine Lake

Clear Lake

Rhumly L.

Spoke Lake

Fog L.

Robbie Lake

CROSSMAN LAKE BATHOLITH

Ducell Lake

Maude Lake

Syenite Lake

SCHREIBER-HEMLO GREENSTONE BELT

Syenite Lake Fault

10

15

5

N

LEGEND

- Phase 2 Assessment Area
- Major Road
- Minor Road
- Watercourse
- Waterbody
- Matachewan mafic dyke
- Dyke (Other)
- Mapped Fault
- Quetico/Wawa Subprovince boundary
- Batholith Contact

Certainty

Lineament

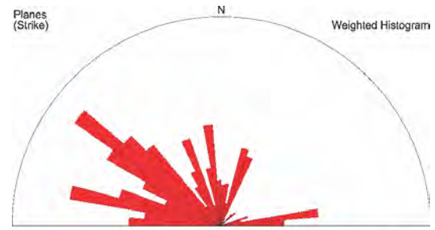
- 1
- 2
- 3

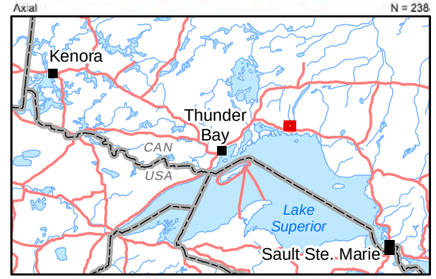
Dyke

- 1
- 2
- 3

Bedrock Geology

- 10 Mafic suite
- 15 Biotite granite suite
- 7 Clastic metasedimentary rocks
- 6 Intermediate to felic metavolcanic rocks
- 5 Mafic metavolcanic rocks
- 11 Tonalite gneiss suite





REFERENCE

Base Data: MNR LIO, obtained 2009-2014,
CanVec topography
Bedrock/Fault/Dyke: OGS MRD 126-REV1 (1:250,000)

2 km

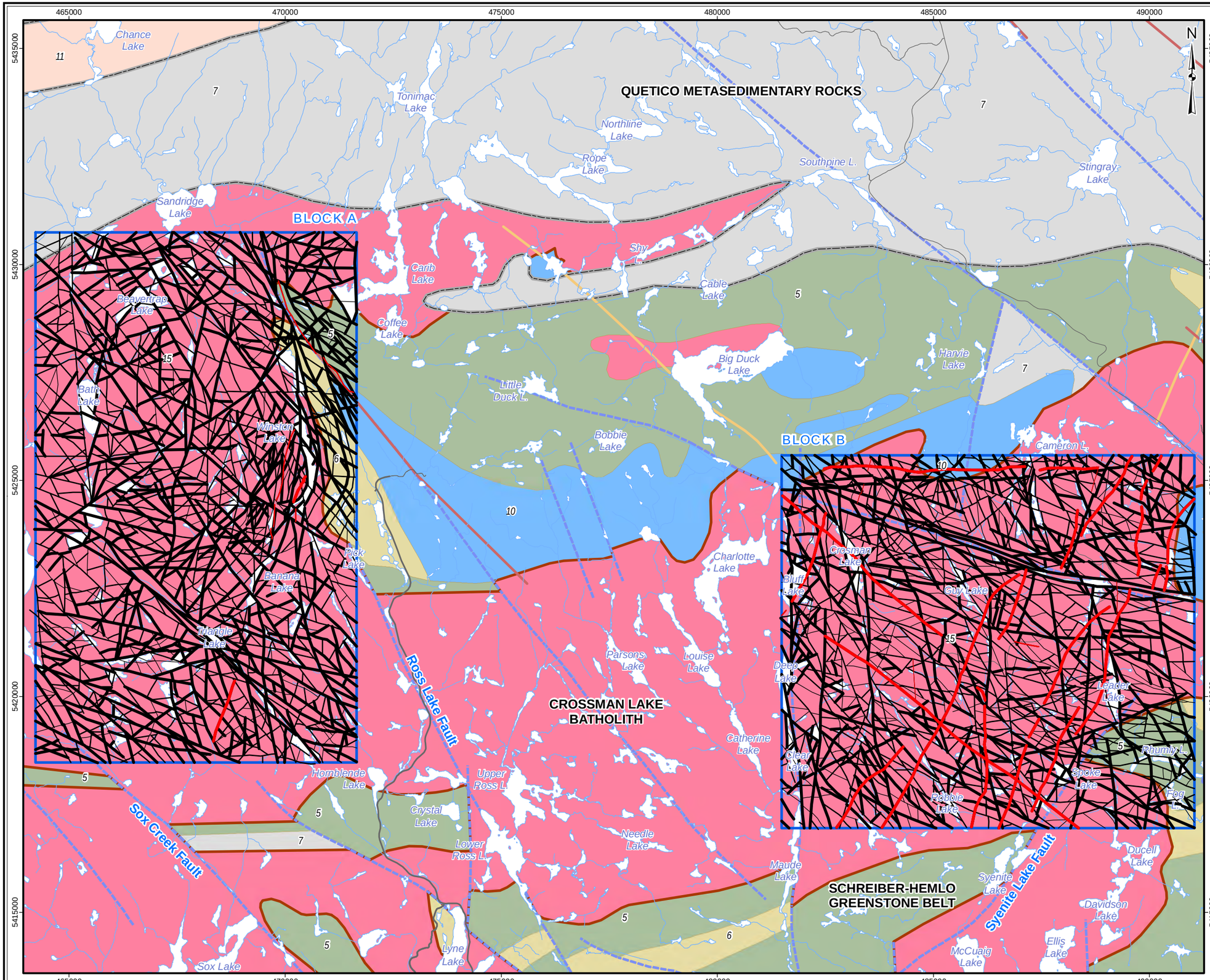
srk consulting

PROJECT
Phase 2 Structural Lineament Interpretation
Schreiber Area, Ontario

TITLE
Interpreted Lineaments from Pole Reduced Magnetic Data of the Schreiber Area - Block B

DESIGN	KR	02 SEP 2014	**Figure 12b**	REVISION 2
GIS	JA	04 FEB 2015		UTM ZONE 16N
CHECK	SDC	04 FEB 2015		NAD 1983
REVIEW	AF	04 FEB 2015		1:48,000

File: SRK_NWMO_SCH_Fig12b_GeophRA1



LEGEND

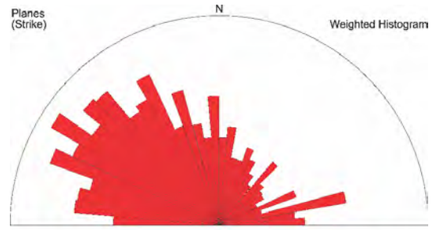
- Phase 2 Assessment Area
- Major Road
- Minor Road
- Watercourse
- Waterbody
- Matachewan mafic dyke
- Dyke (Other)
- Mapped Fault
- Quetico/Wawa Subprovince boundary
- Batholith Contact

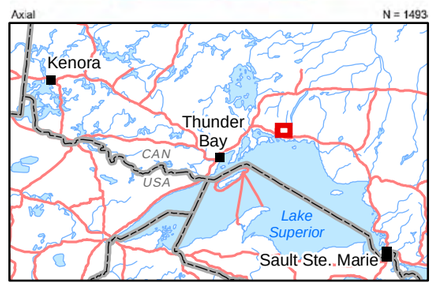
Bedrock Geology

- 10 Mafic suite
- 15 Biotite granite suite
- 7 Clastic metasedimentary rocks
- 6 Intermediate to felsic metavolcanic rocks
- 5 Mafic metavolcanic rocks
- 11 Tonalite gneiss suite

Certainty

Lineament	Dyke
1	1
2	2
3	3





REFERENCE

Base Data: MNR LIO, obtained 2009-2014,
CanVec topography
Bedrock/Fault/Dyke: OGS MRD 126-REV1 (1:250,000)

5 km

srk consulting

PROJECT
Phase 2 Structural Lineament Interpretation
Schreiber Area, Ontario

TITLE
Final Integrated Interpreted Lineaments (RA-2) of the Schreiber Area

DESIGN	KR	02 SEP 2014	**Figure 13**	REVISION 3
GIS	JA	04 FEB 2015		UTM ZONE 16N
CHECK	SDC	04 FEB 2015		NAD 1983
REVIEW	AF	04 FEB 2015		1:85,000

File: SRK_NWMO_SCH_Fig13_FinalRA2

462000 464000 466000 468000 470000 472000 474000

5430000 5428000 5426000 5424000 5422000 5420000

BLOCK A

Beavertrap Lake

Bath Lake

Winston Lake

Banana Lake

Triangle Lake

Carib Lake

Coffee Lake

Little Duck L.

Pick Lake

CROSSMAN LAKE BATHOLITH

Ross Lake Fault

15

5

6

10

N

LEGEND

- Phase 2 Assessment Area
- Major Road
- Minor Road
- Watercourse
- Waterbody
- Matachewan mafic dyke
- Dyke (Other)
- Mapped Fault
- Quetico/Wawa Subprovince boundary
- Batholith Contact

Bedrock Geology

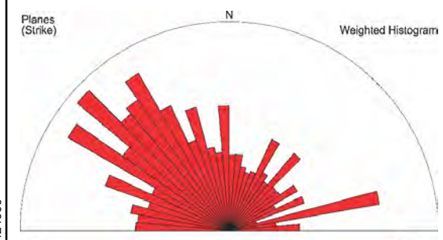
- 10 Mafic suite
- 15 Biotite granite suite
- 7 Clastic metasedimentary rocks
- 6 Intermediate to felsic metavolcanic rocks
- 5 Mafic metavolcanic rocks
- 11 Tonalite gneiss suite

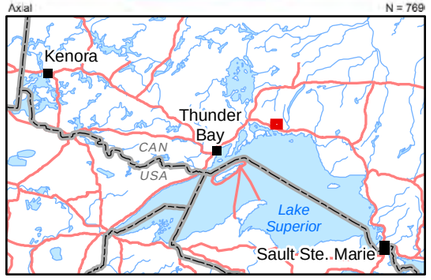
Lineament, Certainty

- 1
- 2
- 3

Dyke, Certainty

- 1
- 2
- 3





REFERENCE

Base Data: MNR LIO, obtained 2009-2014,
CanVec topography
Bedrock/Fault/Dyke: OGS MRD 126-REV1 (1:250,000)

0 1 km

srk consulting

PROJECT
Phase 2 Structural Lineament Interpretation
Schreiber Area, Ontario

TITLE
Final Integrated Interpreted Lineaments (RA-2) of the Schreiber Area - Block A

DESIGN	KR	02 SEP 2014	**Figure 13a**	REVISION 3
GIS	JA	04 FEB 2015		UTM ZONE 16N
CHECK	SDC	04 FEB 2015		NAD 1983
REVIEW	AF	04 FEB 2015		1:48,000

File: SRK_NWMO_SCH_Fig13a_FinalRA2

480000 482000 484000 486000 488000 490000 492000

5426000 5424000 5422000 5420000 5418000 5416000

BLOCK B

Cameron L.

Crosman Lake

Charlotte Lake

Bluff Lake

Guy Lake

Louise Lake

Deep Lake

Leader Lake

Catherine Lake

Clear Lake

Rhumly L.

Spoke Lake

Fog L.

Robbie Lake

CROSSMAN LAKE BATHOLITH

Ducell Lake

Maude Lake

Syenite Lake

Syenite Lake Fault

SCHREIBER-HEMLO GREENSTONE BELT

10

15

5

N

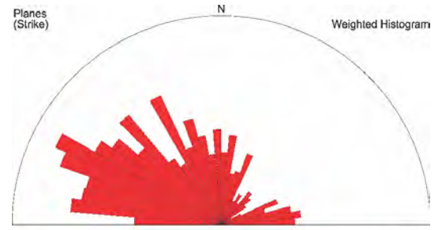
LEGEND

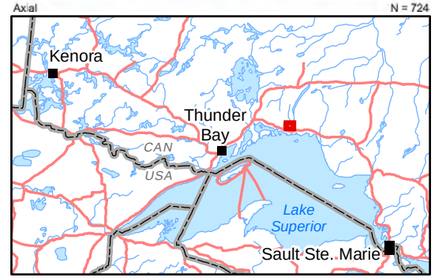
- Phase 2 Assessment Area
- Major Road
- Minor Road
- Watercourse
- Waterbody
- Matachewan mafic dyke
- Dyke (Other)
- Mapped Fault
- Quetico/Wawa Subprovince boundary
- Batholith Contact

Bedrock Geology

- 10 Mafic suite
- 15 Biotite granite suite
- 7 Clastic metasedimentary rocks
- 6 Intermediate to felsic metavolcanic rocks
- 5 Mafic metavolcanic rocks
- 11 Tonalite gneiss suite

Lineament, Certainty	Dyke, Certainty
1	1
2	2
3	3





REFERENCE

Base Data: MNR LIO, obtained 2009-2014,
CanVec topography
Bedrock/Fault/Dyke: OGS MRD 126-REV1 (1:250,000)

2 km

srk consulting

PROJECT
Phase 2 Structural Lineament Interpretation
Schreiber Area, Ontario

TITLE
Final Integrated Interpreted Lineaments (RA-2) of the Schreiber Area - Block B

DESIGN	KR	02 SEP 2014	**Figure 13b**	REVISION 3
GIS	JA	04 FEB 2015		UTM ZONE 16N
CHECK	SDC	04 FEB 2015		NAD 1983
REVIEW	AF	04 FEB 2015		1:48,000

File: SRK_NWMO_SCH_Fig13b_FinalRA2

462000 464000 466000 468000 470000 472000 474000

5430000 5428000 5426000 5424000 5422000 5420000

BLOCK A

Beavertrap Lake

Carib Lake

Coffee Lake

Bath Lake

Winston Lake

Little Duck L.

Pick Lake

Banana Lake

Triangle Lake

CROSSMAN LAKE BATHOLITH

Ross Lake Fault

15

5

6

10

N

LEGEND

- Phase 2 Assessment Area
- Major Road
- Minor Road
- Watercourse
- Waterbody
- Matachewan mafic dyke
- Dyke (Other)
- Mapped Fault
- Quetico/Wawa Subprovince
- Batholith Contact

Dkye, Length

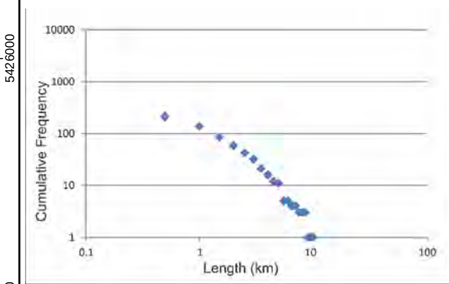
- <1 km
- 1 - 2.5
- 2.5 - 5
- >5 km

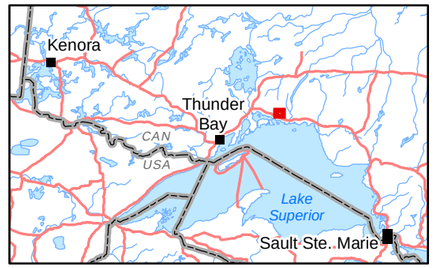
Lineament, Length

- <1 km
- 1 - 2.5
- 2.5 - 5
- >5 km

Bedrock Geology

- 10 Mafic suite
- 15 Biotite granite suite
- 7 Clastic metasedimentary rocks
- 6 Intermediate to felsic metavolcanic rocks
- 5 Mafic metavolcanic rocks
- 11 Tonalite gneiss suite





REFERENCE

Base Data: MNR LIO, obtained 2009-2014,
CanVec topography
Bedrock/Fault/Dyke: OGS MRD 126-REV1 (1:250,000)

0 2 km

srk consulting

PROJECT

Phase 2 Structural Lineament Interpretation
Schreiber Area, Ontario

TITLE

Geophysical Lineaments by Length of the Schreiber Area - Block A

DESIGN	KR	02 SEP 2014	**Figure 14**	REVISION 3
GIS	JA	04 FEB 2015		UTM ZONE 16N
CHECK	SDC	04 FEB 2015		NAD 1983
REVIEW	AF	04 FEB 2015		1:48,000

File: SRK_NWMO_SCH_Fig14_GeophLenA

480000 482000 484000 486000 488000 490000 492000

5426000 5424000 5422000 5420000 5418000 5416000

BLOCK B

Cameron L.

Crosman Lake

Charlotte Lake

Bluff Lake

Guy Lake

Louise Lake

Deep Lake

Catherine Lake

Clear Lake

Leader Lake

Rhumly L.

Spoke Lake

Fog L.

Robbie Lake

Ducell Lake

Maude Lake

Syenite Lake

Syenite Lake Fault

CROSSMAN LAKE BATHOLITH

SCHREIBER-HEMLO GREENSTONE BELT

10 15 5

N

LEGEND

- Phase 2 Assessment Area
- Major Road
- Minor Road
- Watercourse
- Waterbody
- Matachewan mafic dike
- Dyke (Other)
- Mapped Fault
- Quetico/Wawa Subprovince
- Batholith Contact

Dkye, Length

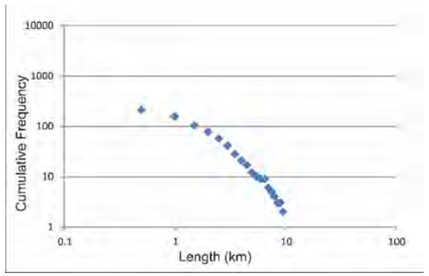
- <1 km
- 1 - 2.5
- 2.5 - 5
- >5 km

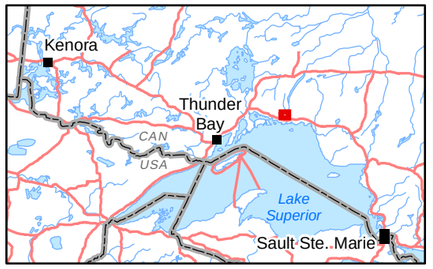
Lineament, Length

- <1 km
- 1 - 2.5
- 2.5 - 5
- >5 km

Bedrock Geology

- 10 Mafic suite
- 15 Biotite granite suite
- 7 Clastic metasedimentary rocks
- 6 Intermediate to felsic metavolcanic rocks
- 5 Mafic metavolcanic rocks
- 11 Tonalite gneiss suite





REFERENCE

Base Data: MNR LIO, obtained 2009-2014,
CanVec topography
Bedrock/Fault/Dyke: OGS MRD 126-REV1 (1:250,000)

2 km

srk consulting

PROJECT

Phase 2 Structural Lineament Interpretation
Schreiber Area, Ontario

TITLE

Geophysical Lineaments by Length of the Schreiber Area - Block B

DESIGN	KR	02 SEP 2014	**Figure 15**	REVISION 3
GIS	JA	04 FEB 2015		UTM ZONE 16N
CHECK	SDC	04 FEB 2015		NAD 1983
REVIEW	AF	04 FEB 2015		1:48,000

File: SRK_NWMO_SCH_Fig15_GeophLenB

462000 464000 466000 468000 470000 472000 474000

5430000 5428000 5426000 5424000 5422000 5420000

BLOCK A

Beavertrap Lake

Bath Lake

Winston Lake

Carib Lake

Coffee Lake

Little Duck L.

Pick Lake

Banana Lake

Triangle Lake

CROSSMAN LAKE BATHOLITH

Ross Lake Fault

15

5

6

10

N

LEGEND

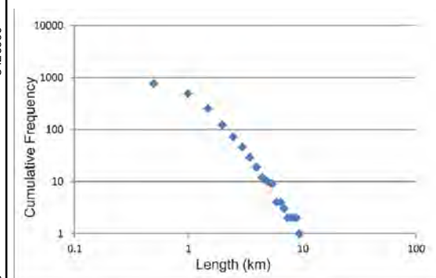
- Phase 2 Assessment Area
- Major Road
- Minor Road
- Watercourse
- Waterbody
- Matachewan mafic dike
- Dyke (Other)
- Mapped Fault
- Quetico/Wawa Subprovince boundary
- Batholith Contact

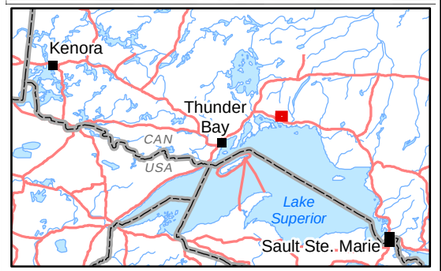
Length

- <1 km
- 1 - 2.5
- 2.5 - 5
- >5 km

Bedrock Geology

- 10 Mafic suite
- 15 Biotite granite suite
- 7 Clastic metasedimentary rocks
- 6 Intermediate to felsic metavolcanic rocks
- 5 Mafic metavolcanic rocks
- 11 Tonalite gneiss suite





REFERENCE

Base Data: MNR LIO, obtained 2009-2014,
CanVec topography
Bedrock/Fault/Dyke: OGS MRD 126-REV1 (1:250,000)

2 km

srk consulting

PROJECT

Phase 2 Structural Lineament Interpretation
Schreiber Area, Ontario

TITLE

Surficial Lineaments by Length of the Schreiber Area - Block A

DESIGN	KR	02 SEP 2014	**Figure 16**	REVISION 3
GIS	JA	04 FEB 2015		UTM ZONE 16N
CHECK	SDC	04 FEB 2015		NAD 1983
REVIEW	AF	04 FEB 2015		1:48,000

File: SRK_NWMO_SCH_Fig16_SurfLenA

480000 482000 484000 486000 488000 490000 492000

5426000 5424000 5422000 5420000 5418000 5416000

BLOCK B

Cameron L.

10

15

5

Crosman Lake

Guy Lake

Charlotte Lake

Bluff Lake

Louise Lake

Deep Lake

Catherine Lake

Clear Lake

Leader Lake

Rhumly L.

Spoke Lake

Fog L.

Robbie Lake

Ducell Lake

Maude Lake

Syenite Lake

Syenite Lake Fault

CROSSMAN LAKE BATHOLITH

SCHREIBER-HEMLO GREENSTONE BELT

N

LEGEND

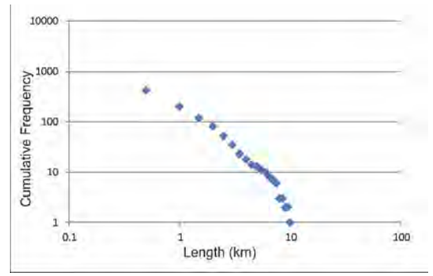
- Phase 2 Assessment Area
- Major Road
- Minor Road
- Watercourse
- Waterbody
- Matachewan mafic dike
- Dyke (Other)
- Mapped Fault
- Quetico/Wawa Subprovince boundary
- Batholith Contact

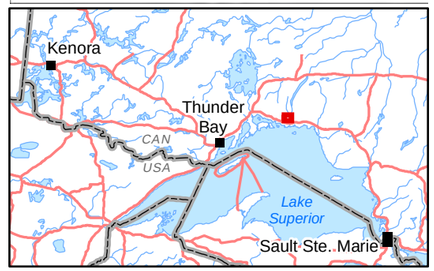
Length

- <1 km
- 1 - 2.5
- 2.5 - 4
- >5 km

Bedrock Geology

- 10 Mafic suite
- 15 Biotite granite suite
- 7 Clastic metasedimentary rocks
- 6 Intermediate to felsic metavolcanic rocks
- 5 Mafic metavolcanic rocks
- 11 Tonalite gneiss suite





REFERENCE

Base Data: MNR LIO, obtained 2009-2014,
CanVec topography
Bedrock/Fault/Dyke: OGS MRD 126-REV1 (1:250,000)

2 km

srk consulting

PROJECT

Phase 2 Structural Lineament Interpretation
Schreiber Area, Ontario

TITLE

Surficial Lineaments by Length of the Schreiber Area - Block B

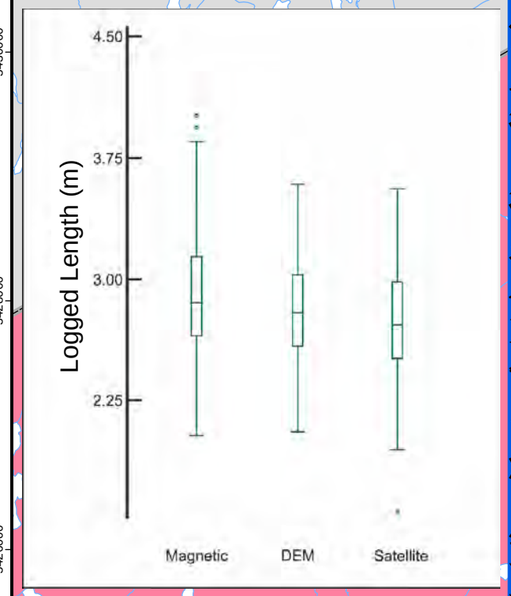
DESIGN	KR	02 SEP 2014	**Figure 17**	REVISION 3
GIS	JA	04 FEB 2015		UTM ZONE 16N
CHECK	SDC	04 FEB 2015		NAD 1983
REVIEW	AF	04 FEB 2015		1:48,000

File: SRK_NWMO_SCH_Fig17_SurfLenB

462000 464000 466000 468000 470000 472000 474000

5430000 5428000 5426000 5424000 5422000 5420000

BLOCK A



Beavertrap Lake

Bath Lake

Winston Lake

Carib Lake

Coffee Lake

Little Duck L.

Pick Lake

Banana Lake

Triangle Lake

CROSSMAN LAKE BATHOLITH

Ross Lake Fault

5 6 10 15

N

LEGEND

- Phase 2 Assessment Area
- Major Road
- Minor Road
- Watercourse
- Waterbody
- Matachewan mafic dike
- Dyke (Other)
- Mapped Fault
- Quetico/Wawa Subprovince
- Batholith Contact

Dyke, Length

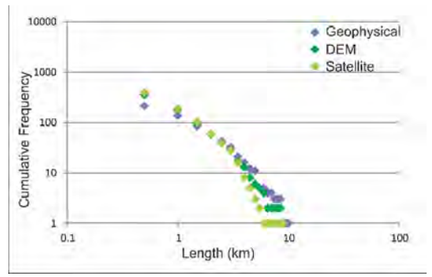
- <1 km
- 1 - 2.5
- 2.5 - 5
- >5 km

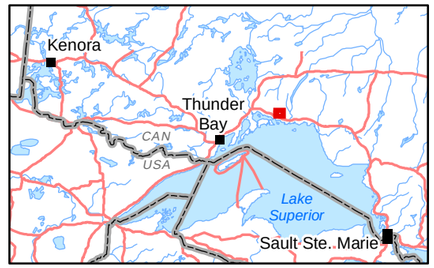
Lineament, Length

- <1 km
- 1 - 2.5
- 2.5 - 5
- >5 km

Bedrock Geology

- 10 Mafic suite
- 15 Biotite granite suite
- 7 Clastic metasedimentary rocks
- 6 Intermediate to felsic metavolcanic rocks
- 5 Mafic metavolcanic rocks
- 11 Tonalite gneiss suite





REFERENCE

Base Data: MNR LIO, obtained 2009-2014,
CanVec topography
Bedrock/Fault/Dyke: OGS MRD 126-REV1 (1:250,000)

2 km

srk consulting

PROJECT

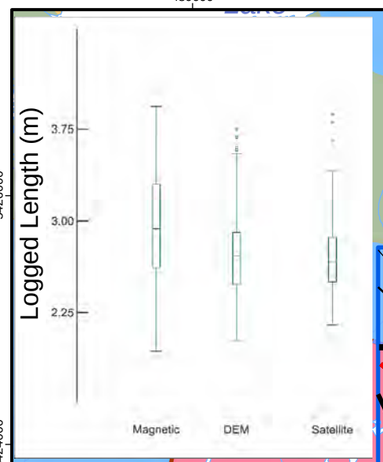
Phase 2 Structural Lineament Interpretation
Schreiber Area, Ontario

TITLE

Final Integrated Lineaments by Length of the Schreiber Area - Block A

DESIGN	KR	02 SEP 2014	**Figure 18**	REVISION 3
GIS	JA	04 FEB 2015		UTM ZONE 16N
CHECK	SDC	04 FEB 2015		NAD 1983
REVIEW	AF	04 FEB 2015		1:48,000

File: SRK_NWMO_SCH_Fig18_FinalLenA



480000 482000 484000 486000 488000 490000 492000

5426000 5424000 5422000 5420000 5418000 5416000

BLOCK B

Cameron L.

Crosman Lake

Guy Lake

Charlotte Lake

Bluff Lake

Louise Lake

Deep Lake

Catherine Lake

Clear Lake

Leader Lake

Rhumly L.

Spoke Lake

Fog L.

Robbie Lake

Ducell Lake

Maude Lake

Syenite Lake

Syenite Lake Fault

CROSSMAN LAKE BATHOLITH

SCHREIBER-HEMLO GREENSTONE BELT

10

15

5

N

LEGEND

- Phase 2 Assessment Area
- Major Road
- Minor Road
- Watercourse
- Waterbody
- Matachewan mafic dike
- Dyke (Other)
- Mapped Fault
- Quetico/Wawa Subprovince
- Batholith Contact

Dyke, Length

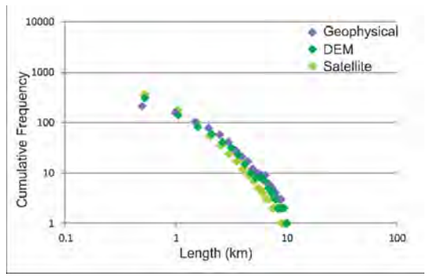
- <1 km
- 1 - 2.5
- 2.5 - 5
- >5 km

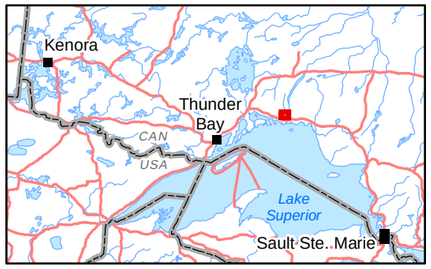
Lineament, Length

- <1 km
- 1 - 2.5
- 2.5 - 5
- >5 km

Bedrock Geology

- 10 Mafic suite
- 15 Biotite granite suite
- 7 Clastic metasedimentary rocks
- 6 Intermediate to felsic metavolcanic rocks
- 5 Mafic metavolcanic rocks
- 11 Tonalite gneiss suite





REFERENCE

Base Data: MNR LIO, obtained 2009-2014,
CanVec topography
Bedrock/Fault/Dyke: OGS MRD 126-REV1 (1:250,000)

2 km

srk consulting

PROJECT

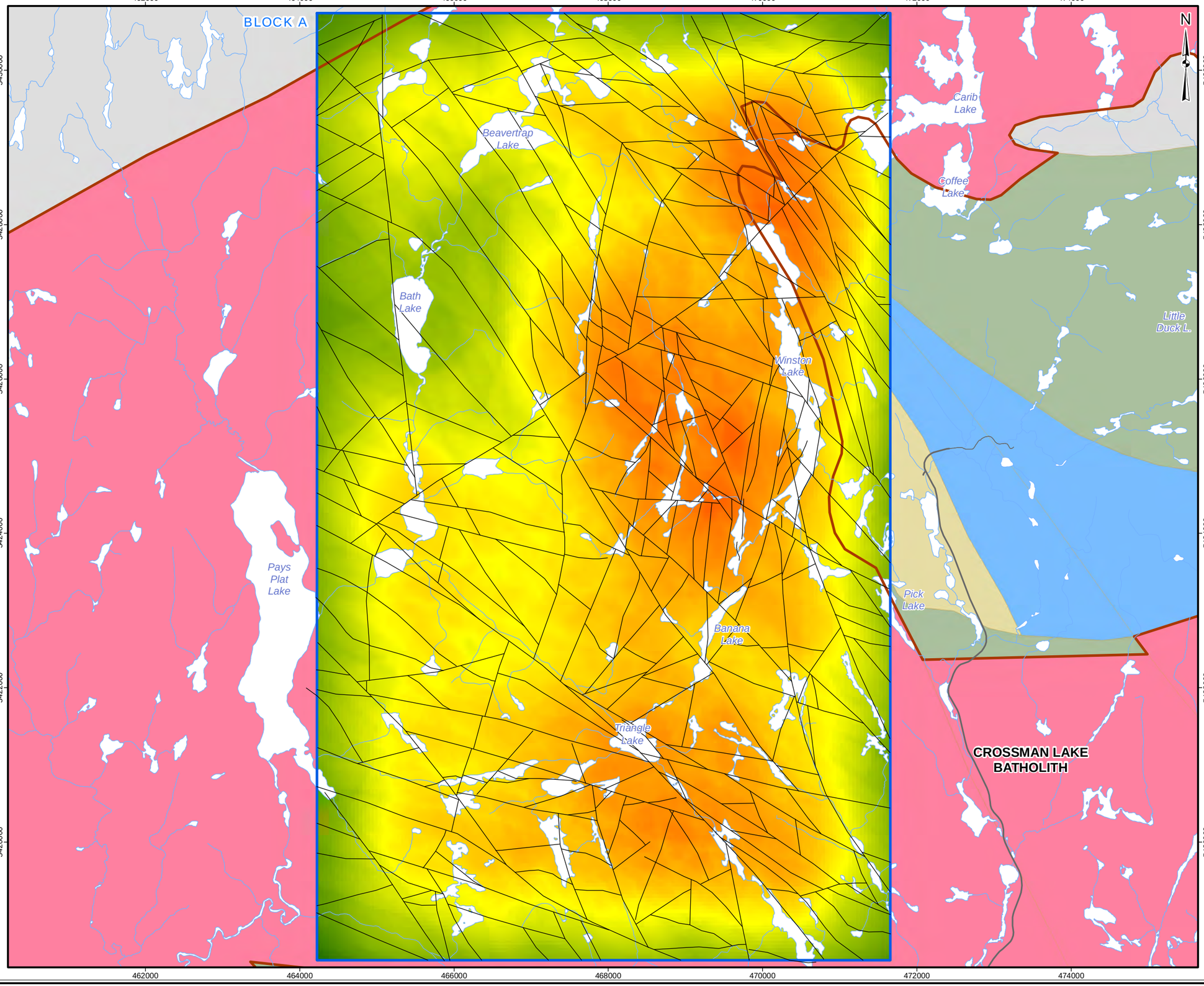
Phase 2 Structural Lineament Interpretation
Schreiber Area, Ontario

TITLE

Final Integrated Lineaments by Length of the Schreiber Area - Block B

DESIGN	KR	02 SEP 2014	Figure 19	REVISION 3
GIS	JA	04 FEB 2015		UTM ZONE 16N
CHECK	SDC	04 FEB 2015		NAD 1983
REVIEW	AF	04 FEB 2015		1:48,000

File: SRK_NWMO_SCH_Fig19_FinalLenB



LEGEND

- Phase 2 Assessment Area
- Major Road
- Minor Road
- Watercourse
- Waterbody
- Batholith Contact
- Lineament - Geophysical

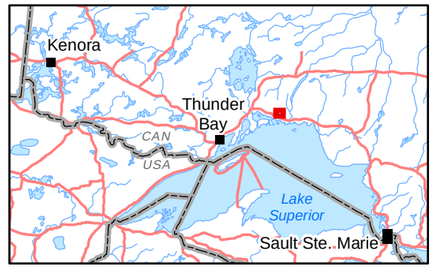
Bedrock Geology

- 10 Mafic suite
- 15 Biotite granite suite
- 7 Clastic metasedimentary rocks
- 6 Intermediate to felsic metavolcanic rocks
- 5 Mafic metavolcanic rocks
- 11 Tonalite gneiss suite

Geophysical Lineament Density

High : 7.26 (km/km²)

Low : 0



REFERENCE

Base Data: MNR LIO, obtained 2009-2014,
CanVec topography
Bedrock: OGS MRD 126-REV1 (1:250,000)

2 km

srk consulting

PROJECT

Phase 2 Structural Lineament Interpretation
Schreiber Area, Ontario

TITLE

Geophysical Lineament Density of the Schreiber Area - Block A

DESIGN	KR	02 SEP 2014	**Figure 20**	REVISION 3
GIS	JA	04 FEB 2015		UTM ZONE 16N
CHECK	SDC	04 FEB 2015		NAD 1983
REVIEW	AF	04 FEB 2015		1:48,000

File: SRK_NWMO_SCH_Fig20_DensMAGa

480000 482000 484000 486000 488000 490000 492000

5426000 5424000 5422000 5420000 5418000 5416000

BLOCK B

Cameron L.

Crosman Lake

Guy Lake

Charlotte Lake

Bluff Lake

Louise Lake

Deep Lake

Catherine Lake

Clear Lake

Leader Lake

Rhumly L.

Spoke Lake

Fog L.

Robbie Lake

Maude Lake

Syenite Lake

Ducell Lake

CROSSMAN LAKE BATHOLITH

SCHREIBER-HEMLO GREENSTONE BELT

N

LEGEND

- Phase 2 Assessment Area
- Major Road
- Minor Road
- Watercourse
- Waterbody
- Batholith Contact
- Lineament - Geophysical

Bedrock Geology

- 10 Mafic suite
- 15 Biotite granite suite
- 7 Clastic metasedimentary rocks
- 6 Intermediate to felsic metavolcanic rocks
- 5 Mafic metavolcanic rocks
- 11 Tonalite gneiss suite

Geophysical Lineament Density

High : 7.26 (km/km²)

Low : 0

Kenora

Thunder Bay

CAN

USA

Lake Superior

Sault Ste. Marie

REFERENCE

Base Data: MNR LIO, obtained 2009-2014,
CanVec topography
Bedrock: OGS MRD 126-REV1 (1:250,000)

2 km

srk consulting

PROJECT

Phase 2 Structural Lineament Interpretation
Schreiber Area, Ontario

TITLE

Geophysical Lineament Density of the Schreiber Area - Block B

DESIGN	KR	02 SEP 2014	**Figure 21**	REVISION 3
GIS	JA	04 FEB 2015		UTM ZONE 16N
CHECK	SDC	04 FEB 2015		NAD 1983
REVIEW	AF	04 FEB 2015		1:48,000

File: SRK_NWMO_SCH_Fig21_DensMAGb

462000 464000 466000 468000 470000 472000 474000

5430000 5428000 5426000 5424000 5422000 5420000

BLOCK A

Beavertrap Lake

Bath Lake

Pays Plat Lake

Carib Lake

Coffee Lake

Little Duck L.

Winston Lake

Pick Lake

Banana Lake

Triangle Lake

CROSSMAN LAKE BATHOLITH

N

LEGEND

- Phase 2 Assessment Area
- Major Road
- Minor Road
- Watercourse
- Waterbody
- Batholith Contact
- Lineament - Surficial

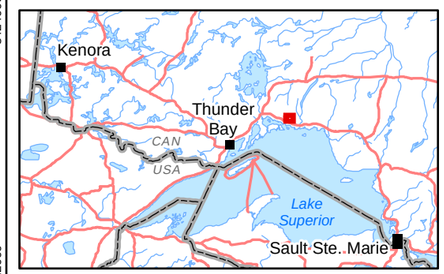
Bedrock Geology

- 10 Mafic suite
- 15 Biotite granite suite
- 7 Clastic metasedimentary rocks
- 6 Intermediate to felsic metavolcanic rocks
- 5 Mafic metavolcanic rocks
- 11 Tonalite gneiss suite

Surficial Lineament Density

High : 11.00 (km/km²)

Low : 0



REFERENCE

Base Data: MNR LIO, obtained 2009-2014,
CanVec topography
Bedrock: OGS MRD 126-REV1 (1:250,000)

2 km

srk consulting

PROJECT

Phase 2 Structural Lineament Interpretation
Schreiber Area, Ontario

TITLE

Surficial Lineament Density of the Schreiber Area - Block A

DESIGN	KR	02 SEP 2014	**Figure 22**	REVISION 3
GIS	JA	04 FEB 2015		UTM ZONE 16N
CHECK	SDC	04 FEB 2015		NAD 1983
REVIEW	AF	04 FEB 2015		1:48,000

File: SRK_NWMO_SCH_Fig22_DensSURFa

480000 482000 484000 486000 488000 490000 492000

5426000 5424000 5422000 5420000 5418000 5416000

BLOCK B

Cameron L.

Charlotte Lake

Bluff Lake

Crosman Lake

Guy Lake

Louise Lake

Deep Lake

Leader Lake

Catherine Lake

Clear Lake

Rhumly L.

Spoke Lake

Fog L.

Robbie Lake

CROSSMAN LAKE BATHOLITH

Maude Lake

Syenite Lake

Ducell Lake

SCHREIBER-HEMLO GREENSTONE BELT

N

LEGEND

- Phase 2 Assessment Area
- Major Road
- Minor Road
- Watercourse
- Waterbody
- Batholith Contact
- Lineament - Surficial

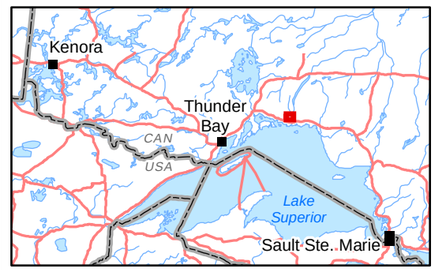
Bedrock Geology

- 10 Mafic suite
- 15 Biotite granite suite
- 7 Clastic metasedimentary rocks
- 6 Intermediate to felsic metavolcanic rocks
- 5 Mafic metavolcanic rocks
- 11 Tonalite gneiss suite

Surficial Lineament Density

High : 11.00 (km/km²)

Low : 0



REFERENCE

Base Data: MNR LIO, obtained 2009-2014,
CanVec topography
Bedrock: OGS MRD 126-REV1 (1:250,000)

2 km

srk consulting

PROJECT

Phase 2 Structural Lineament Interpretation
Schreiber Area, Ontario

TITLE

Surficial Lineament Density of the Schreiber Area - Block B

DESIGN	KR	02 SEP 2014	**Figure 23**	REVISION 3
GIS	JA	04 FEB 2015		UTM ZONE 16N
CHECK	SDC	04 FEB 2015		NAD 1983
REVIEW	AF	04 FEB 2015		1:48,000

File: SRK_NWMO_SCH_Fig23_DensSURFb

462000 464000 466000 468000 470000 472000 474000

5430000 5428000 5426000 5424000 5422000 5420000

BLOCK A

Beavertrap Lake

Bath Lake

Pays Plat Lake

Banana Lake

Triangle Lake

Winston Lake

Carib Lake

Coffee Lake

Little Duck L.

Pick Lake

CROSSMAN LAKE BATHOLITH

N

LEGEND

- Phase 2 Assessment Area
- Major Road
- Minor Road
- Watercourse
- Waterbody
- Batholith Contact
- Lineament - Final Integrated

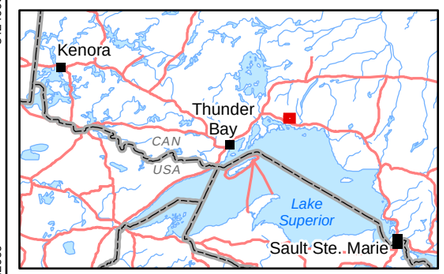
Bedrock Geology

- 10 Mafic suite
- 15 Biotite granite suite
- 7 Clastic metasedimentary rocks
- 6 Intermediate to felsic metavolcanic rocks
- 5 Mafic metavolcanic rocks
- 11 Tonalite gneiss suite

Integrated Lineament Density

High : 12.25 (km/km²)

Low : 0



REFERENCE

Base Data: MNR LIO, obtained 2009-2014,
CanVec topography
Bedrock: OGS MRD 126-REV1 (1:250,000)

2 km

srk consulting

PROJECT

Phase 2 Structural Lineament Interpretation
Schreiber Area, Ontario

TITLE

Final Integrated Lineament Density of the Schreiber Area - Block A

DESIGN	KR	02 SEP 2014	**Figure 24**	REVISION 3
GIS	JA	04 FEB 2015		UTM ZONE 16N
CHECK	SDC	04 FEB 2015		NAD 1983
REVIEW	AF	04 FEB 2015		1:48,000

File: SRK_NWMO_SCH_Fig24_DensFINALa

480000 482000 484000 486000 488000 490000 492000

5426000 5424000 5422000 5420000 5418000 5416000

BLOCK B

Cameron L.

Crosman Lake

Guy Lake

Charlotte Lake

Bluff Lake

Louise Lake

Deep Lake

Catherine Lake

Clear Lake

Leader Lake

Rhumly L.

Spoke Lake

Fog L.

Robbie Lake

Maude Lake

Syenite Lake

Ducell Lake

CROSSMAN LAKE BATHOLITH

SCHREIBER-HEMLO GREENSTONE BELT

N

LEGEND

- Phase 2 Assessment Area
- Major Road
- Minor Road
- Watercourse
- Waterbody
- Batholith Contact
- Lineament - Final Integrated

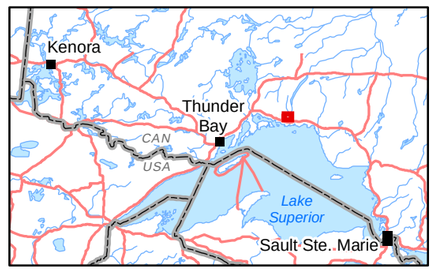
Bedrock Geology

- 10 Mafic suite
- 15 Biotite granite suite
- 7 Clastic metasedimentary rocks
- 6 Intermediate to felsic metavolcanic rocks
- 5 Mafic metavolcanic rocks
- 11 Tonalite gneiss suite

Integrated Lineament Density

High : 12.25 (km/km²)

Low : 0



REFERENCE

Base Data: MNR LIO, obtained 2009-2014,
CanVec topography
Bedrock: OGS MRD 126-REV1 (1:250,000)

2 km

srk consulting

PROJECT

Phase 2 Structural Lineament Interpretation
Schreiber Area, Ontario

TITLE

Final Integrated Lineament Density of the Schreiber Area - Block B

DESIGN	KR	02 SEP 2014	**Figure 25**	REVISION 3
GIS	JA	04 FEB 2015		UTM ZONE 16N
CHECK	SDC	04 FEB 2015		NAD 1983
REVIEW	AF	04 FEB 2015		1:48,000

File: SRK_NWMO_SCH_Fig25_DensFINALb

462000 464000 466000 468000 470000 472000 474000

5430000 5428000 5426000 5424000 5422000 5420000

BLOCK A

Beavertrap Lake
Bath Lake
Winston Lake
Banana Lake
Triangle Lake
Pays Plat Lake
Pick Lake
Carib Lake
Coffee Lake
Little Duck L.

CROSSMAN LAKE BATHOLITH

N

LEGEND

- Phase 2 Assessment Area
- Major Road
- Minor Road
- Watercourse
- Waterbody
- Batholith Contact
- Lineament - Geophysical

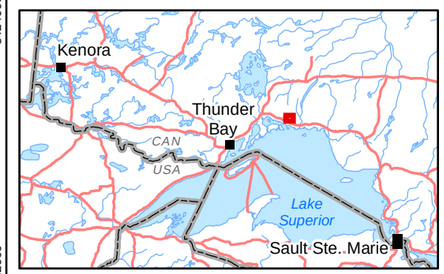
Bedrock Geology

- 10 Mafic suite
- 15 Biotite granite suite
- 7 Clastic metasedimentary rocks
- 6 Intermediate to felsic metavolcanic rocks
- 5 Mafic metavolcanic rocks
- 11 Tonalite gneiss suite

Geophysical Intersection Density

High : 56.23 (/km²)

Low : 0



REFERENCE

Base Data: MNR LIO, obtained 2009-2014,
CanVec topography
Bedrock: OGS MRD 126-REV1 (1:250,000)

2 km

srk consulting

PROJECT

Phase 2 Structural Lineament Interpretation
Schreiber Area, Ontario

TITLE

Geophysical Lineament Intersection Density of the Schreiber Area - Block A

DESIGN	KR	02 SEP 2014	**Figure 26**	REVISION 3
GIS	JA	04 FEB 2015		UTM ZONE 16N
CHECK	SDC	04 FEB 2015		NAD 1983
REVIEW	AF	04 FEB 2015		1:48,000

File: SRK_NWMO_SCH_Fig26_DensptMAGa

480000 482000 484000 486000 488000 490000 492000

5426000 5424000 5422000 5420000 5418000 5416000

BLOCK B

Cameron L.

Crosman Lake

Guy Lake

Charlotte Lake

Bluff Lake

Louise Lake

Deep Lake

Catherine Lake

Clear Lake

Leader Lake

Rhumly L.

Spoke Lake

Fog L.

Robbie Lake

Maude Lake

Syenite Lake

Ducell Lake

CROSSMAN LAKE BATHOLITH

SCHREIBER-HEMLO GREENSTONE BELT

N

LEGEND

- Phase 2 Assessment Area
- Major Road
- Minor Road
- Watercourse
- Waterbody
- Batholith Contact
- Lineament - Geophysical

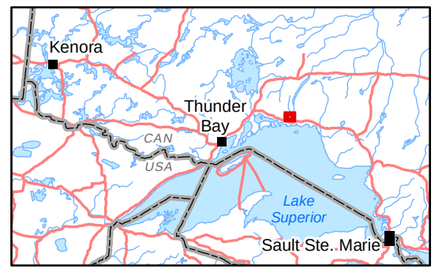
Bedrock Geology

- 10 Mafic suite
- 15 Biotite granite suite
- 7 Clastic metasedimentary rocks
- 6 Intermediate to felsic metavolcanic rocks
- 5 Mafic metavolcanic rocks
- 11 Tonalite gneiss suite

Geophysical Intersection Density

High : 56.23 (/km²)

Low : 0



REFERENCE

Base Data: MNR LIO, obtained 2009-2014,
CanVec topography
Bedrock: OGS MRD 126-REV1 (1:250,000)

2 km

srk consulting

PROJECT

Phase 2 Structural Lineament Interpretation
Schreiber Area, Ontario

TITLE

Geophysical Lineament Intersection Density of the Schreiber Area - Block B

DESIGN	KR	02 SEP 2014	**Figure 27**	REVISION 3
GIS	JA	04 FEB 2015		UTM ZONE 16N
CHECK	SDC	04 FEB 2015		NAD 1983
REVIEW	AF	04 FEB 2015		1:48,000

File: SRK_NWMO_SCH_Fig27_DensptMAGb

462000 464000 466000 468000 470000 472000 474000

5430000 5428000 5426000 5424000 5422000 5420000

BLOCK A

Beavertrap Lake
Bath Lake
Winston Lake
Banana Lake
Triangle Lake
Pays Plat Lake
Carib Lake
Coffee Lake
Little Duck L.
Pick Lake
CROSSMAN LAKE BATHOLITH

N

LEGEND

- Phase 2 Assessment Area
- Major Road
- Minor Road
- Watercourse
- Waterbody
- Batholith Contact
- Lineament - Surficial

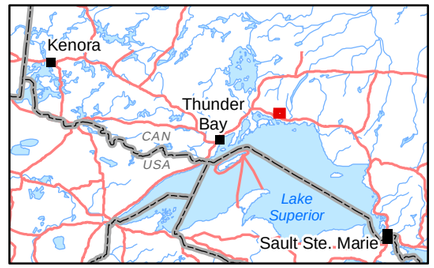
Bedrock Geology

- 10 Mafic suite
- 15 Biotite granite suite
- 7 Clastic metasedimentary rocks
- 6 Intermediate to felsic metavolcanic rocks
- 5 Mafic metavolcanic rocks
- 11 Tonalite gneiss suite

Surficial Intersection Density

High : 42.37 (/km²)

Low : 0



REFERENCE

Base Data: MNR LIO, obtained 2009-2014,
CanVec topography
Bedrock: OGS MRD 126-REV1 (1:250,000)

2 km

srk consulting

PROJECT

Phase 2 Structural Lineament Interpretation
Schreiber Area, Ontario

TITLE

Surficial Lineament Intersection Density of the Schreiber Area - Block A

DESIGN	KR	02 SEP 2014	**Figure 28**	REVISION 3
GIS	JA	04 FEB 2015		UTM ZONE 16N
CHECK	SDC	04 FEB 2015		NAD 1983
REVIEW	AF	04 FEB 2015		1:48,000

File: SRK_NWMO_SCH_Fig28_DensptSURFa

480000 482000 484000 486000 488000 490000 492000

5426000 5424000 5422000 5420000 5418000 5416000

BLOCK B

Cameron L.

Charlotte Lake

Bluff Lake

Crosman Lake

Guy Lake

Louise Lake

Deep Lake

Catherine Lake

Clear Lake

Leader Lake

Rhumly L.

Spoke Lake

Fog L.

Robbie Lake

Maude Lake

Syenite Lake

Ducell Lake

CROSSMAN LAKE BATHOLITH

SCHREIBER-HEMLO GREENSTONE BELT

N

LEGEND

- Phase 2 Assessment Area
- Major Road
- Minor Road
- Watercourse
- Waterbody
- Batholith Contact
- Lineament - Surficial

Bedrock Geology

- 10 Mafic suite
- 15 Biotite granite suite
- 7 Clastic metasedimentary rocks
- 6 Intermediate to felsic metavolcanic rocks
- 5 Mafic metavolcanic rocks
- 11 Tonalite gneiss suite

Surficial Intersection Density

High : 42.37 (/km²)

Low : 0

Kenora

Thunder Bay

CAN

USA

Lake Superior

Sault Ste. Marie

REFERENCE

Base Data: MNR LIO, obtained 2009-2014,
CanVec topography
Bedrock: OGS MRD 126-REV1 (1:250,000)

2 km

srk consulting

PROJECT

Phase 2 Structural Lineament Interpretation
Schreiber Area, Ontario

TITLE

Surficial Lineament Intersection Density of the Schreiber Area - Block B

DESIGN	KR	02 SEP 2014	Figure 29	REVISION 3
GIS	JA	04 FEB 2015		UTM ZONE 16N
CHECK	SDC	04 FEB 2015		NAD 1983
REVIEW	AF	04 FEB 2015		1:48,000

File: SRK_NWMO_SCH_Fig29_DensptSURFb

462000 464000 466000 468000 470000 472000 474000

5430000 5428000 5426000 5424000 5422000 5420000

BLOCK A

Beavertrap Lake

Bath Lake

Winston Lake

Carib Lake

Coffee Lake

Little Duck L.

Pays Plat Lake

Banana Lake

Triangle Lake

Pick Lake

CROSSMAN LAKE BATHOLITH

N

LEGEND

- Phase 2 Assessment Area
- Major Road
- Minor Road
- Watercourse
- Waterbody
- Batholith Contact
- Lineament - Final Integrated

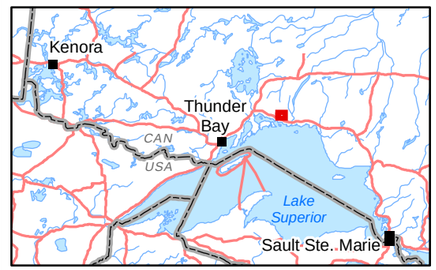
Bedrock Geology

- 10 Mafic suite
- 15 Biotite granite suite
- 7 Clastic metasedimentary rocks
- 6 Intermediate to felsic metavolcanic rocks
- 5 Mafic metavolcanic rocks
- 11 Tonalite gneiss suite

Integrated Intersection Density

High : 51.78 (/km²)

Low : 0



REFERENCE

Base Data: MNR LIO, obtained 2009-2014,
CanVec topography
Bedrock: OGS MRD 126-REV1 (1:250,000)

2 km

srk consulting

PROJECT

Phase 2 Structural Lineament Interpretation
Schreiber Area, Ontario

TITLE

Final Integrated Lineament Intersection Density of the Schreiber Area - Block A

DESIGN	KR	02 SEP 2014	**Figure 30**	REVISION 3
GIS	JA	04 FEB 2015		UTM ZONE 16N
CHECK	SDC	04 FEB 2015		NAD 1983
REVIEW	AF	04 FEB 2015		1:48,000

File: SRK_NWMO_SCH_Fig30_DensptFINALa

480000 482000 484000 486000 488000 490000 492000

5426000 5424000 5422000 5420000 5418000 5416000

BLOCK B

Cameron L.

Crosman Lake

Guy Lake

Charlotte Lake

Bluff Lake

Louise Lake

Deep Lake

Catherine Lake

Clear Lake

Leader Lake

Rhumly L.

Spoke Lake

Fog L.

Robbie Lake

Maude Lake

Syenite Lake

Ducell Lake

CROSSMAN LAKE BATHOLITH

SCHREIBER-HEMLO GREENSTONE BELT

N

LEGEND

- Phase 2 Assessment Area
- Major Road
- Minor Road
- Watercourse
- Waterbody
- Batholith Contact
- Lineament - Final Integrated

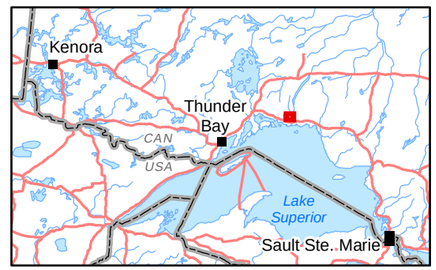
Bedrock Geology

- 10 Mafic suite
- 15 Biotite granite suite
- 7 Clastic metasedimentary rocks
- 6 Intermediate to felsic metavolcanic rocks
- 5 Mafic metavolcanic rocks
- 11 Tonalite gneiss suite

Integrated Intersection Density

High : 51.78 (/km²)

Low : 0



REFERENCE

Base Data: MNR LIO, obtained 2009-2014,
CanVec topography
Bedrock: OGS MRD 126-REV1 (1:250,000)

2 km

srk consulting

PROJECT

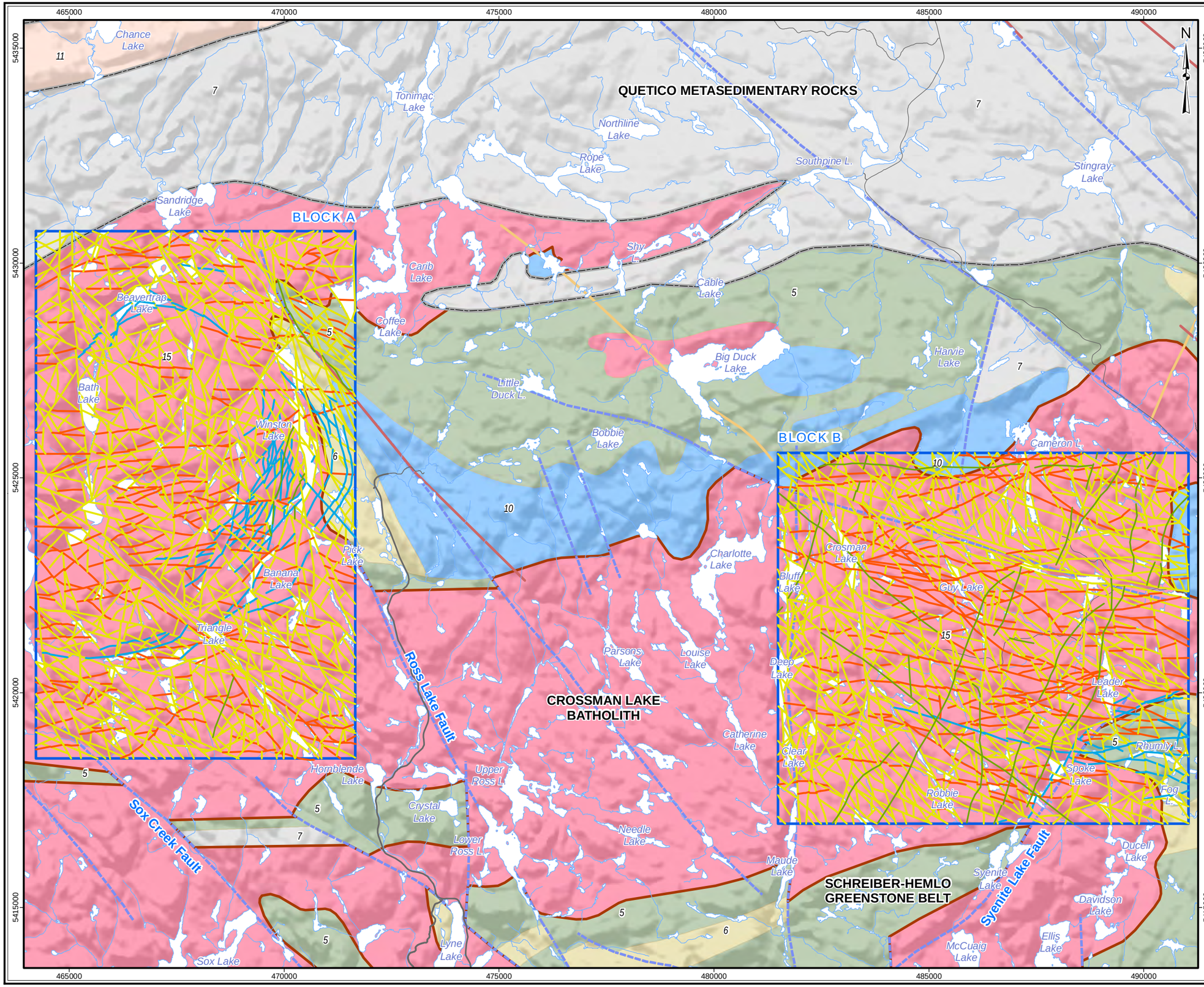
Phase 2 Structural Lineament Interpretation
Schreiber Area, Ontario

TITLE

Final Integrated Lineament Intersection Density of the Schreiber Area - Block B

DESIGN	KR	02 SEP 2014	Figure 31	REVISION 3
GIS	JA	04 FEB 2015		UTM ZONE 16N
CHECK	SDC	04 FEB 2015		NAD 1983
REVIEW	AF	04 FEB 2015		1:48,000

File: SRK_NWMO_SCH_Fig31_DensptFINALb



LEGEND

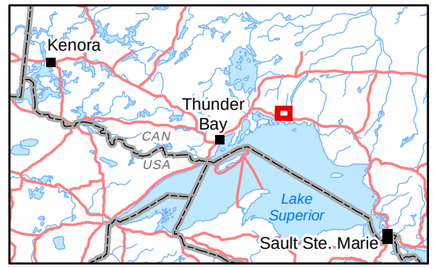
- Phase 2 Assessment Area
- Major Road
- Minor Road
- Watercourse
- Waterbody
- Matachewan mafic dike
- Dyke (Other)
- Mapped Fault
- Quetico/Wawa Subprovince boundary
- Batholith Contact

Relative Age

- Dyke
- D6 (brittle)
- D5 (brittle)
- D1-D4 (brittle-ductile)

Bedrock Geology

- 10 Mafic suite
- 15 Biotite granite suite
- 7 Clastic metasedimentary rocks
- 6 Intermediate to felsic metavolcanic rocks
- 5 Mafic metavolcanic rocks
- 11 Tonalite gneiss suite



REFERENCE

Base Data: MNR LIO, obtained 2009-2014,
CanVec topography
Bedrock/Fault/Dyke: OGS MRD 126-REV1 (1:250,000)

5 km

srk consulting

PROJECT
Phase 2 Structural Lineament Interpretation
Schreiber Area, Ontario

TITLE
Relative Age Relationships
Interpreted Lineaments (RA-2)
of the Schreiber Area

DESIGN	KR	02 SEP 2014	**Figure 32**	REVISION 3
GIS	JA	04 FEB 2015		UTM ZONE 16N
CHECK	SDC	04 FEB 2015		NAD 1983
REVIEW	AF	04 FEB 2015		1:85,000

File: SRK_NWMO_SCH_Fig32_RelAge